

AN ABSTRACT OF THE THESIS OF

SOON-JAI KHANG for the MASTER OF SCIENCE
(Name) (Degree)

in CHEMICAL ENGINEERING presented on Oct. 7, 1971
(Major) (Date)

Title: CATALYST DEACTIVATION

Abstract approved: *Redacted for Privacy*
Octave Levenspiel

This thesis deals with a simple kinetic form to describe an observed first order reaction on a progressively deactivating porous catalyst pellet with all its diffusional effects, or

$$\left(\begin{array}{l} \text{rate of reaction of gas} \\ \text{phase reactant A} \end{array} \right) = k_A C_A a$$

$$-\frac{da}{dt} = k_d C_i a^d$$

where a is the activity of the pellet and d is the order of deactivation. We here explore whether this equation form is derivable in a simple way from the mechanism of deactivation.

The basic differential equations are set up to account for homogeneous surface deactivation and pore diffusion effects, and the appropriate Thiele modulus is found to be the proper parameter for describing the system. For both parallel and side-by-side deactivation, analytical solution of the equations is possible for the extremes of high and low Thiele modulus, however numerical solutions are required for intermediate values of the Thiele modulus.

Results of this analysis show the following.

a) For parallel deactivation, the mechanism study yields the above equations with constant value of d varying from $d = 0.8$ to $d = 3$ depending on the value of the Thiele modulus.

b) For side-by-side deactivation, similar results are obtained except when deactivation by poison is vigorous. In this case the order d varies while the particle deactivates.

Catalyst Deactivation

by

Soon-Jai Khang

A THESIS

submitted to

Oregon State University

in partial fulfillment of
the requirements for the
degree of

Master of Science

June 1972

APPROVED:

Redacted for Privacy

Professor of Chemical Engineering
in charge of major

Redacted for Privacy

Head of Department of Chemical Engineering

Redacted for Privacy

Dean of Graduate School

Date thesis is presented Oct. 7. 1971

Typed by Mary Jo Stratton for Soon-Jai Khang

ACKNOWLEDGMENT

I wish to express my sincere thanks to Dr. Octave Levenspiel, my major professor, for his excellent advice, encouragement and patience during the course of this study. His teachings have helped me to develop an understanding of chemical reaction engineering.

Thanks are also due the Chemical Engineering Department, Dr. Charles E. Wicks, Head, for use of its facilities, and the Oregon State University Computer Center for financial assistance and services rendered by their personnel.

I would like to thank the National Science Foundation for their financial assistance.

A special note of thanks is extended to my mother, Kyonghai Lim, for her encouragement and support.

TABLE OF CONTENTS

	<u>Page</u>
I. INTRODUCTION	1
II. MECHANISMS OF CATALYST DEACTIVATION	6
General Description	6
Previous Work	8
Parallel Deactivation	11
Series Deactivation	18
Side-by-side Deactivation	23
III. RESULTS	28
Parallel Deactivation	28
Discussion	47
Side-by-side Deactivation	47
Discussion	48
IV. LIMITING CASES	70
Parallel Deactivation	70
Case i) $h_A \rightarrow 0$	70
Case ii) $h_A \rightarrow \infty$	72
Side-by-side Deactivation	75
Case i) $\left\{ \begin{array}{l} h_A \rightarrow 0 \\ h_P \rightarrow 0 \end{array} \right.$	76
Case ii) $\left\{ \begin{array}{l} h_A \rightarrow \infty \\ h_P \rightarrow 0 \end{array} \right.$	77
Case iii) $\left\{ \begin{array}{l} h_A \rightarrow 0 \\ h_P \rightarrow \infty \end{array} \right.$	78
Case iv) $\left\{ \begin{array}{l} h_A \rightarrow \infty \\ h_P \rightarrow \infty \end{array} \right.$	86
V. CONCLUSIONS	88
VI. RECOMMENDATIONS FOR FUTURE WORK	90

	<u>Page</u>
BIBLIOGRAPHY	91
APPENDICES	
Appendix I. Nomenclature	93
Appendix II. Solutions of Tridiagonal Linear Equations	96
Appendix III. Difference Equations and Program Listings for Parallel Deactivation	98
Appendix IV. Difference Equations and Program Listings for Side-by-side Deactivation	103

LIST OF TABLES

<u>Table</u>		<u>Page</u>
1	Summary of equations for parallel deactivation.	19
2	Summary of equations for series deactivation.	24
3	Summary of equations for side-by-side deactivation.	27

LIST OF FIGURES

<u>Figure</u>		<u>Page</u>
1	Setting up the material balance.	12
2	Parallel deactivation, C_A^* vs. r^* ($h_A = 0.1$).	31
3	Parallel deactivation, α vs. r^* ($h_A = 0.1$).	31
4	Parallel deactivation, C_A^* vs. r^* ($h_A = 1$).	32
5	Parallel deactivation, α vs. r^* ($h_A = 1$).	32
6	Parallel deactivation, C_A^* vs. r^* ($h_A = 5$).	33
7	Parallel deactivation, α vs. r^* ($h_A = 5$).	33
8	Parallel deactivation, C_A^* vs. r^* ($h_A = 100$).	34
9	Parallel deactivation, α vs. r^* ($h_A = 100$).	34
10	Parallel deactivation, C_A^* vs. r^* ($h_A = 1000$).	35
11	Parallel deactivation, α vs. r^* ($h_A = 1000$).	35
12	Parallel deactivation, a vs. Θ .	36
13	Parallel deactivation, $-\frac{da}{d\Theta}$ vs. a ($h_A = 0.1$).	37
14	Parallel deactivation, $-\frac{da}{d\Theta}$ vs. a ($h_A = 0.5$).	37

<u>Figure</u>		<u>Page</u>
15	Parallel deactivation, $-\frac{da}{d\Theta}$ vs. a ($h_A = 0.65$).	38
16	Parallel deactivation, $-\frac{da}{d\Theta}$ vs. a ($h_A = 0.8$).	38
17	Parallel deactivation, $-\frac{da}{d\Theta}$ vs a ($h_A = 1$).	39
18	Parallel deactivation, $-\frac{da}{d\Theta}$ vs a ($h_A = 1.2$).	39
19	Parallel deactivation, $-\frac{da}{d\Theta}$ vs a ($h_A = 1.5$).	40
20	Parallel deactivation, $-\frac{da}{d\Theta}$ vs a ($h_A = 2$).	40
21	Parallel deactivation, $-\frac{da}{d\Theta}$ vs a ($h_A = 2.5$).	41
22	Parallel deactivation, $-\frac{da}{d\Theta}$ vs a ($h_A = 3$).	41
23	Parallel deactivation, $-\frac{da}{d\Theta}$ vs a ($h_A = 5$).	42
24	Parallel deactivation, $-\frac{da}{d\Theta}$ vs a ($h_A = 7$).	42
25	Parallel deactivation, $-\frac{da}{d\Theta}$ vs a ($h_A = 15$).	43
26	Parallel deactivation, $-\frac{da}{d\Theta}$ vs. a ($h_A = 30$).	43
27	Parallel deactivation, $-\frac{da}{d\Theta}$ vs. a ($h_A = 60$).	44

<u>Figure</u>		<u>Page</u>
28	Parallel deactivation, $-\frac{da}{d\Theta}$ vs. a ($h_A = 100$).	44
29	Parallel deactivation, $-\frac{da}{d\Theta}$ vs. a ($h_A = 1000$).	45
30	Parallel deactivation, d vs. h_A .	46
31	Side-by-side deactivation, C_A^* , C_P^* vs. r^* ($h_A = 0.1$, $h_P = 0.1$).	49
32	Side-by-side deactivation, α vs. r^* ($h_A = 0.1$, $h_P = 0.1$).	49
33	Side-by-side deactivation, C_A^* vs. r^* ($h_A = 0.1$, $h_P = 1$).	50
34	Side-by-side deactivation, C_P^* vs. r^* ($h_A = 0.1$, $h_P = 1$).	50
35	Side-by-side deactivation, α vs. r^* ($h_A = 0.1$, $h_P = 1$).	51
36	Side-by-side deactivation, C_A^* vs. r^* ($h_A = 0.1$, $h_P = 10$).	51
37	Side-by-side deactivation, C_P^* vs. r^* ($h_A = 0.1$, $h_P = 10$).	52
38	Side-by-side deactivation, α vs. r^* ($h_A = 0.1$, $h_P = 10$).	52
39	Side-by-side deactivation, a vs. Θ ($h_A = 0.1$).	53
40	Side-by-side deactivation, $-\frac{da}{d\Theta}$ vs. a ($h_A = 0.1$, $h_P = 0.1$).	54

<u>Figure</u>		<u>Page</u>
41	Side-by-side deactivation, $-\frac{da}{d\Theta}$ vs. a ($h_A = 0.1, h_P = 1$).	54
42	Side-by-side deactivation, $-\frac{da}{d\Theta}$ vs. a ($h_A = 0.1, h_P = 10$).	55
43	Side-by-side deactivation, C_A^* vs. r^* ($h_A = 1, h_P = 0.1$).	55
44	Side-by-side deactivation, C_P^* vs. r^* ($h_A = 1, h_P = 0.1$).	56
45	Side-by-side deactivation, α vs. r^* ($h_A = 1, h_P = 0.1$).	56
46	Side-by-side deactivation, C_A^*, C_P^* vs. r^* ($h_A = 1, h_P = 1$).	57
47	Side-by-side deactivation, α vs. r^* ($h_A = 1, h_P = 1$).	57
48	Side-by-side deactivation, C_A^* vs. r^* ($h_A = 1, h_P = 10$).	58
49	Side-by-side deactivation, C_P^* vs. r^* ($h_A = 1, h_P = 10$).	58
50	Side-by-side deactivation, α vs. r^* ($h_A = 1, h_P = 10$).	59
51	Side-by-side deactivation, a vs. Θ ($h_A = 1$).	60
52	Side-by-side deactivation, $-\frac{da}{d\Theta}$ vs. a ($h_A = 1, h_P = 0.1$).	61

<u>Figure</u>		<u>Page</u>
53	Side-by-side deactivation, $-\frac{da}{d\Theta}$ vs a ($h_A = 1, h_P = 1$).	61
54	Side-by-side deactivation, $-\frac{da}{d\Theta}$ vs. a ($h_A = 1, h_P = 10$).	62
55	Side-by-side deactivation, C_A^* vs. r^* ($h_A = 10, h_P = 0.1$).	62
56	Side-by-side deactivation, C_P^* vs. r^* ($h_A = 10, h_P = 0.1$).	63
57	Side-by-side deactivation, α vs. r^* ($h_A = 10, h_P = 0.1$).	63
58	Side-by-side deactivation, C_A^* vs. r^* ($h_A = 10, h_P = 1$).	64
59	Side-by-side deactivation, C_P^* vs. r^* ($h_A = 10, h_P = 1$).	64
60	Side-by-side deactivation, α vs. r^* ($h_A = 10, h_P = 1$).	65
61	Side-by-side deactivation, C_A^*, C_P^* vs. r^* ($h_A = 10, h_P = 10$).	65
62	Side-by-side deactivation, α vs. r^* ($h_A = 10, h_P = 10$).	66
63	Side-by-side deactivation, a vs. Θ ($h_A = 10$).	67
64	Side-by-side deactivation, $-\frac{da}{d\Theta}$ vs. a ($h_A = 10, h_P = 0.1$).	68
65	Side-by-side deactivation, $-\frac{da}{d\Theta}$ vs a ($h_A = 10, h_P = 10$).	68

<u>Figure</u>		<u>Page</u>
66	Parallel deactivation, $h_A \longrightarrow 0$.	71
67	Parallel deactivation, $h_A \longrightarrow \infty$.	73
68	Side-by-side deactivation, $h_A \longrightarrow 0$ and $h_P \longrightarrow \infty$.	79
69	Side-by-side deactivation, limiting case ($h_A \longrightarrow 0$, $h_P = 50$).	85

CATALYST DEACTIVATION

I. INTRODUCTION

Catalysts are the substances which speed up or slow down the approach to equilibrium of chemical changes. Catalysts may be solids or fluids. Especially, solid catalyzed gas-phase reactions play an important role in many industrial processes such as hydrogenations, dehydrogenations, oxidations, reductions, dehydrations, polymerizations, cracking and reforming. Usually, solid catalysts consist of catalytically active substances, carrier materials, promoters and inhibitors. Promoters improve activity or selectivity of the catalyst or stabilize the catalytic agents. Inhibitors have the opposite effects. Since a large active surface area is desirable, most solid catalysts are in the form of porous pellets. Such materials can provide hundreds of square meters of solid surface per gram of solid.

Usually, a pellet of solid catalyst is in contact with a fluid in which reactants are present. The reactants must diffuse from the bulk of the fluid to the exterior surface of the pellet, and from the exterior surface of the pellet into the interior active surface through the pores. Then, adsorption to the active sites, surface reaction and desorption take place. The products must diffuse back to the bulk of the fluid. Normally, the diffusion step from the bulk of fluid to the exterior

surface of the pellet is negligible compared to the diffusion step inside the pellet.

Often, the activity of a catalyst decreases with operating time. This deactivation makes the process difficult to operate, and requires periodic or continual replacement of catalyst. The following are main causes of deactivation:

- 1) Deposition and physical blocking of the active surface by poisoning substances; carbon deposition on cracking catalyst is a typical example.
- 2) Physical adsorption or chemisorption on the active sites by poisoning substances; poisoning of metallic catalysts by the compounds of S, Se, As is in this group. If the adsorption is not reversible, the poisoning is permanent.
- 3) Structural changes of the catalyst surface such as sintering, localized melting and abrasion of the pellets.

The study of catalyst deactivation can be conducted on four different levels (Butt, 1970). Firstly, microscopic systems or the intrinsic kinetics for the reaction and deactivation: this deals with the kinetics on solid surfaces without consideration of diffusional effects. Adsorption, desorption and surface reaction kinetics come into the picture at this stage. Secondly, an analysis of the behavior of an intermediate system such as the single catalyst pellet: the details of reaction and deactivation kinetics are combined with effects

of pore diffusion. If the intrinsic kinetics are complicated, this is not an easy job. Thirdly, the intrinsic kinetics and the behavior of single catalyst pellets are incorporated into the macroscopic system to give estimates of reactor performance. Finally, the behavior of reactor performance leads to optimization problems for the design and operation of reactors.

This thesis deals with the second level of study of deactivating catalytic systems. It is concerned with the proper or useful description and the mathematical modeling of the action of single pellets of deactivating pellets, accounting for both the surface kinetics and pore diffusion effects.

The first step in treating the problem is to describe the behavior of an intermediate system. As mentioned above, direct mathematical modeling starting with the basic intrinsic kinetics is complicated and yet there is not a simple analytical expression for general behavior of the system. Recently, a new model was proposed for a single catalyst pellet system and has been proved to be useful for many practical applications (Szépe and Levenspiel, 1968a, b; Gwyn, 1970; Levenspiel, 1972). This model assumes that the rate equations of reaction and deactivation are termed separable for the single pellet system as well as for the microscopic system. For the main reaction

$$\text{Reaction rate} = f_1(\text{Temperature}) \cdot f_3(\text{Concentration}) \cdot f_5(\text{activity of catalyst}) \quad (1)$$

and for the deactivation

$$\begin{aligned} \text{Deactivation rate} &= f_2(\text{Temperature}) \cdot f_4(\text{Concentration}) \\ &\cdot f_6(\text{Present condition of catalyst}) \end{aligned} \quad (2)$$

The activity of a catalyst is defined as

$$a = \frac{-r_A}{-r_{A_0}} \quad (3)$$

where $-r_A$ is the observed rate of the main reaction and $-r_{A_0}$ is some specified reference rate, usually the reaction rate with fresh catalyst.

Introducing nth order kinetics and Arrhenius temperature dependencies, the reaction rate becomes

$$-r_A = k_A C_A^n a = k_{A_0} e^{-E/RT} C_A^n a \quad (4)$$

And the deactivation rate which is dependent on the concentration of the poison-producing species i becomes

$$-\frac{da}{dt} = k_d C_i^{n'} a^d = k_{d_0} e^{-E_d/RT} C_i^{n'} a^d \quad (5)$$

where E_d , n' and d denote the activation energy of deactivation, the dependency on poison concentration outside the pellet, and the order of deactivation, respectively. Sometimes, the deactivation is independent of concentration of any material in the gas stream such as in temperature caused changes in surface structure. In that case, equation (5) becomes

$$-\frac{da}{dt} = k''_d a^d = k''_d e^{-E_d/RT} a^d \quad (5a)$$

The purpose of this thesis is to study the behavior of single catalyst pellets as a result of the interaction of various simple surface kinetics and the different kinds of pore diffusion processes which may be operating.

We will also show the relationship between order of deactivation, d , with the various mechanisms which may be operating. The importance of this is that a knowledge of this order of deactivation will give a valuable clue to the mechanism of action of the deactivation process.

II. MECHANISMS OF CATALYST DEACTIVATION

General Description

There are several ways for a catalyst to deactivate. And for the catalyst decay, different authors have used different terminologies such as poisoning, fouling, aging and deactivation. Although each term has a slightly different meaning, we will use the term deactivation. Levenspiel (1972) summarized general mechanisms of deactivation as follows:

A) Form of surface attack by poison

I) Homogeneous site-attack

Under an uniform environment, all active sites on the catalyst surface are attacked indiscriminately. Therefore, all active sites are deactivated uniformly. Poisoning by physical deposition on the surface is in this group.

II) Preferential site-attack

More active sites are preferentially attacked and deactivated. Poisoning by chemisorption on the active surface is likely to be in this group.

B) Decay reactions

I) Parallel deactivation



or



The reaction product may deposit on and deactivate the active surface.

II) Series deactivation



The reaction product may decompose or further react to produce a material which deposits on and deactivates the active surface.

III) Side-by-side deactivation



An impurity in the feed may deposit on the active surface or react to produce a material which deposits on and deactivates the surface.

IV) Independent deactivation

In some cases, the deactivation is independent on the composition of reactants, products and some other substances in the feed. This decaying process involves the structural change or sintering of the active surface under extreme physical conditions such as high pressure or high temperature environment. This type of decay is called independent deactivation.

This thesis develops the general differential equations for homogeneous site attack, the different decay reactions and pore

diffusional effects. The case of parallel and side-by-side deactivation will be solved numerically and the results displayed graphically.

Previous Work

Though many works have been done for various chemical aspects, we will emphasize on the engineering point of view.

Systematic observation and interpretation of deactivating catalysts have a relatively short history. In 1945, Voorhies reported an empirical correlation of coke deposition rates on cracking catalysts. The result, for various catalysts, is in the form

$$C_c = At^n \quad (9)$$

where C_c is the concentration of carbon and t is the operating time. A and n are the constants and n has the value of about 0.5. A few years later, Wheeler (1951, 1955) first introduced diffusion effects on the deactivation, and classified the poisoning in terms of two limiting cases; pore mouth poisoning and uniform poisoning. Pore mouth poisoning is the diffusion limiting case where the outer shell of the pellet becomes completely deactivated, where the completely deactivated zone has a distinct boundary from the active zone, and where the boundary moves toward the interior of the catalyst pellet. On the contrary, the uniform poisoning has no diffusion effect. The poison material is distributed uniformly throughout the pellet and

hence the deactivation takes place uniformly throughout the pellet. Experimentally, Balder and Peterson (1966) examined Wheeler's concepts. They developed a new experimental technique, a method using a single pellet reactor of slab geometry. It has two exposed ends, one is for the centerplane concentration measurement, the other is for the bulk concentration measurement. By plotting activity versus centerplane concentration, they were able to differentiate between pore-mouth poisoning and uniform poisoning for a first-order reaction. Furthermore, Jeffery and Peterson (1970) extended this method to determine whether the poisoning of the catalysts was uniform, simply switching the centerplane and the bulk concentration faces. Dougharty (1970) employed the same idea, but he used the different intrinsic kinetics for deactivation.

Masamune and Smith (1966) presented a more general treatment of a single pellet system. They considered three different decay reactions; parallel, series and side-by-side deactivation. First-order intrinsic kinetics were assumed for reaction and deactivation. Homogeneous site-attack for microscopic scale of deactivation was combined with intraparticle diffusion resistances, so that the extremes of uniform poisoning or pore-mouth poisoning were possible depending on relative rates of diffusion and intrinsic deactivation. Particle effectiveness factor was introduced and calculated numerically as a function of time and Thiele modulus. Also, they used the

numerical results of a single pellet system for the calculation of conversion in a fixed-bed reactor, a typical macroscopic system.

Ozawa and Bishoff (1968) gave a similar analysis for coke formation on cracking catalysts. For their experimental data, the Thiele modulus was so small that the effectiveness factor was taken as unity. Their conclusion was that the parallel mechanism and first-order linear kinetics were suitable for coke formation. Chu (1968) extended Masamune and Smith's work by using Langmuir-Hinshelwood type rate forms. However, his results did not agree with the correlation of Voorhies. Murakami et al. (1968) also presented similar analyses, for parallel and series deactivation. They assumed a fast poisoning reaction comparing to the diffusion process and hence used an unsteady state analysis for the diffusion of poison. For series deactivation, they showed that by changing the Thiele modulus the poisoned area moved toward the interior of a catalyst pellet. This behavior is not possible if we assume pseudo steady-state for the diffusion of poison material. Gioia (1971) gave further analysis of side-by-side deactivation. He used the same technique as Masamune and Smith's, except employing Langmuir-Hinshelwood type rate forms for poisoning. His experimental data showed good agreement with his analysis.

So far, most of the investigators have paid little attention to independent deactivation, and there are few works on this subject.

Thermal sintering is considered as an important factor of independent deactivation. Herrmann et al. (1961) reported experimental results of thermal sintering on platinum-alumina reforming catalysts. The intrinsic kinetics of deactivation on thermal sintering was established to be second-order with respect to remaining intrinsic activity. But later, Chu (1963) reported his experimental results of the sintering of platinum supported on alumina and could not find any order for the thermal sintering reaction because of inaccuracy of his data. Russian researchers (Zaidmann et al., 1969) briefly discussed the mechanisms of thermal sintering. They said that the sintering rate can be represented as the probability of collision of platinum particles and the probability is determined by the size of the particles, by the energy of their interaction with the surface and by the concentration of platinum. Dougharty (1970) employed results of Herrmann et al. for the intrinsic kinetics of deactivation.

Parallel Deactivation

Let us consider the control volume of a thin shell shape inside a spherical catalyst pellet as shown in Figure 1. Reactant A diffuses in a porous catalyst pellet, with a first-order reaction



The material balance for reactant A in the control volume is

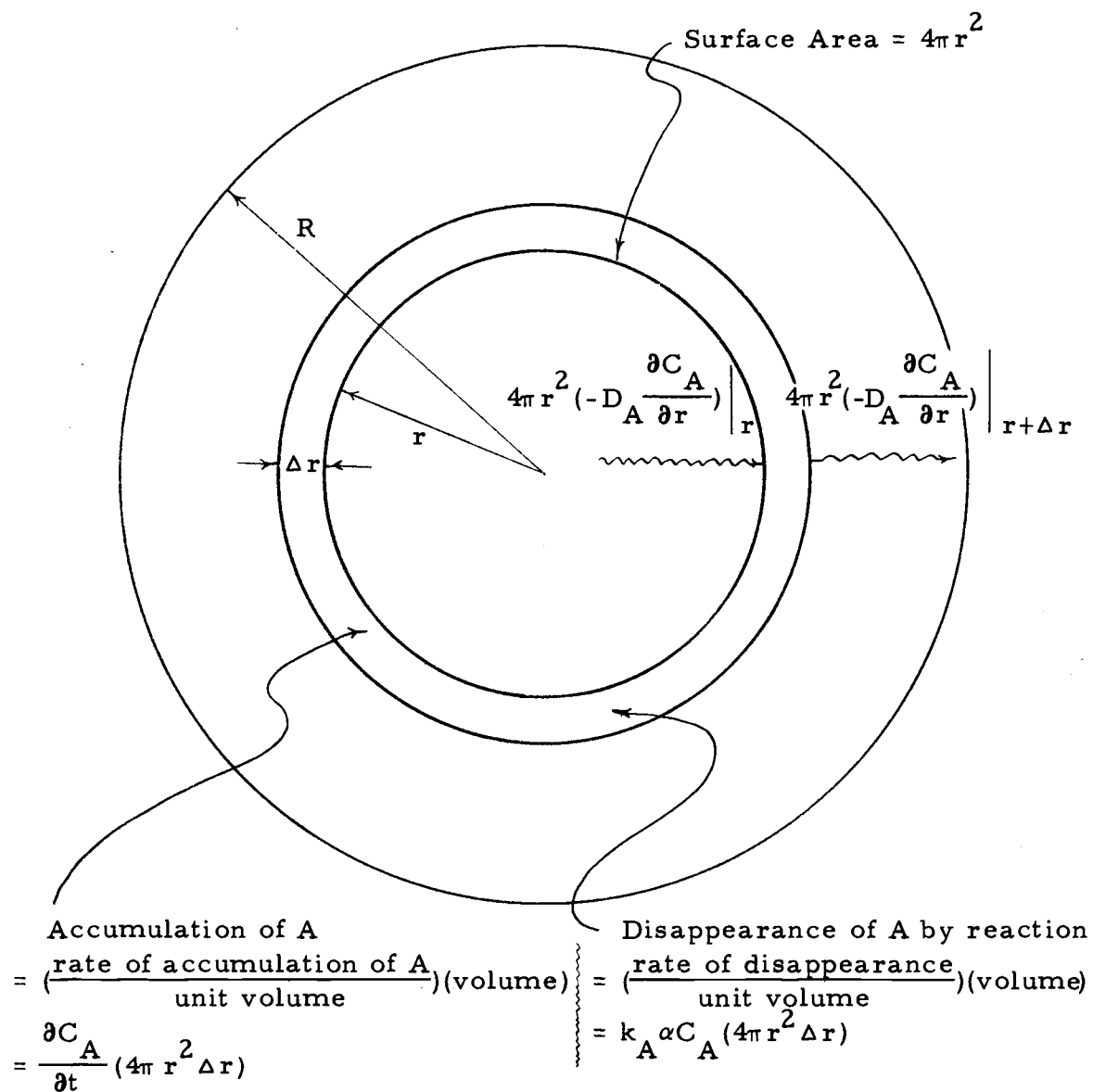


Figure 1. Setting up the material balance.

(rate of reactant diffusion into the control volume)

- (rate of reactant diffusion out of the control volume)

- (rate of reactant loss due to reaction within the control volume)

= (rate of accumulation of reactant in the control volume) (10)

or with the quantities shown in Figure 1,

$$4\pi r^2 \left(-D_A \frac{\partial C_A}{\partial r}\right) \Big|_r - 4\pi r^2 \left(-D_A \frac{\partial C_A}{\partial r}\right) \Big|_{r+\Delta r} - 4\pi r^2 \Delta r k_A \alpha C_A = 4\pi r^2 \Delta r \frac{\partial C_A}{\partial t}$$

where D_A is effective diffusivity of reactant A inside the porous pellet, and α is called point activity. α is 1 on the fresh surface and decreases as the active sites are deactivated.

Rearranging the above equation,

$$\frac{r^2 \frac{\partial C_A}{\partial r} \Big|_{r+\Delta r} - r^2 \frac{\partial C_A}{\partial r} \Big|_r}{\Delta r} - r^2 \frac{k_A}{D_A} \alpha C_A = \frac{r^2}{D_A} \frac{\partial C_A}{\partial t}$$

and taking the limit as Δr approaches zero, we have

$$\frac{\partial}{\partial r} \left(r^2 \frac{\partial C_A}{\partial r} \right) - r^2 \frac{k_A}{D_A} \alpha C_A = \frac{r^2}{D_A} \frac{\partial C_A}{\partial t}$$

or

$$\frac{\partial^2 C_A}{\partial r^2} + \frac{2}{r} \frac{\partial C_A}{\partial r} - \frac{k_A}{D_A} \alpha C_A = \frac{1}{D_A} \frac{\partial C_A}{\partial t} \quad (11)$$

Similarly, for the parallel deactivation of the form



we have

$$\frac{\partial^2 C_A}{\partial r^2} + \frac{2}{r} \frac{\partial C_A}{\partial r} - \frac{1}{D_A} (k_{A1} + k_{A2}) \alpha C_A = \frac{1}{D_A} \frac{\partial C_A}{\partial t} \quad (11a)$$

Replacing the sum of the rate constants, $k_{A1} + k_{A2}$, by another constant, k_A' , we get the same expression as Equation (11).

We assume that the rate of decrease of the point activity, α , has the linear relationship,

$$\frac{\partial \alpha}{\partial t} = -k_d \alpha C_A \quad (12)$$

We can easily recognize that Equation (12) represents homogeneous site-attack as well as the first-order intrinsic kinetics for deactivation.

Initial and boundary conditions for Equations (11) and (12) are

$$C_A(r, t) = C_{As} \quad \text{at } r = R, \quad t \geq 0 \quad (13)$$

$$\frac{\partial C_A(r, t)}{\partial r} = 0 \quad \text{at } r = 0, \quad t \geq 0 \quad (14)$$

$$\alpha(r, t) = 1 \quad \text{at } t = 0, \quad 0 \leq r \leq R \quad (15)$$

$$C_A(r, t) = 0 \quad \text{at } t = 0, \quad 0 \leq r < R \quad (16)$$

In the boundary condition, Equation (13), the reactant concentration, C_{As} , at the surface of a pellet can be considered as the bulk

concentration, since the gas-film resistance of mass transfer outside the pellet is much lower than the resistance inside the pellet.

At this moment, it is convenient to make the equations dimensionless, so let us define the following dimensionless quantities;

$$C_A^* = C_A / C_{As} \quad (17)$$

$$r^* = r/R \quad (18)$$

$$\Theta = k_d C_{As} t \quad (19)$$

$$h_A = \sqrt{\frac{k_A}{D_A}} \frac{R}{3} \quad (20)$$

$$h_{dA} = \sqrt{\frac{k_d C_{As}}{D_A}} \frac{R}{3} \quad (21)$$

where h_A is the Thiele modulus for slab geometry.

Rewriting Equations (11) to (16) with above dimensionless quantities, we obtain

$$\frac{\partial^2 C_A^*}{\partial r^{*2}} + \frac{2}{r^*} \frac{\partial C_A^*}{\partial r^*} - \eta h_A^2 \alpha C_A^* = \eta h_{dA}^2 \frac{\partial C_A^*}{\partial \Theta} \quad (22)$$

$$\frac{\partial \alpha}{\partial \Theta} = -\alpha C_A^* \quad (23)$$

$$C_A^*(r^*, \Theta) = 1 \quad \text{at } r^* = 1, \Theta \geq 0 \quad (24)$$

$$\frac{\partial C_A^*(r^*, \Theta)}{\partial r^*} = 0 \quad \text{at } r^* = 0, \Theta \geq 0 \quad (25)$$

$$\alpha(r^*, \Theta) = 1 \quad \text{at } \Theta = 0, 0 \leq r^* \leq 1 \quad (26)$$

$$C_A^*(r^*, \Theta) = 0 \quad \text{at } \Theta = 0, 0 \leq r^* < 1 \quad (27)$$

Furthermore, noticing that the poisoning reaction is usually much slower than the diffusion process, we assume pseudo steady-state with respect to the accumulation of mass inside the pellet.

Therefore, we can neglect the accumulation term in Equation (22), or

$$\frac{\partial^2 C_A^*}{\partial r^{*2}} + \frac{2}{r^*} \frac{\partial C_A^*}{\partial r^*} - 9h_A^2 C_A^* = 0 \quad (28)$$

In this case, the initial condition, Equation (27), is not valid, and other initial condition can be found from the initial steady-state solution. As stated above, at $t = 0$, α is 1. Eliminating the time variable from Equation (28), we have the ordinary differential equation

$$\frac{d^2 C_A^*}{dr^{*2}} + \frac{2}{r^*} \frac{dC_A^*}{dr^*} - 9h_A^2 C_A^* = 0 \quad (29)$$

or

$$\frac{d}{dr^*} \left(r^{*2} \frac{dC_A^*}{dr^*} \right) = 9r^{*2} h_A^2 C_A^*$$

with the boundary conditions

$$C_A^* = 1 \quad \text{at } r^* = 1 \quad (30)$$

$$\frac{dC_A^*}{dr^*} = 0 \quad \text{at } r^* = 0 \quad (31)$$

The solution of Equation (29) with the boundary conditions,

Equations (30) and (31), becomes

$$C_A^* = \frac{1}{r^*} \frac{\sinh(3h_A r^*)}{\sinh(3h_A)} \quad \text{at } \Theta = 0, \quad 0 \leq r^* \leq 1 \quad (32)$$

Equation (32) is a new initial condition for the differential equation (29).

Reaction rates at any instant for reactant A is defined as

$$-r_A = \frac{(\text{Moles A disapp.})}{(\text{Time})(\text{Vol. of pellet})}$$

or

$$\begin{aligned} -r_A &= \frac{\int_0^1 \alpha(r^*, \Theta) C_A^*(r^*, \Theta) 4\pi r^{*2} dr^*}{\int_0^1 4\pi r^{*2} dr^*} \\ &= 3 \int_0^1 r^{*2} \alpha(r^*, \Theta) C_A^*(r^*, \Theta) dr^* \end{aligned} \quad (33)$$

From Equation (3), the activity of a catalyst pellet is

$$a = \frac{-r_A}{-r_{A0}}$$

We will choose the maximum reaction rate as a reference reaction rate, r_{A0} , so that maximum value of the activity cannot exceed unity. For slow deactivation (using Equation (28)), the initial reaction rate is the maximum reaction rate because reactant can penetrate throughout the pellet, and each element of catalyst surface "sees" fluid at bulk condition. For fast deactivation, things are more complex. The instant a pellet is bathed in reactant starts diffusion into the interior of the pellet, thus the rate of reaction will rise and reach a maximum value a short time after exposing the

catalyst pellet to the reactant gas.

All necessary equations for analysis of parallel deactivation are summarized in Table 1.

Series Deactivation



Consider the same control volume shown in Figure 1. The material balance for reactant A in the control volume is the same as Equation (10). Taking the same steps, we arrive finally at the differential equation,

$$\frac{\partial^2 C_A}{\partial r^2} + \frac{2}{r} \frac{\partial C_A}{\partial r} - \frac{k_A}{D_A} C_A = \frac{1}{D_A} \frac{\partial C_A}{\partial t} \quad (34)$$

The material balance for product R in the control volume is

$$\begin{aligned} & \text{(rate of product diffusion into the control volume)} \\ & - \text{(rate of product diffusion out of the control volume)} \\ & - \text{(rate of product loss due to poisoning reaction within} \\ & \quad \text{the control volume)} \\ & + \text{(rate of production due to main reaction within the} \\ & \quad \text{control volume)} \\ & = \text{(rate of accumulation of product in the control volume)} \end{aligned}$$

The product loss due to the poisoning reaction is much smaller than the diffusion process and the production rate due to the main reaction. If it were not much smaller, then hardly any product R

Table 1. Summary of equations for parallel deactivation.

Parameters of the system	Differential equations	Initial and boundary conditions	Activity
h_A, h_{dA}	<p style="text-align: center;"><u>Fast Deactivation</u></p> $\nabla_r^2 C_A^* - 9h_A^2 \alpha C_A^* = 9h_{dA}^2 \frac{\partial C_A^*}{\partial \Theta} \quad (22)$ $\frac{\partial \alpha}{\partial \Theta} = -\alpha C_A^* \quad (23)$	$C_A^* = 1 \quad \text{at } r^* = 1, \Theta \geq 0 \quad (24)$ $\frac{\partial C_A^*}{\partial r^*} = 0 \quad \text{at } r^* = 0, \Theta \geq 0 \quad (25)$ $\alpha = 1 \quad \text{at } \Theta = 0, 0 \leq r^* \leq 1 \quad (26)$ $C_A^* = 0 \quad \text{at } \Theta = 0, 0 \leq r^* < 1 \quad (27)$	$a = \frac{-r_A}{-r_{Ao}} \quad (3)$ <p>where</p>
h_A	<p style="text-align: center;"><u>Slow Deactivation</u></p> $\nabla_r^2 C_A^* - 9h_A^2 \alpha C_A^* = 0 \quad (28)$ $\frac{\partial \alpha}{\partial \Theta} = -\alpha C_A^* \quad (23)$	$C_A^* = 1 \quad \text{at } r^* = 1, \Theta \geq 0 \quad (24)$ $\frac{\partial C_A^*}{\partial r^*} = 0 \quad \text{at } r^* = 0, \Theta \geq 0 \quad (25)$ $\alpha = 1 \quad \text{at } \Theta = 0, 0 \leq r^* \leq 1 \quad (26)$ $C_A^* = \frac{1}{r^*} \frac{\sinh(3h_A r^*)}{\sinh(3h_A)} \quad (32)$ <p style="text-align: center;">at $\Theta = 0, 0 \leq r^* \leq 1$</p>	$-r_A = 3 \int_0^1 r^{*2} \alpha C_A^* dr^* \quad (33)$ <p>$-r_{Ao}$; maximum value of $-r_A$</p>

would escape from the pellet, this would represent a poor catalyst, and this is an uninteresting case. Thus, eliminating the third term of above equation, we have

$$4\pi r^2 \left(-D_R \frac{\partial C_R}{\partial r}\right) \Big|_r - 4\pi r^2 \left(-D_R \frac{\partial C_R}{\partial r}\right) \Big|_{r+\Delta r} + 4\pi r^2 \Delta r k_A \alpha C_A = 4\pi r^2 \Delta r \frac{\partial C_R}{\partial t}$$

Rearranging the above equation and taking the limit as Δr approaches zero,

$$\frac{\partial^2 C_R}{\partial r^2} + \frac{2}{r} \frac{\partial C_R}{\partial r} + \frac{k_A}{D_R} \alpha C_A = \frac{1}{D_R} \frac{\partial C_R}{\partial t} \quad (35)$$

In this case, the point activity has the relationship,

$$\frac{\partial \alpha}{\partial t} = -k_d \alpha C_R \quad (36)$$

Initial and boundary conditions for Equations (34), (35), and (36) are

$$C_A(r, t) = C_{As} \quad \text{at } r = R, t \geq 0 \quad (37)$$

$$C_R(r, t) = C_{Rs} \quad \text{at } r = R, t \geq 0 \quad (38)$$

$$\frac{\partial C_A(r, t)}{\partial r} = \frac{\partial C_R(r, t)}{\partial r} = 0 \quad \text{at } r = 0, t \geq 0 \quad (39)$$

$$\alpha(r, t) = 1 \quad \text{at } t = 0, 0 \leq r \leq R \quad (40)$$

$$C_A(r, t) = C_R(r, t) = 0 \quad \text{at } t = 0, 0 \leq r < R \quad (41)$$

Introducing the dimensionless quantities defined by Equations (17) to (21) and defining the following additional dimensionless quantities

$$C_R^* = \frac{C_R}{C_{As}} \quad (42)$$

$$h_{AR} = \sqrt{\frac{k_A}{D_R}} \frac{R}{3} \quad (43)$$

$$h_{dR} = \sqrt{\frac{k_d C_{As}}{D_R}} \frac{R}{3} \quad (44)$$

we can rewrite Equations (35) to (44) as

$$\frac{\partial^2 C_A^*}{\partial r^{*2}} + \frac{2}{r^*} \frac{\partial C_A^*}{\partial r^*} - 9h_A^2 \alpha C_A^* = 9h_{dA}^2 \frac{\partial C_A^*}{\partial \Theta} \quad (45)$$

$$\frac{\partial^2 C_R^*}{\partial r^{*2}} + \frac{2}{r^*} \frac{\partial C_R^*}{\partial r^*} + 9h_{AR}^2 \alpha C_A^* = 9h_{dR}^2 \frac{\partial C_R^*}{\partial \Theta} \quad (46)$$

$$\frac{\partial \alpha}{\partial \Theta} = -\alpha C_R^* \quad (47)$$

$$C_A^*(r^*, \Theta) = 1 \quad \text{at } r^* = 1, \Theta \geq 0 \quad (48)$$

$$C_R^*(r^*, \Theta) = C_{Rs}/C_{As} \quad \text{at } r^* = 1, \Theta \geq 0 \quad (49)$$

$$\frac{\partial C_A^*(r^*, \Theta)}{\partial r^*} = \frac{\partial C_R^*(r^*, \Theta)}{\partial r^*} = 0 \quad \text{at } r^* = 0, \Theta \geq 0 \quad (50)$$

$$\alpha(r^*, \Theta) = 1 \quad \text{at } \Theta = 0, 0 \leq r^* \leq 1 \quad (51)$$

$$C_A^*(r^*, \Theta) = C_R^*(r^*, \Theta) = 0 \quad \text{at } \Theta = 0, 0 \leq r^* < 1 \quad (52)$$

For slow deactivation, we may assume pseudo steady-state with

respect to the accumulation of mass inside the pellet. Thus, the accumulation terms in Equations (45) and (46) are neglected and these expressions reduce to

$$\frac{\partial^2 C_A^*}{\partial r^{*2}} + \frac{2}{r^*} \frac{\partial C_A^*}{\partial r^*} - 9h_A^2 \alpha C_A^* = 0 \quad (53)$$

$$\frac{\partial^2 C_R^*}{\partial r^{*2}} + \frac{2}{r^*} \frac{\partial C_R^*}{\partial r^*} + 9h_{AR}^2 \alpha C_A^* = 0 \quad (54)$$

In this case, the initial condition, Equation (52), is not valid. The proper initial condition for C_A^* for this case can be found by the same treatment given in the previous section, or

$$C_A^*(r^*, \Theta) = \frac{1}{r^*} \frac{\sinh(3h_A r^*)}{\sinh(3h_A)} \quad \text{at } \Theta = 0, \quad 0 \leq r^* \leq 1 \quad (55)$$

Initial condition for C_R^* can be found easily from the properties of a harmonic function. Combining Equation (53) with Equation (54),

$$\nabla_r^2 (h_{AR}^2 C_A^* + h_A^2 C_R^*) = 0 \quad (56)$$

where ∇_r^2 denotes the Laplacian in spherical coordinates which only has an r-component.

Integrating Equation (56) with respect to r^* ,

$$r^{*2} \frac{d}{dr^*} (h_{AR}^2 C_A^* + h_A^2 C_R^*) = C_1$$

Using Equation (50), the constant C_1 becomes zero.

$$\frac{d}{dr^*} (h_{AR}^2 C_A^* + h_A^2 C_R^*) = 0$$

Integrating once more,

$$h_{AR}^2 C_A^* + h_A^2 C_R^* = C_2$$

and from Equations (48) and (49), we have

$$C_R^*(r^*, \Theta) = \frac{C_{Rs}}{C_{As}} + \left(\frac{h_{AR}}{h_A}\right)^2 [1 - C_A^*(r^*, \Theta)] \quad (57)$$

$$\text{at } \Theta = 0, \quad 0 \leq r^* \leq 1$$

Equations (55) and (57) are new initial conditions for C_A^* and C_R^* . Activity and reaction rates for reactant A can be calculated by the method of the previous section. All necessary equations are tabulated in Table 2.

Side-by-side Deactivation



By a procedure similar to that of the previous sections, we find that for fast deactivation,

$$\nabla_r^2 C_A - \frac{k_A}{D_A} \alpha C_A = \frac{1}{D_A} \frac{\partial C_A}{\partial t} \quad (58)$$

$$\nabla_r^2 C_P - \frac{k_P}{D_P} \alpha C_P = \frac{1}{D_P} \frac{\partial C_P}{\partial t} \quad (59)$$

$$\frac{\partial \alpha}{\partial t} = -k_d \alpha C_P \quad (60)$$

Table 2. Summary of equations for series deactivation.

Parameters of the system	Differential equations	Initial and boundary conditions	Activity
$h_A, h_{AR},$ $h_{dA}, C_{Rs}/C_{As}$	<p style="text-align: center;"><u>Fast Deactivation</u></p> $\nabla_r^2 C_A^* - 9h_A^2 \alpha C_A^* = 9h_{dA}^2 \frac{\partial C_A^*}{\partial \Theta} \quad (45)$ $\nabla_r^2 C_R^* + 9h_{AR}^2 \alpha C_A^* = 9h_{dR}^2 \frac{\partial C_R^*}{\partial \Theta} \quad (46)$ $\frac{\partial \alpha}{\partial \Theta} = -\alpha C_R^* \quad (47)$	$C_A^* = 1 \text{ at } r^* = 1, \Theta \geq 0 \quad (48)$ $C_R^* = C_{Rs}/C_{As} \text{ at } r^* = 1, \Theta \geq 0 \quad (49)$ $\frac{\partial C_A^*}{\partial r^*} = \frac{\partial C_R^*}{\partial r^*} = 0, \text{ at } r^* = 0, \Theta \geq 0 \quad (50)$ $\alpha = 1 \text{ at } \Theta = 0, 0 \leq r^* \leq 1 \quad (51)$ $C_A^* = C_R^* = 0 \text{ at } \Theta = 0, 0 \leq r^* < 1 \quad (52)$	$a = \frac{-r_A}{-r_{Ao}} \quad (3)$ <p>where</p> $-r_A = 3 \int_0^1 r^{*2} \alpha C_A^* dr^* \quad (33)$ <p>$-r_{Ao}$; maximum value of $-r_A$</p>
$h_A, h_{AR},$ C_{Rs}/C_{As}	<p style="text-align: center;"><u>Slow Deactivation</u></p> $\nabla_r^2 C_A^* - 9h_A^2 \alpha C_A^* = 0 \quad (53)$ $\nabla_r^2 C_R^* + 9h_{AR}^2 \alpha C_A^* = 0 \quad (54)$ $\frac{\partial \alpha}{\partial \Theta} = -\alpha C_R^* \quad (47)$	$C_A^* = 1 \text{ at } r^* = 1, \Theta \geq 0 \quad (48)$ $C_R^* = C_{Rs}/C_{As} \text{ at } r^* = 1, \Theta \geq 0 \quad (49)$ $\frac{\partial C_A^*}{\partial r^*} = \frac{\partial C_R^*}{\partial r^*} = 0 \text{ at } r^* = 0, \Theta \geq 0 \quad (50)$ $\alpha = 1 \text{ at } \Theta = 0, 0 \leq r^* \leq 1 \quad (51)$ $C_A^* = \frac{1}{r^*} \frac{\sinh(3h_A r^*)}{\sinh(3h_A)} \quad (56)$ $C_R^* = \frac{C_{Rs}}{C_{As}} + \left(\frac{h_{AR}}{h_A}\right)^2 (1 - C_A^*) \quad (57)$ <p>at $\Theta = 0, 0 \leq r^* \leq 1$</p>	

The initial and boundary conditions are

$$C_A(r, t) = C_{As} \quad \text{at } r = R, t \geq 0 \quad (61)$$

$$C_P(r, t) = C_{Ps} \quad \text{at } r = R, t \geq 0 \quad (62)$$

$$\frac{\partial C_A(r, t)}{\partial r} = \frac{\partial C_P(r, t)}{\partial r} = 0 \quad \text{at } r = 0, t \geq 0 \quad (63)$$

$$\alpha(r, t) = 1 \quad \text{at } t = 0, 0 \leq r \leq R \quad (64)$$

$$C_A(r, t) = C_P(r, t) = 0 \quad \text{at } t = 0, 0 \leq r < R \quad (65)$$

where C_{Ps} denotes the concentration of poison on the exterior surface of a catalyst pellet.

Using the same dimensionless quantities introduced in Equations (17), (18), (20) and (21), and defining additional dimensionless quantities;

$$\Theta = k_d C_{Ps} t, \quad C_P^* = C_P / C_{Ps} \quad (66)$$

$$h_P = \sqrt{\frac{k_P}{D_P} \frac{R}{3}} \quad (67)$$

$$h_{dP} = \sqrt{\frac{k_d C_{Ps}}{D_P} \frac{R}{3}} \quad (68)$$

Equations (58) to (65) are rewritten in dimensionless form as follows,

$$\nabla_r^2 C_A^* - \eta h_A^2 \alpha C_A^* = \eta h_{dA}^2 \frac{\partial C_A^*}{\partial \Theta} \quad (69)$$

$$\nabla_r^2 C_P^* - \eta h_P^2 \alpha C_P^* = \eta h_{dP}^2 \frac{\partial C_P^*}{\partial \Theta} \quad (70)$$

$$\frac{\partial \alpha}{\partial \Theta} = -\alpha C_P^* \quad (71)$$

The initial and boundary conditions are

$$C_A^*(r^*, \Theta) = C_P^*(r^*, \Theta) = 1 \quad \text{at } r^* = 1, \Theta \geq 0 \quad (72)$$

$$\frac{\partial C_A^*(r^*, \Theta)}{\partial r^*} = \frac{\partial C_P^*(r^*, \Theta)}{\partial r^*} = 0 \quad \text{at } r^* = 0, \Theta \geq 0 \quad (73)$$

$$\alpha(r^*, \Theta) = 1 \quad \text{at } \Theta = 0, 0 \leq r^* \leq 1 \quad (74)$$

$$C_A^*(r^*, \Theta) = C_P^*(r^*, \Theta) = 0 \quad \text{at } \Theta = 0, 0 \leq r^* < 1 \quad (75)$$

For slow deactivation for the same reason as given in the previous sections, we can neglect the accumulation terms in Equations (69) and (70);

$$\nabla_r^2 C_A^* - 9h_A^2 \alpha C_A^* = 0 \quad (76)$$

$$\nabla_r^2 C_P^* - 9h_P^2 \alpha C_P^* = 0 \quad (77)$$

In that case, the initial conditions, Equation (75), should be changed to

$$C_A^*(r^*, \Theta) = \frac{1}{r^*} \frac{\sinh(3h_A r^*)}{\sinh(3h_A)} \quad (78)$$

at $\Theta = 0, 0 \leq r^* \leq 1$

$$C_P^*(r^*, \Theta) = \frac{1}{r^*} \frac{\sinh(3h_P r^*)}{\sinh(3h_P)} \quad (79)$$

Resulting equations are tabulated in Table 3.

Table 3. Summary of equations for side-by-side deactivation.

Parameters of the system	Differential equations	Initial and boundary conditions	Activity
$h_A, h_P,$ h_{dA}, h_{dP}	<p style="text-align: center;"><u>Fast Deactivation</u></p> $\nabla_r^2 C_A^* - 9h_A^2 \alpha C_A^* = 9h_{dA}^2 \frac{\partial C_A^*}{\partial \Theta} \quad (69)$ $\nabla_r^2 C_P^* - 9h_P^2 \alpha C_P^* = 9h_{dP}^2 \frac{\partial C_P^*}{\partial \Theta} \quad (70)$ $\frac{\partial \alpha}{\partial \Theta} = -\alpha C_P^* \quad (71)$	$C_A^* = C_P^* = 1 \text{ at } r^* = 1, \Theta \geq 0 \quad (72)$ $\frac{\partial C_A^*}{\partial r^*} = \frac{\partial C_P^*}{\partial r^*} = 0 \text{ at } r^* = 0, \Theta \geq 0 \quad (73)$ $\alpha = 1 \text{ at } \Theta = 0, 0 \leq r^* \leq 1 \quad (74)$ $C_A^* = C_P^* = 0, \text{ at } \Theta = 0, 0 \leq r^* < 1 \quad (75)$	$a = \frac{-r_A}{-r_{Ao}} \quad (3)$ <p>where</p> $-r_A = 3 \int_0^1 r^{*2} \alpha C_A^* dr^* \quad (33)$ <p>$-r_{Ao}$; maximum value of $-r_A$</p>
h_A, h_P	<p style="text-align: center;"><u>Slow Deactivation</u></p> $\nabla_r^2 C_A^* - 9h_A^2 \alpha C_A^* = 0 \quad (76)$ $\nabla_r^2 C_P^* - 9h_P^2 \alpha C_P^* = 0 \quad (77)$ $\frac{\partial \alpha}{\partial \Theta} = -\alpha C_P^* \quad (71)$	$C_A^* = C_P^* = 1 \text{ at } r^* = 1, \Theta \geq 0 \quad (72)$ $\frac{\partial C_A^*}{\partial r^*} = \frac{\partial C_P^*}{\partial r^*} = 0, \text{ at } r^* = 0, \Theta \geq 0 \quad (73)$ $C_A^* = \frac{1}{r^*} \frac{\sinh(3h_A r^*)}{\sinh(3h_A)} \text{ at } \Theta = 0, \quad (78)$ $0 \leq r^* \leq 1$ $C_P^* = \frac{1}{r^*} \frac{\sinh(3h_P r^*)}{\sinh(3h_P)} \quad (79)$	

III. RESULTS

The equations tabulated in Tables 1, 2 and 3 can be solved numerically by changing them into difference equations. We can find the standard procedures for partial differential equations and other numerical methods elsewhere (Carnahan et al., 1969).

Only cases of slow deactivation will be solved, because these cases are more realistic and have less parameters to describe the systems. We will consider Parallel and Side-by-side deactivation in turn.

Parallel Deactivation

In difference form, partial differential equations (28), (23) and the initial and boundary conditions (24), (25), (26) and (32) become

$$C_{m+1, n}^A = \left(\frac{m-1}{m}\right)(2 + 9h_A^2 \Delta r^2)C_{m, n}^A - \left(\frac{m-2}{m}\right)C_{m-1, n}^A + 0(\Delta\Theta) + 0(\Delta r^2) \quad (80)$$

$$\alpha_{m, n} = (-\Delta\Theta C_{m, n-1}^A + 1) \alpha_{m, n-1} + 0(\Delta\Theta) \quad (81)$$

the boundary conditions;

$$C_{M, n}^A = 1 \quad (82)$$

$$C_{2, n}^A - C_{1, n}^A = 0 \quad (83)$$

and the initial conditions;

$$\alpha_{m, 1} = 1 \quad (84)$$

$$C_{m,1}^A = \frac{\sinh [3h_A \Delta r(m-1)]}{\Delta r(m-1) \sinh(3h_A)} \quad (85)$$

where

$$\Delta r = \frac{1}{(M-1)}$$

Rearranging Equations (80), (82) and (83), gives the following set of linear equations,

$$-\left(\frac{m-2}{m}\right)C_{m-1,n}^A + \left(\frac{m-1}{m}\right)(9h_A^2 \Delta r^2 \alpha_{m,n} + 2)C_{m,n}^A - C_{m+1,n}^A = 0$$

$$; m = 3, \dots, M-2 \quad (86)$$

$$-\left(\frac{M-3}{M-1}\right)C_{M-2,n}^A + \left(\frac{M-2}{M-1}\right)(9h_A^2 \Delta r^2 \alpha_{M-1,n} + 2)C_{M-1,n}^A = 1$$

The coefficient matrix of the above equations is in the tridiagonal form, and the method of solution is given in Appendix II.

Combining Euler's second-order method for the time increments, Equation (81) is regarded as the first approximation of the point activity, $\bar{\alpha}_{m,n}$,

$$\bar{\alpha}_{m,n} = \alpha_{m,n-1} (-\Delta \Theta C_{m,n-1}^A + 1) \quad (87)$$

Using these $\bar{\alpha}_{m,n}$ values, the tridiagonal matrix of Equation (86) is solved, and the first approximation of the reactant concentration, $\bar{C}_{m,n}^A$, is obtained. The second approximation of the point activity, $\alpha_{m,n}$, can be calculated from

$$\alpha_{m,n} = \alpha_{m,n-1} - \frac{\Delta \Theta}{2} (C_{m,n-1}^A \alpha_{m,n-1} + \bar{C}_{m,n}^A \bar{\alpha}_{m,n}) \quad (88)$$

Using the above second approximate values, $\alpha_{m,n}$, we can solve the tridiagonal matrix, Equation (86), again, and have the second approximate values, $C_{m,n}^A$.

Then, we can evaluate the rate of reaction for the whole pellet as a function of time from Equation (33) and from this, the activity of the whole pellet as a function of time from Equation (3). The derivative of activity with respect to time, $\frac{da}{d\Theta}$, is also evaluated numerically as a function of time.

These procedures are given in Appendix III for both slow and fast deactivation, and are programmed in FORTRAN IV language for CDC 3300 Computer System. However, the results are given only for the slow deactivation. These are shown as follows.

- (1) For various values of Thiele modulus ($h_A = 0.1, 1, 5, 100, 1000$) graphs of reactant concentration and point activity vs. radial position are given in Figures 2 to 11.
- (2) For all these cases the activity, a , is plotted as a function of time and Thiele modulus in Figure 12.
- (3) To test the validity of Equation (5a), the plot of $-\frac{da}{d\Theta}$ vs. a is made on log-log scales for these and numerous other values of Thiele modulus (Figures 13 to 29). The results are generally acceptable as straight lines. The slopes turn out to be the order of deactivation, \underline{d} .
- (4) Finally, the order of deactivation, \underline{d} , is plotted as a function of Thiele modulus in Figure 30.

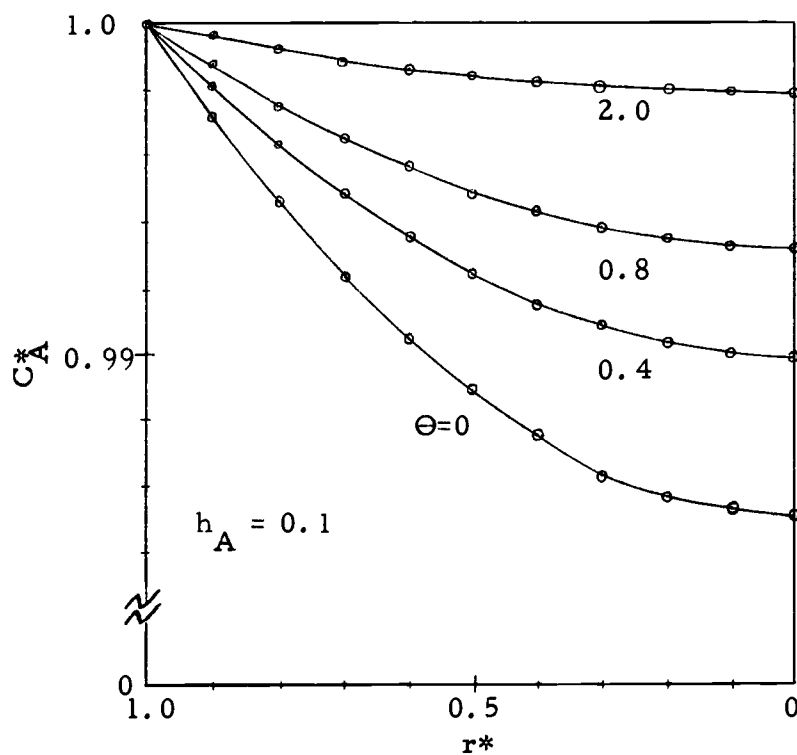


Figure 2. Parallel deactivation, C_A^* vs. r^* .

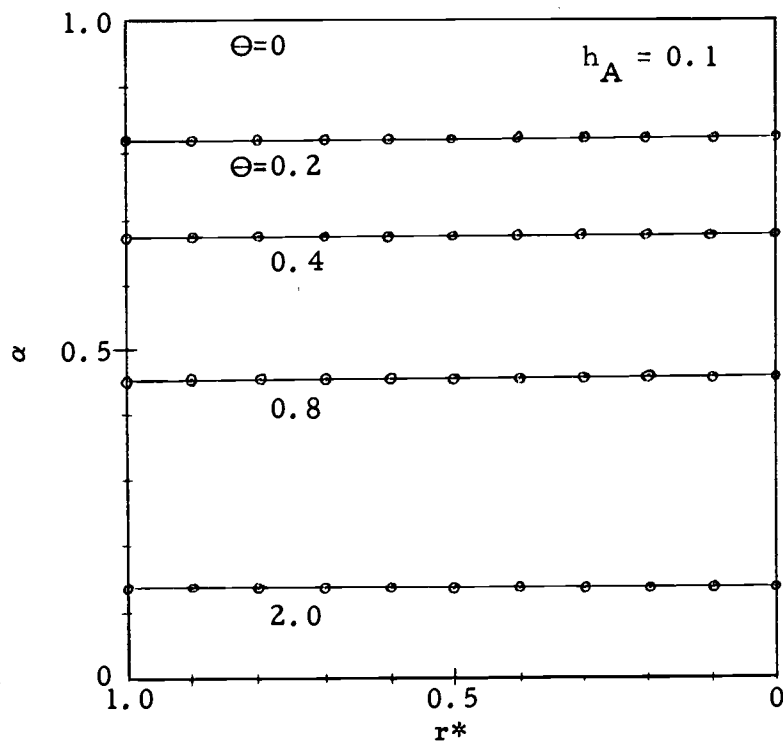


Figure 3. Parallel deactivation, α vs. r^* .

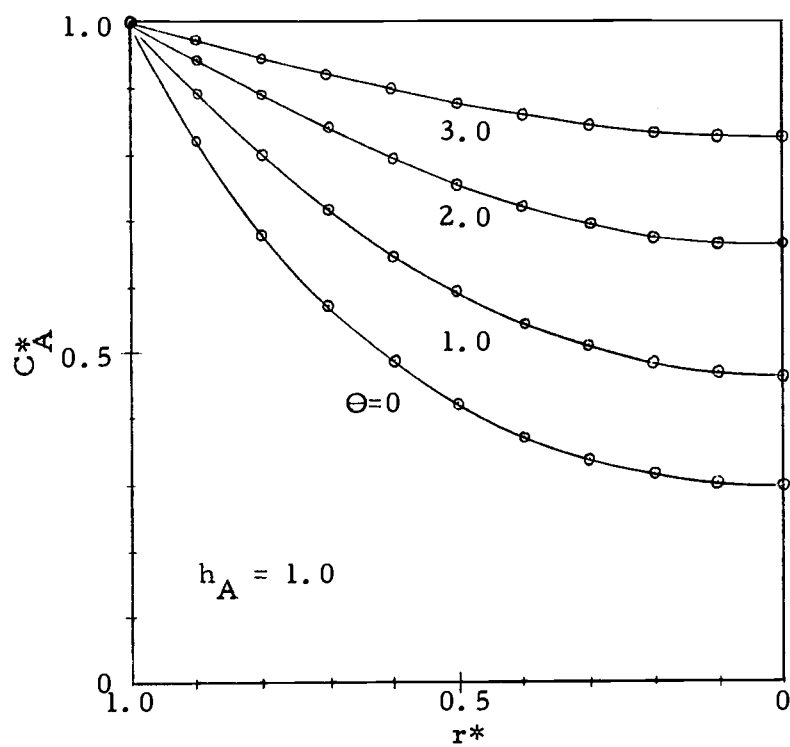


Figure 4. Parallel deactivation, C_A^* vs. r^* .

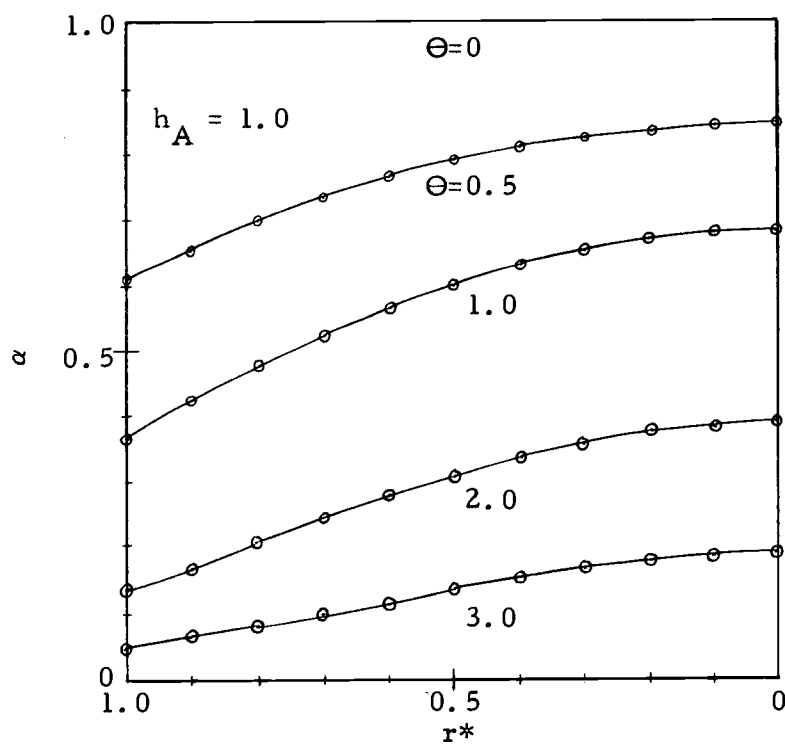


Figure 5. Parallel deactivation, α vs. r^* .

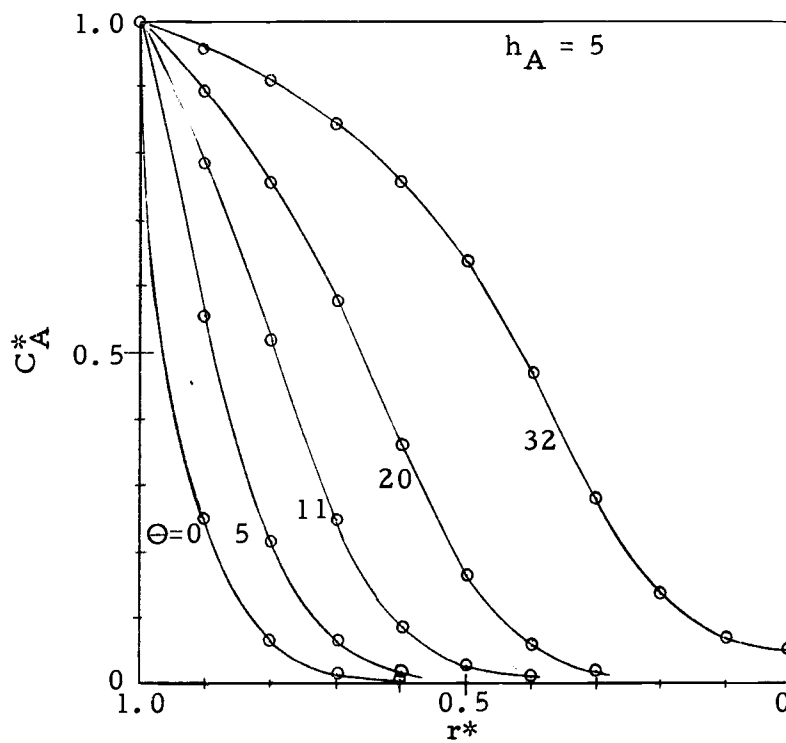


Figure 6. Parallel deactivation, C_A^* vs r^* .

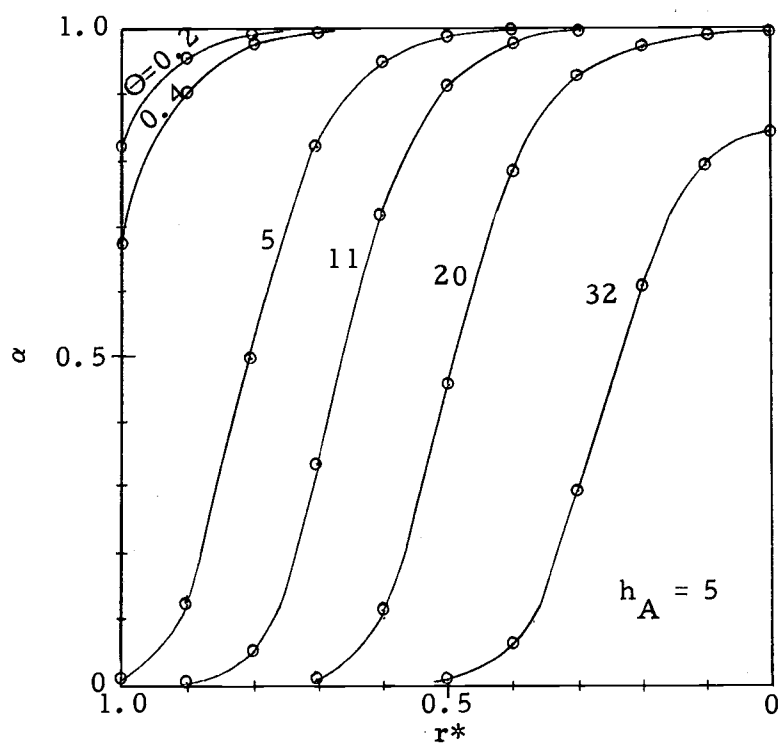


Figure 7. Parallel deactivation, α vs r^* .

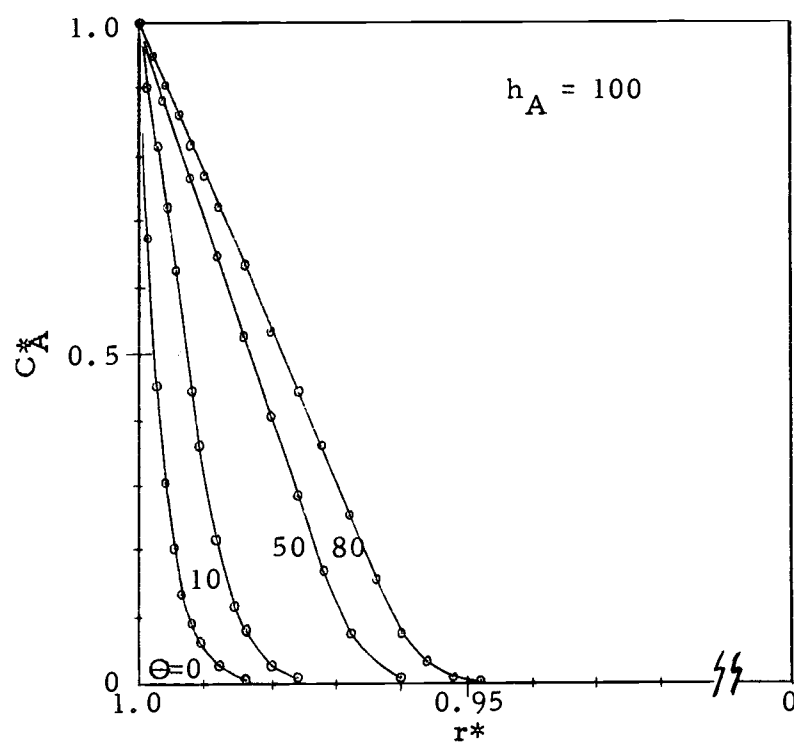


Figure 8. Parallel deactivation, C_A^* vs r^*

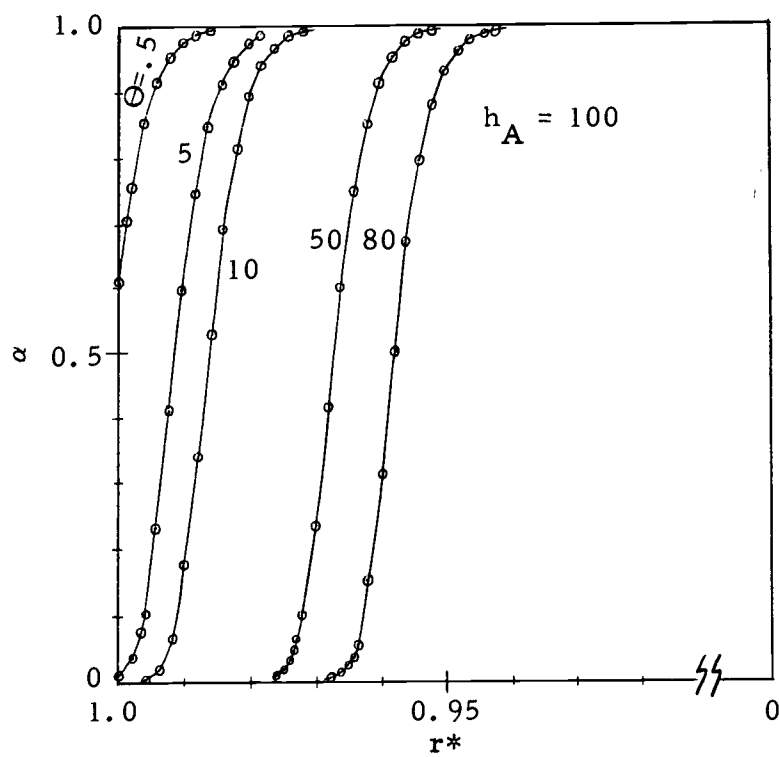


Figure 9. Parallel deactivation, α vs r^* .

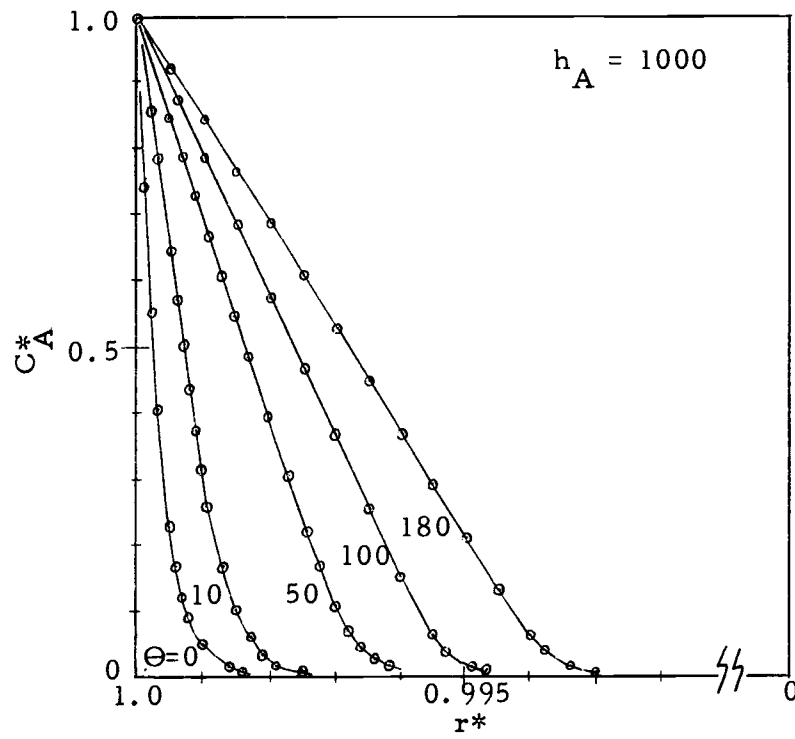


Figure 10. Parallel deactivation, C_A^* vs r^*

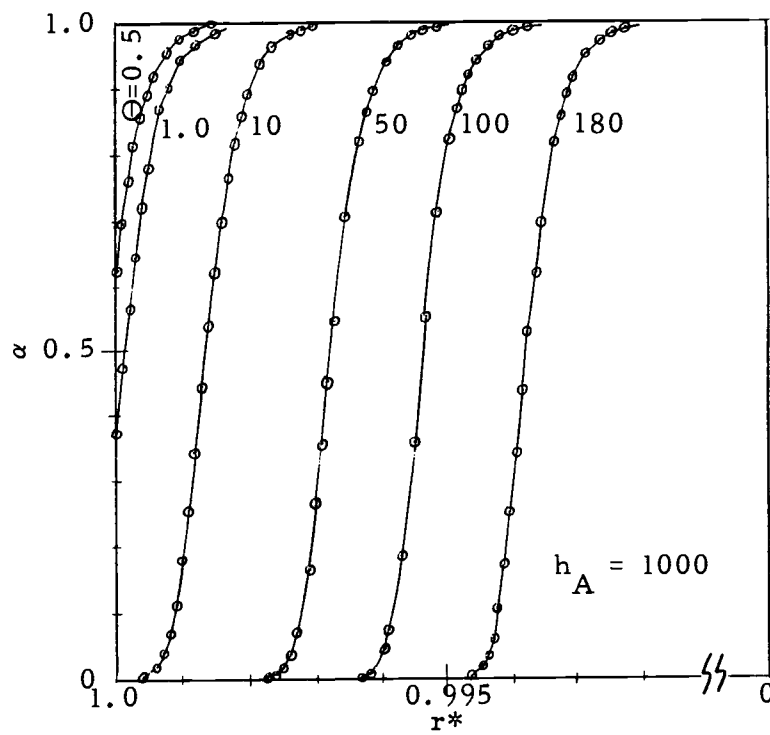


Figure 11. Parallel deactivation, α vs. r^* .

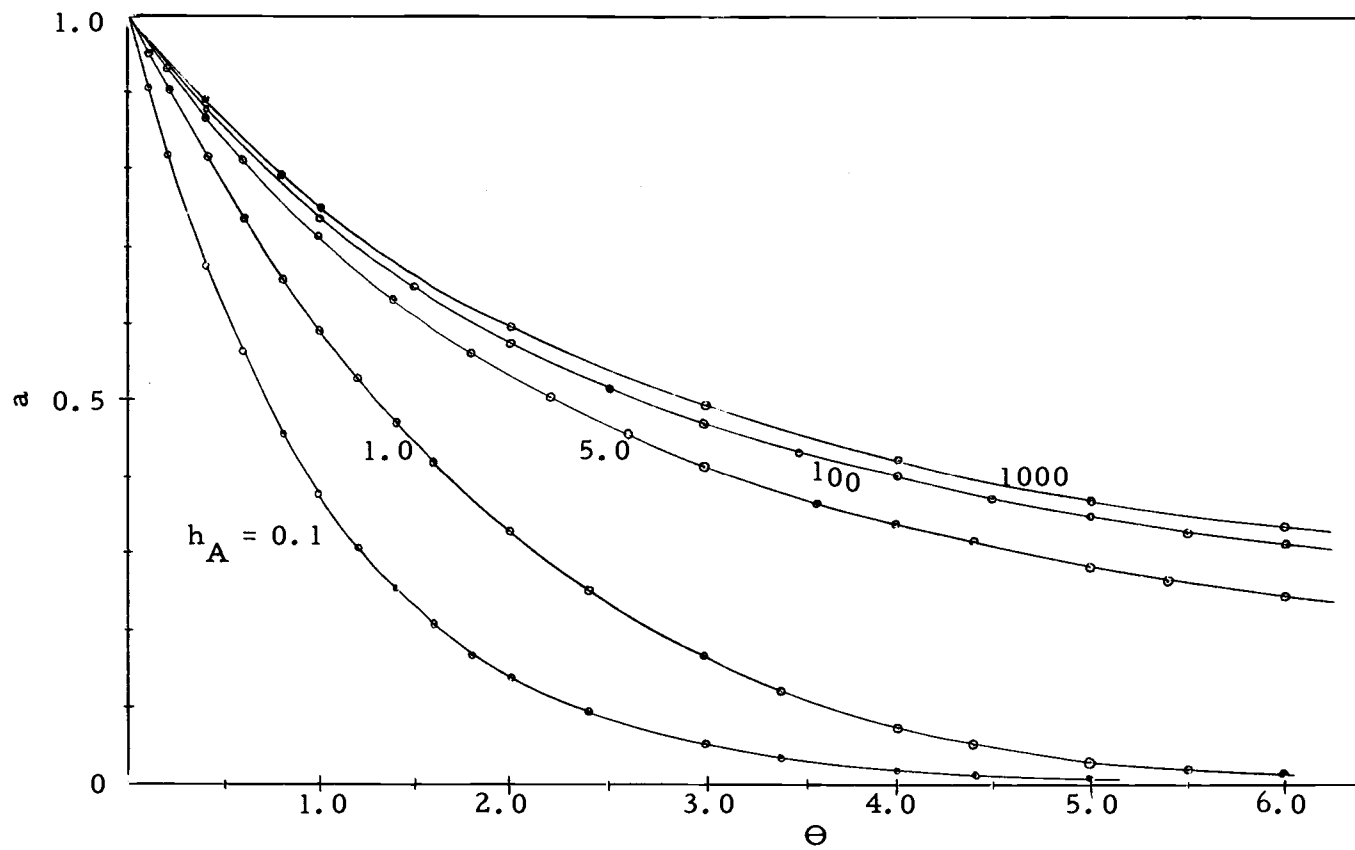


Figure 12. Parallel deactivation, a vs Θ .

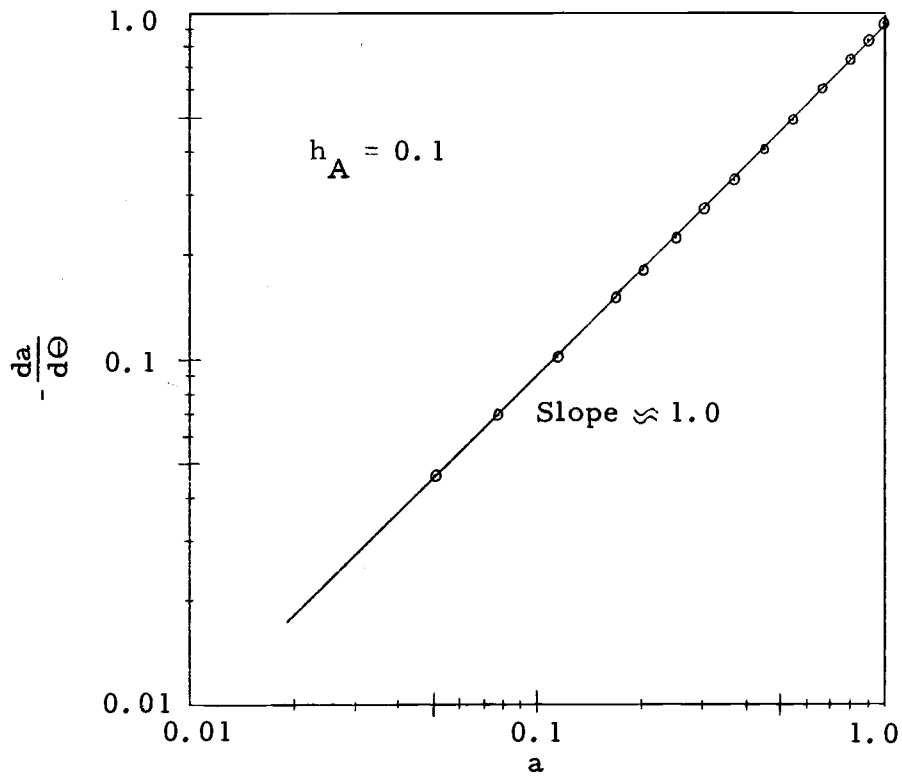


Figure 13. Parallel deactivation, $-\frac{da}{d\Theta}$ vs. a .

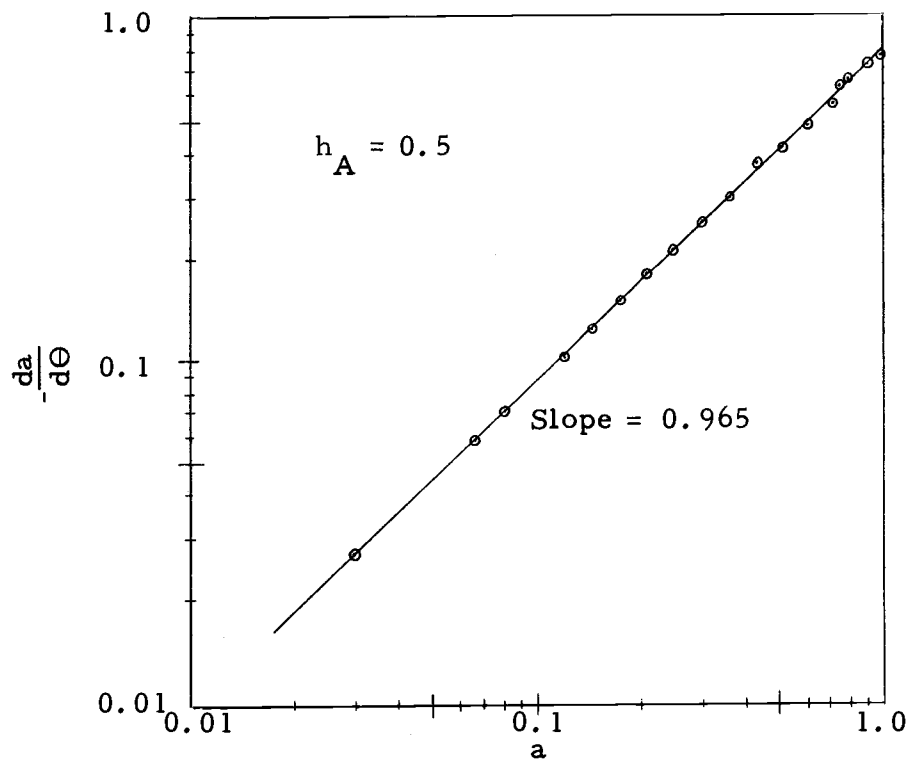


Figure 14. Parallel deactivation, $-\frac{da}{d\Theta}$ vs. a .

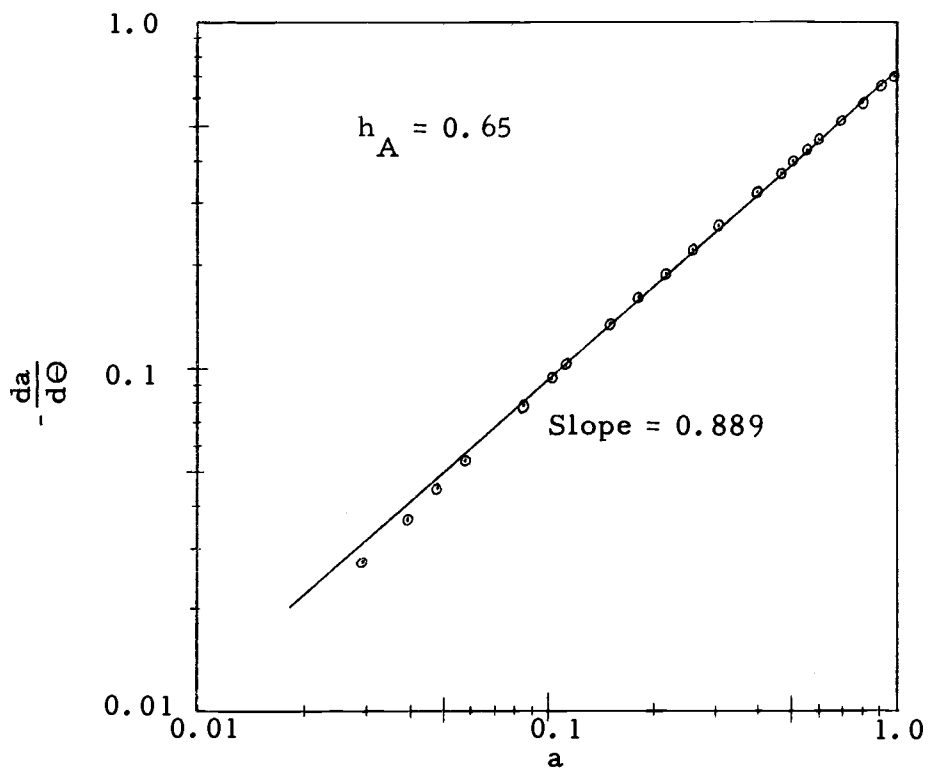


Figure 15. Parallel deactivation, $-\frac{da}{d\Theta}$ vs. a .

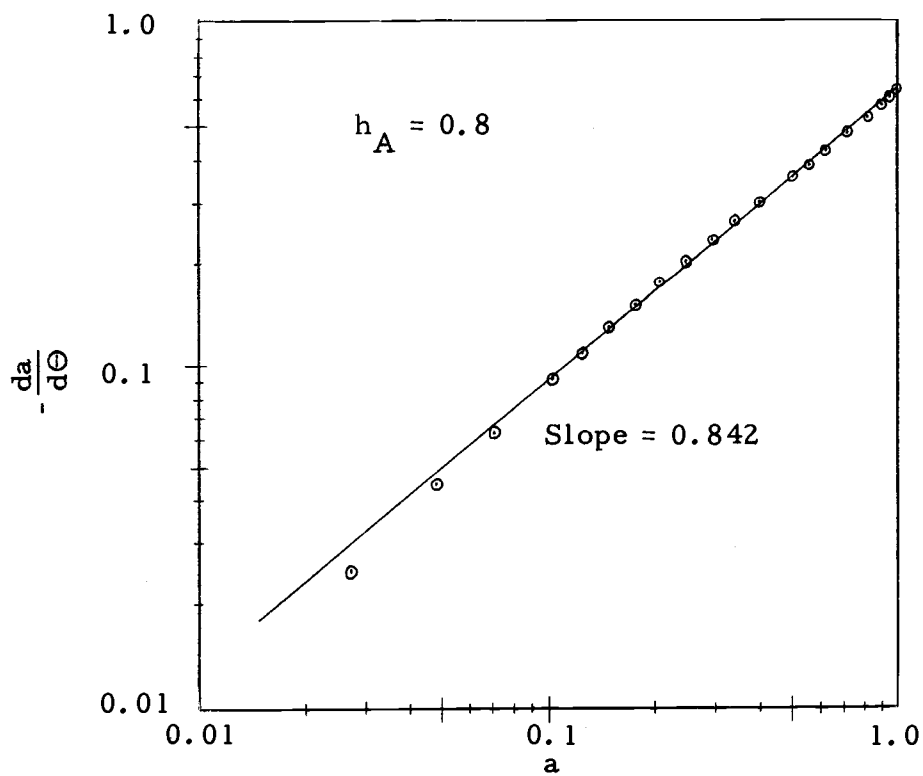


Figure 16. Parallel deactivation, $-\frac{da}{d\Theta}$ vs. a .

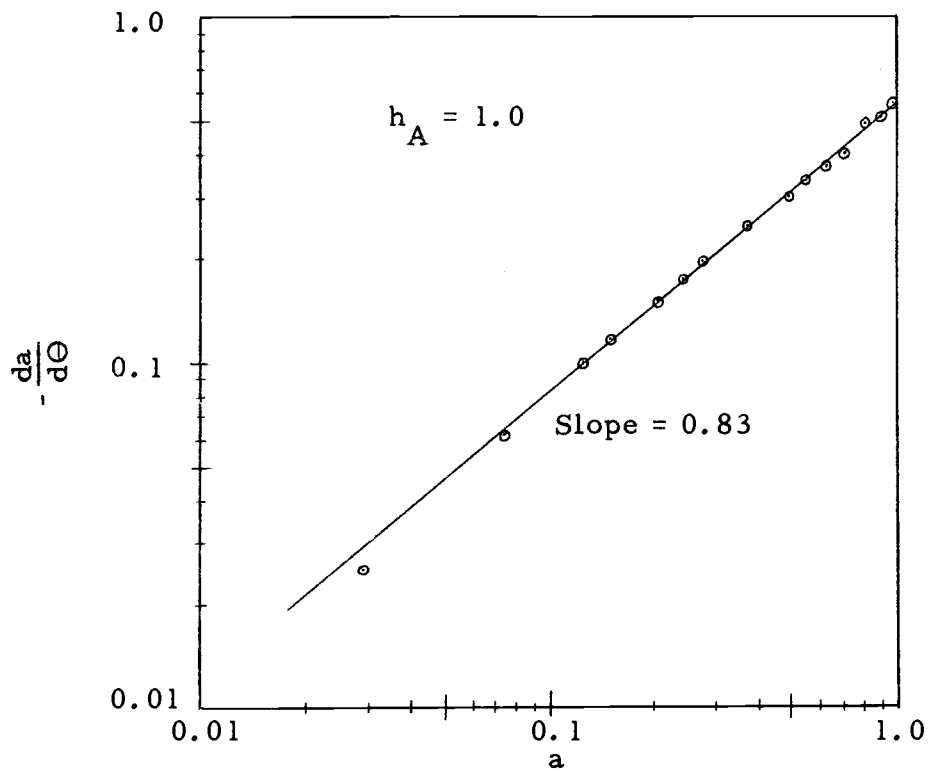


Figure 17. Parallel deactivation, $-\frac{da}{d\Theta}$ vs. a .

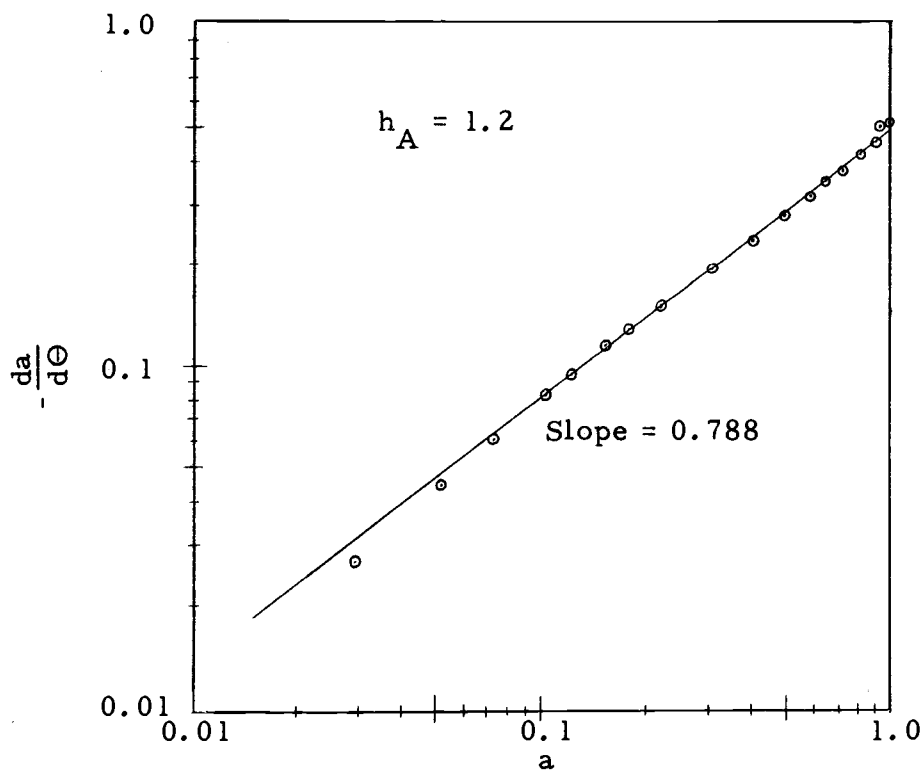


Figure 18. Parallel deactivation, $-\frac{da}{d\Theta}$ vs. a .

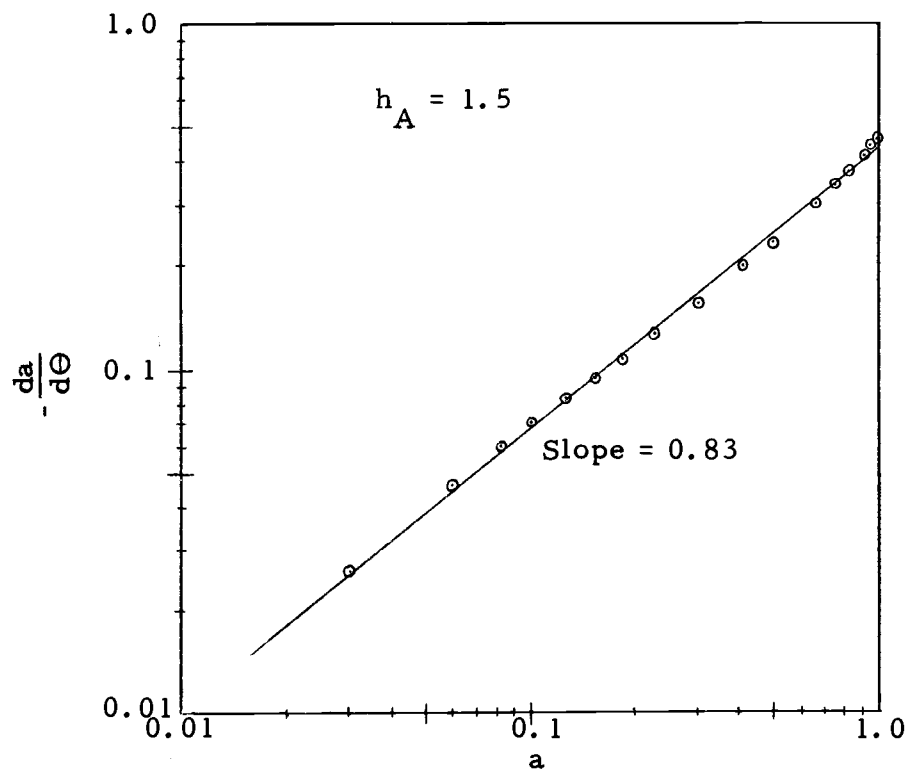


Figure 19. Parallel deactivation, $-\frac{da}{d\Theta}$ vs. a .

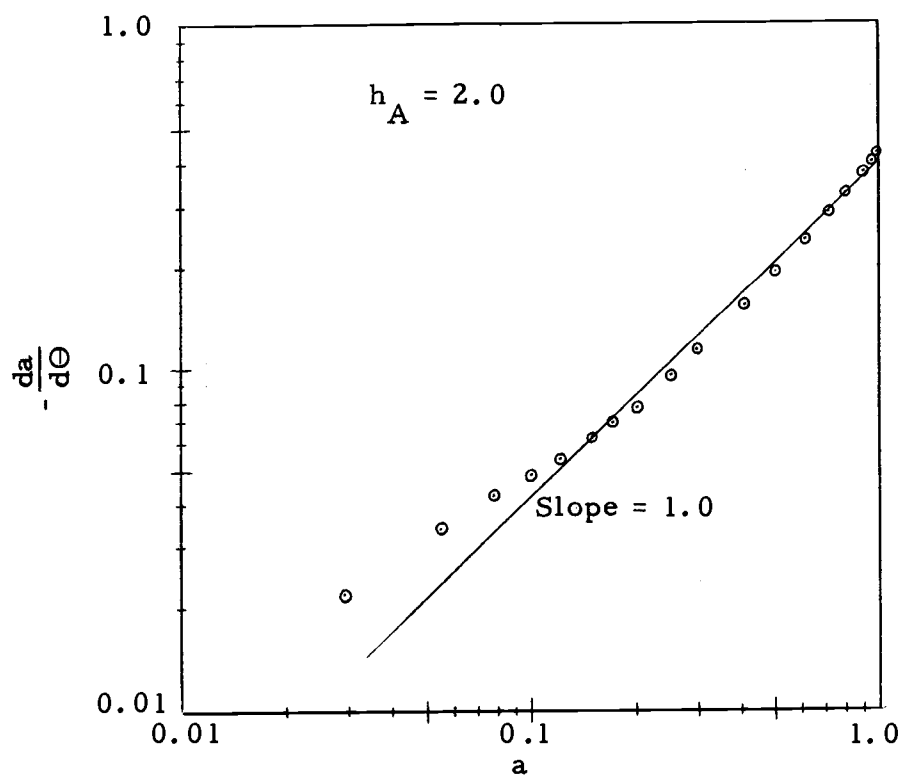


Figure 20. Parallel deactivation, $-\frac{da}{d\Theta}$ vs. a .

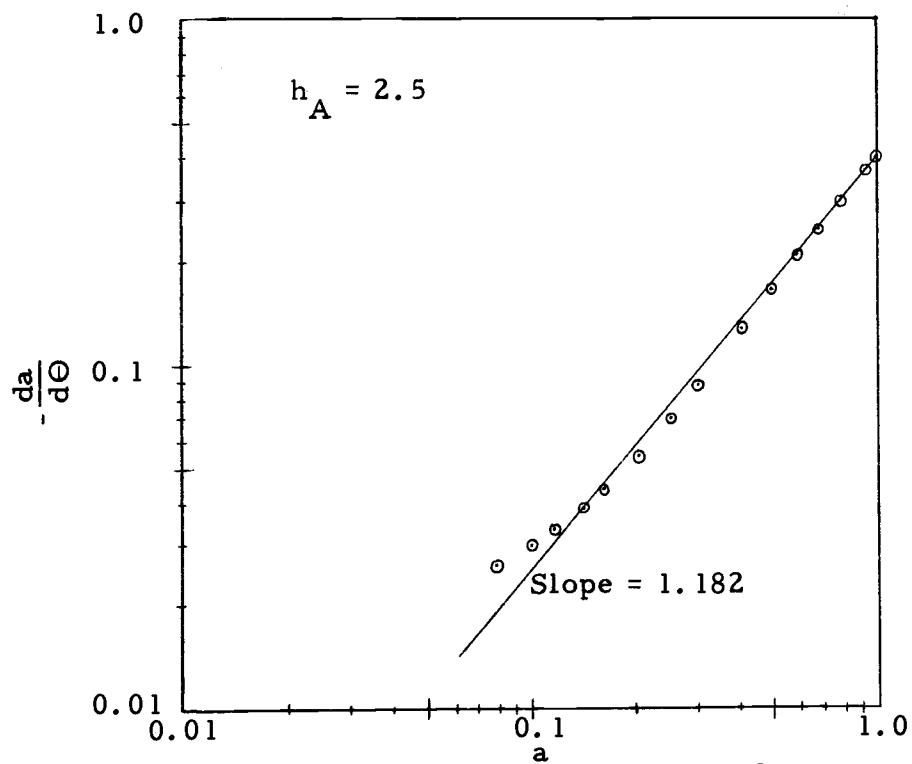


Figure 21. Parallel deactivation, $-\frac{da}{d\Theta}$ vs. a .

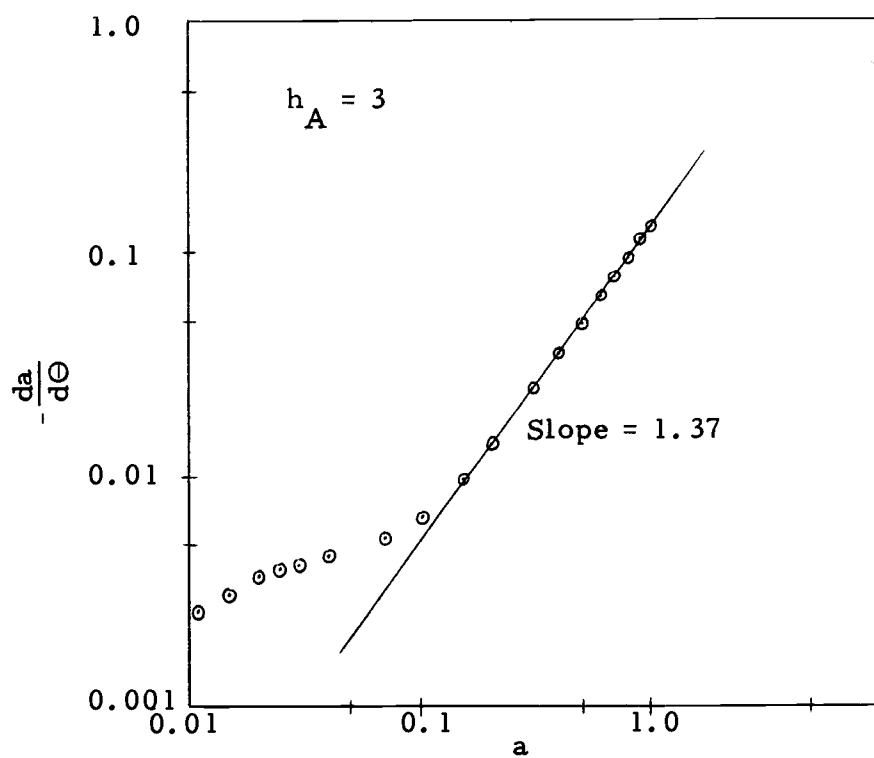


Figure 22. Parallel deactivation, $-\frac{da}{d\Theta}$ vs. a .

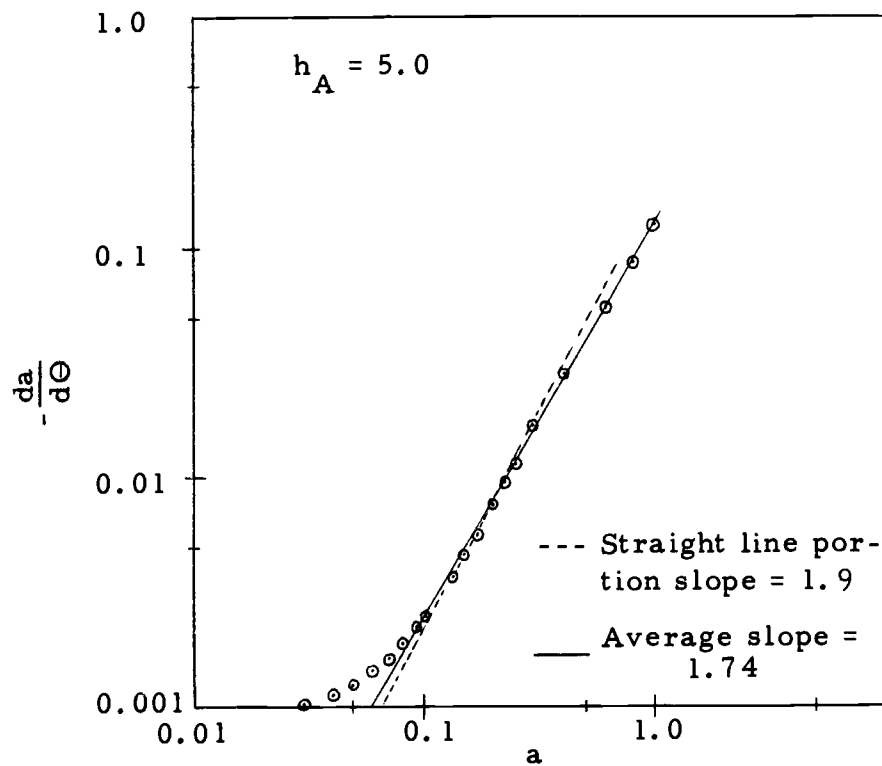


Figure 23. Parallel deactivation, $-\frac{da}{d\Theta}$ vs. a .

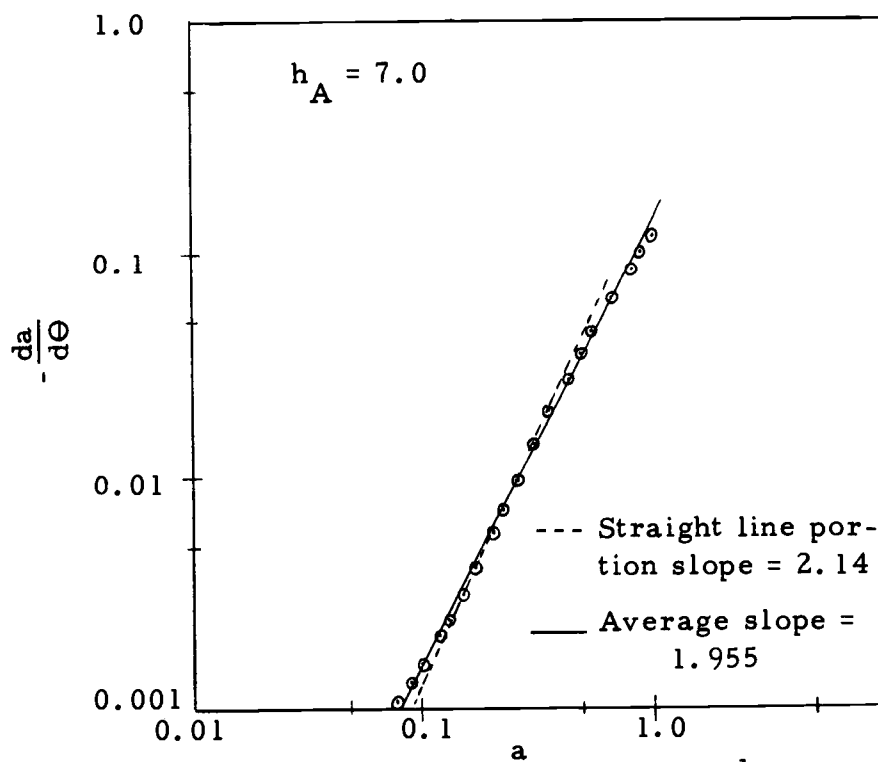


Figure 24. Parallel deactivation, $-\frac{da}{d\Theta}$ vs. a .

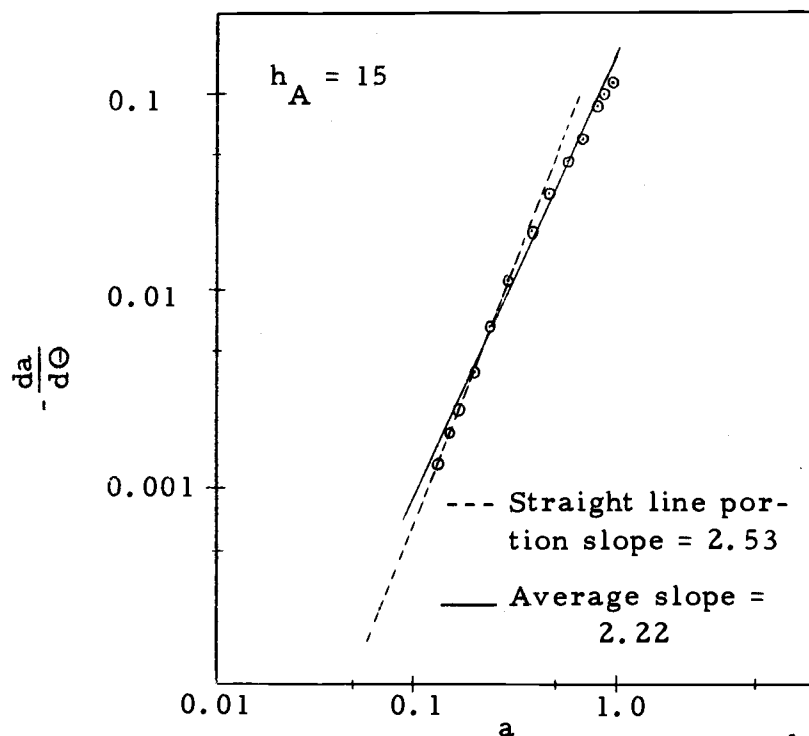


Figure 25. Parallel deactivation, $-\frac{da}{d\Theta}$ vs. a .

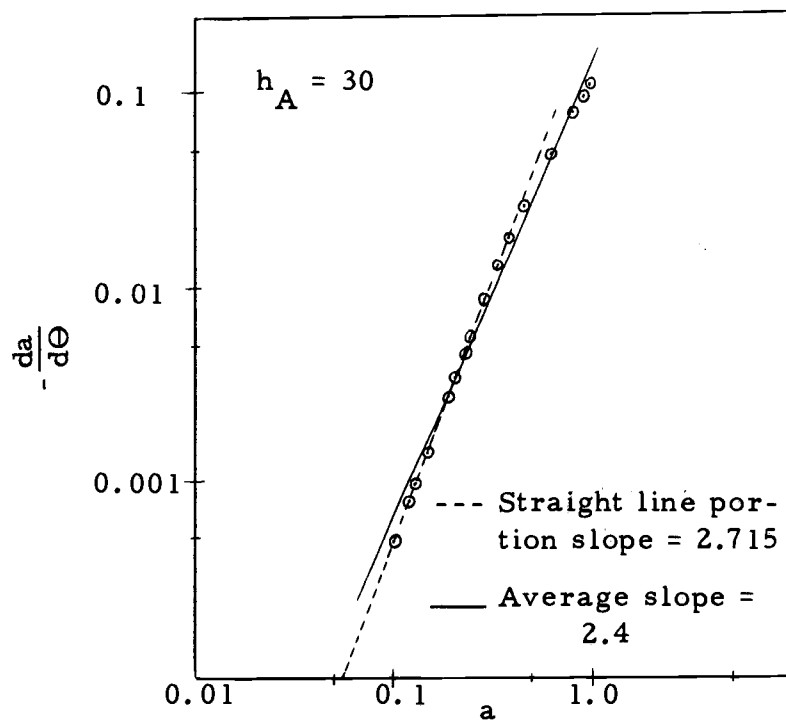


Figure 26. Parallel deactivation, $-\frac{da}{d\Theta}$ vs. a .

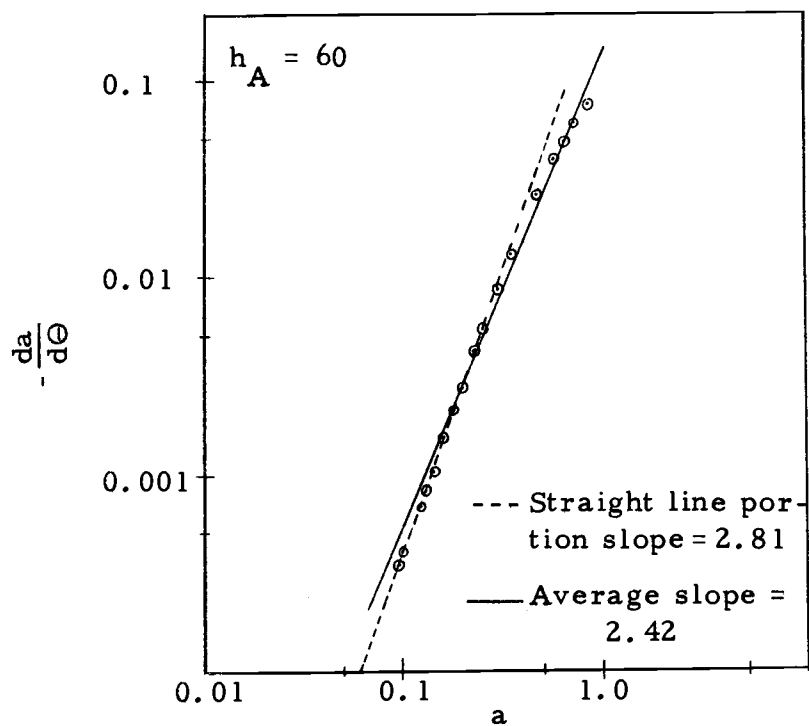


Figure 27. Parallel deactivation, $-\frac{da}{d\Theta}$ vs. a .

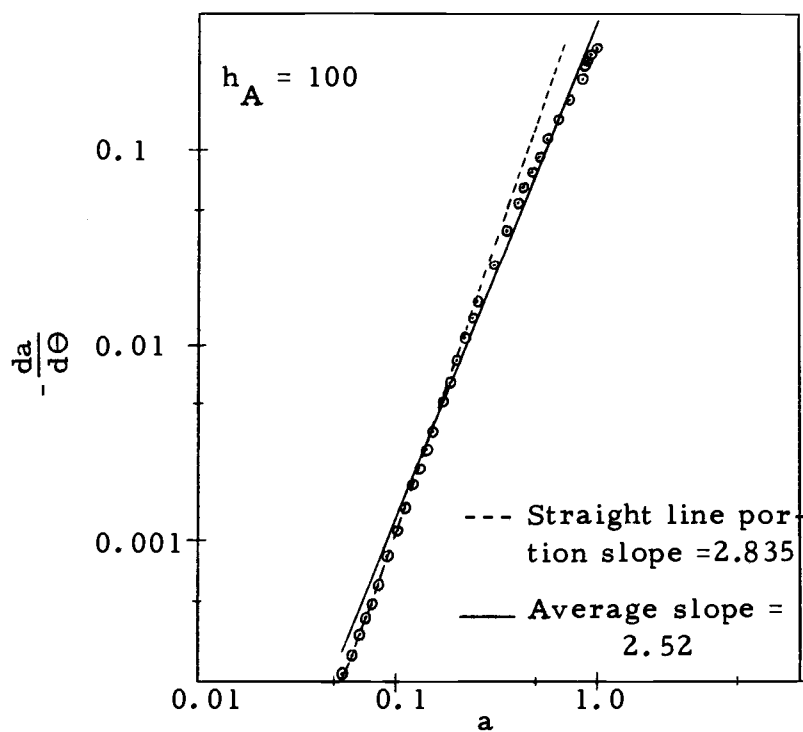


Figure 28. Parallel deactivation, $-\frac{da}{d\Theta}$ vs. a .

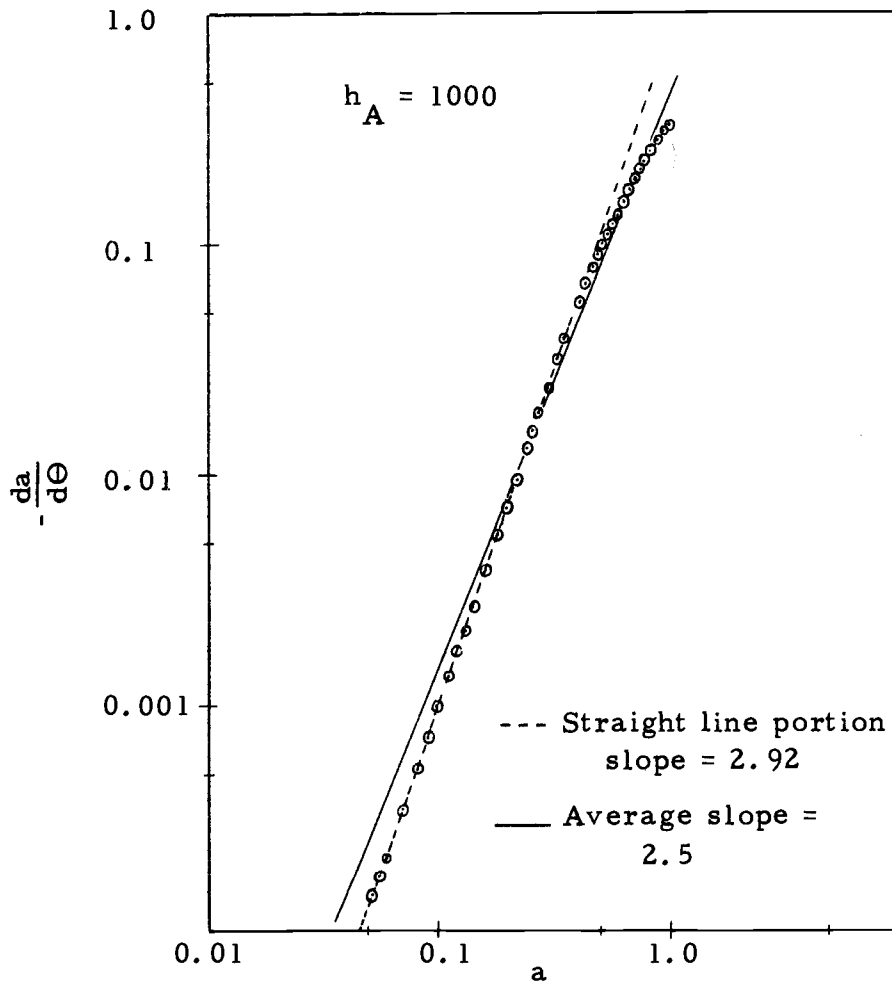


Figure 29. Parallel deactivation, $-\frac{da}{d\Theta}$ vs. a .

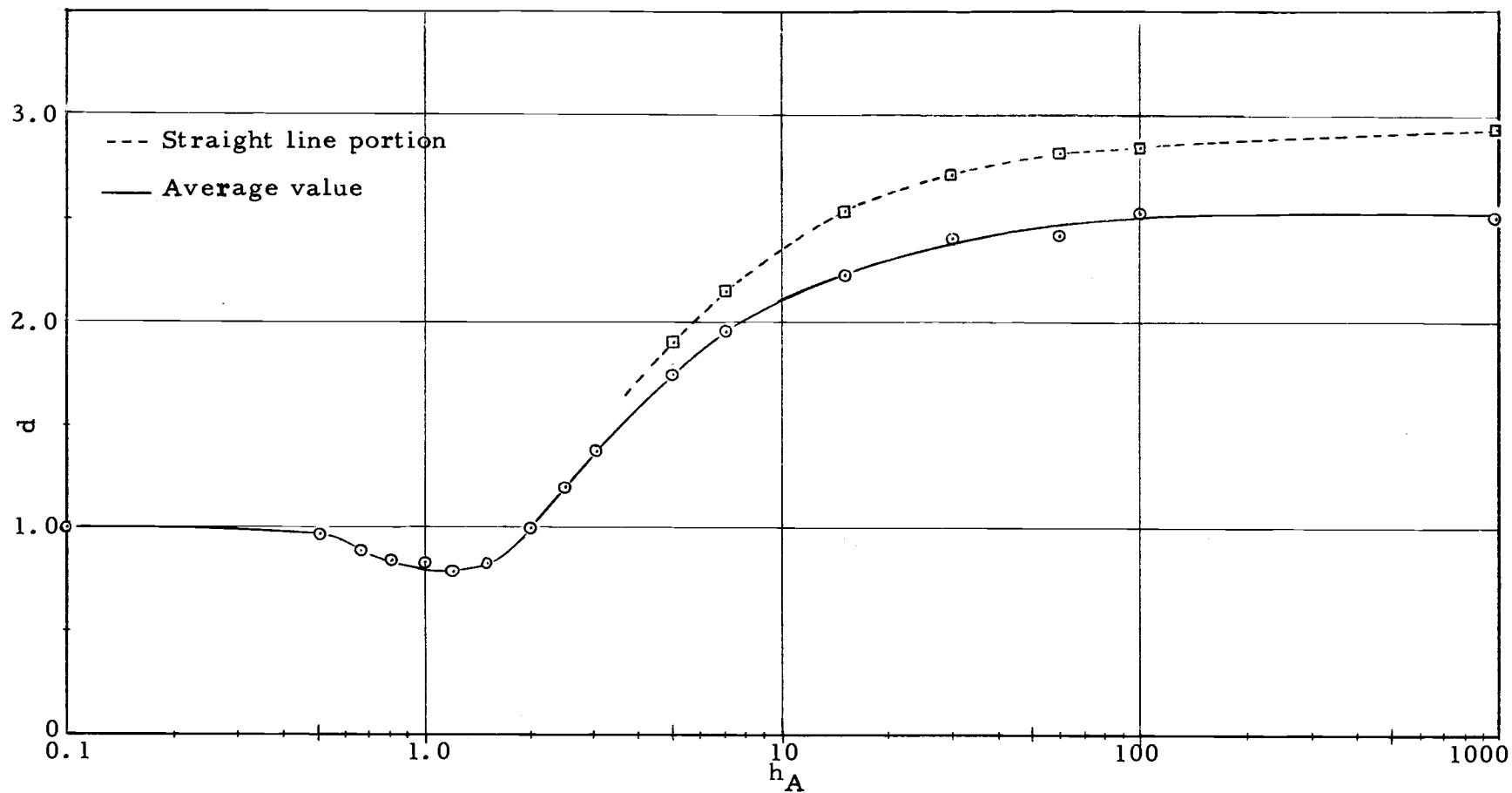


Figure 30. Parallel deactivation, d vs h_A .

Discussion

Figure 30 summarizes the results of this analysis. Let us examine the various regimes in this plot.

For the extreme of rapid diffusion with respect to reaction and deactivation, the Thiele modulus is small ($h_A < 1$) and α vs. r^* curve is horizontal (Figure 3) and the order of deactivation, d , is close to unity (Figure 13).

For slow diffusion with respect to reaction, $h_A > 1$. Here the α vs. r^* curve is S-shaped (Figure 7) and the order of deactivation is somewhat higher than unity.

For the extreme of very fast reaction, $h_A \rightarrow \infty$, and the S-shaped α vs. r^* curve becomes practically vertical and the order of deactivation approaches 3. The curved portion in Figures 25 to 29 represents the initial period of deactivation where the α -profiles have not yet become S-shaped (Figures 9 and 11).

In the intermediate range between a flat and S-shaped α vs. r^* profile (Thiele modulus ≈ 1), the order of deactivation drops to less than unity. This strange behavior is a consequence of the shape of the α vs. r^* curve, as shown in Figure 5.

Side-by-side Deactivation

Partial differential equations and their initial and boundary conditions given in Table 3 can be changed into difference form. The

method of solution is similar to the method given in the previous section. Again, we use Euler's second-order approximation for the time increment. Necessary difference equation and the FORTRAN programs are listed in Appendix IV.

Three typical values of h_A and h_P are selected (0.1, 1.0 and 10.0), and the combination of these gives nine distinct cases. Figures 31 to 42 present the results for the three cases where $h_A = 0.1$. For each of the three h_P values, C_A^* , C_P^* and α are given as a function of radial position and time in Figures 31 to 38. The plot of activity vs. time is given in Figure 39. To test the validity of Equation (5a), plots of $-\frac{da}{d\theta}$ vs. \underline{a} are made (Figures 40 to 42).

For other values of h_A , 1.0 and 10.0, the corresponding graphs are presented in the same order (Figures 43 to 65).

Discussion

When $h_A = h_P$, the equations of side-by-side deactivation reduce to the parallel deactivation case which has already been solved in the previous section. Thus, Figures 31, 32, 40, 46, 47 and 53 turn out to be the same as Figures 2, 3, 13, 4, 5 and 17, respectively.

If the Thiele modulus for poison is small ($h_P < 1$), the plot of $-\frac{da}{d\theta}$ vs. \underline{a} is acceptable as a straight line and the order of deactivation, \underline{d} , approaches unity as h_P goes to zero (Figures 40, 41, 52,

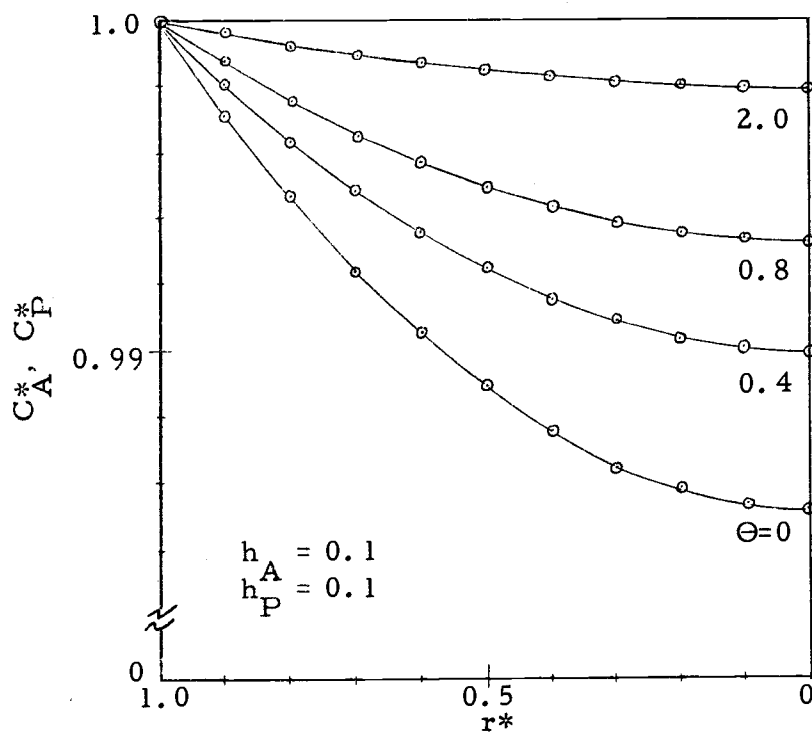


Figure 31. Side-by-side deactivation, C_A^*, C_P^* vs. r^* .

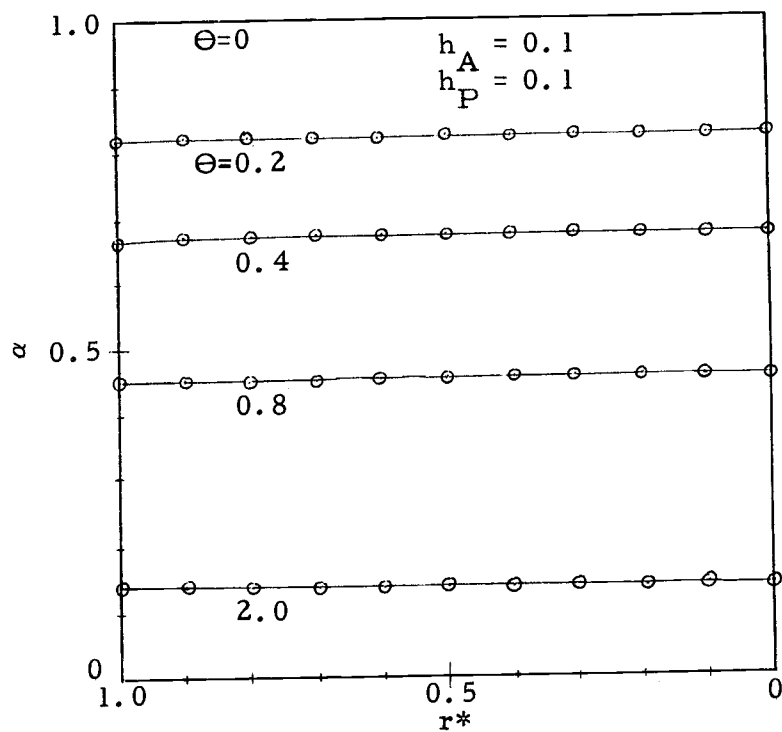


Figure 32. Side-by-side deactivation, α vs. r^* .

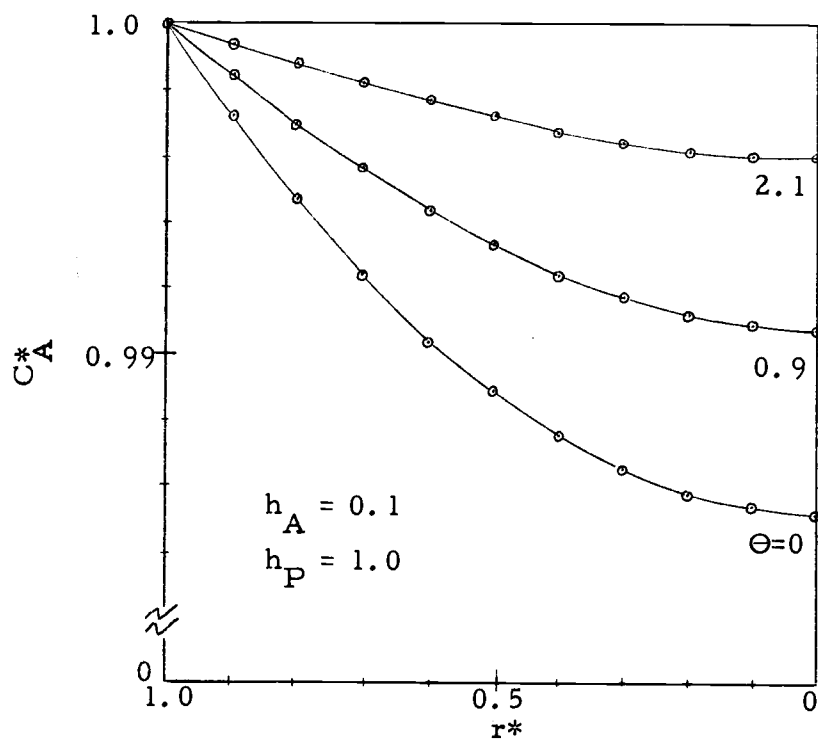


Figure 33. Side-by-side deactivation, C_A^* vs. r^* .

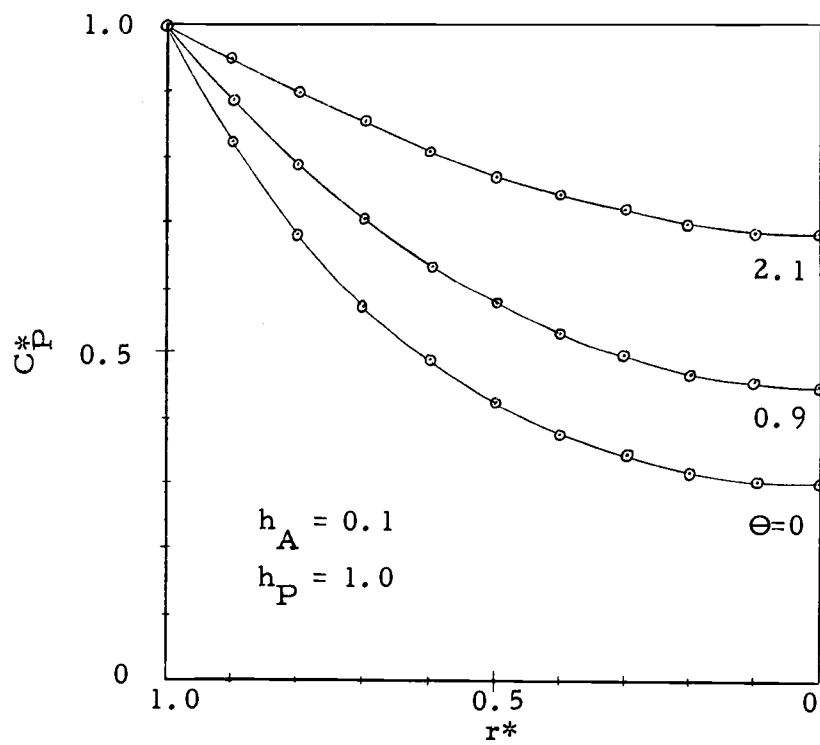


Figure 34. Side-by-side deactivation, C_P^* vs. r^* .

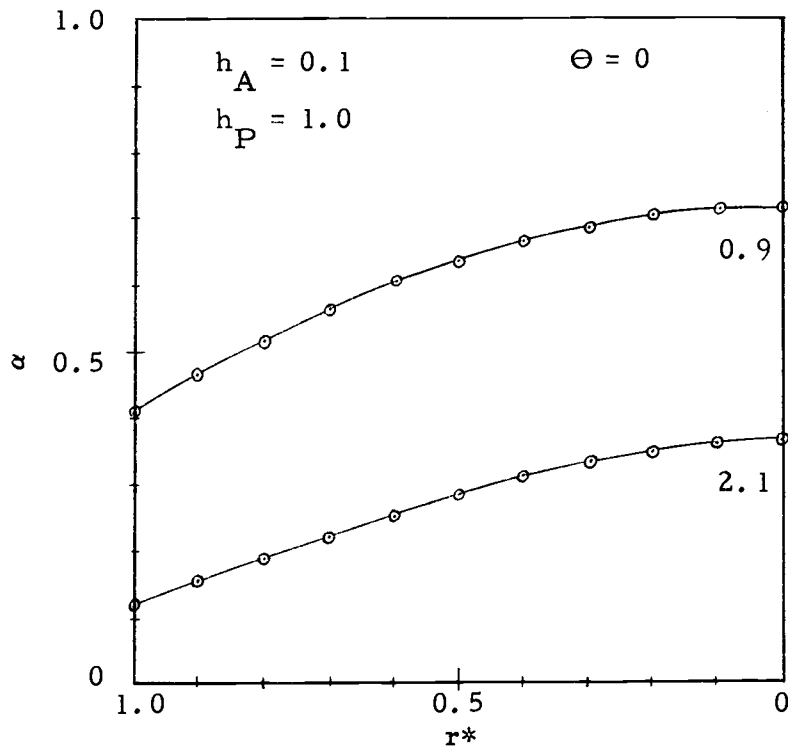


Figure 35. Side-by-side deactivation, α vs. r^* .

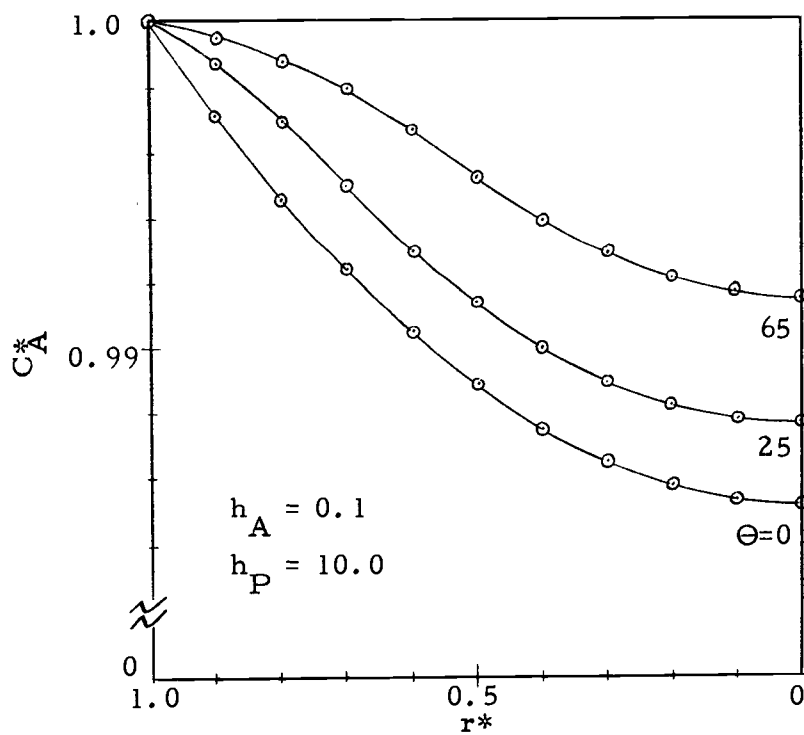


Figure 36. Side-by-side deactivation, C_A^* vs. r^* .

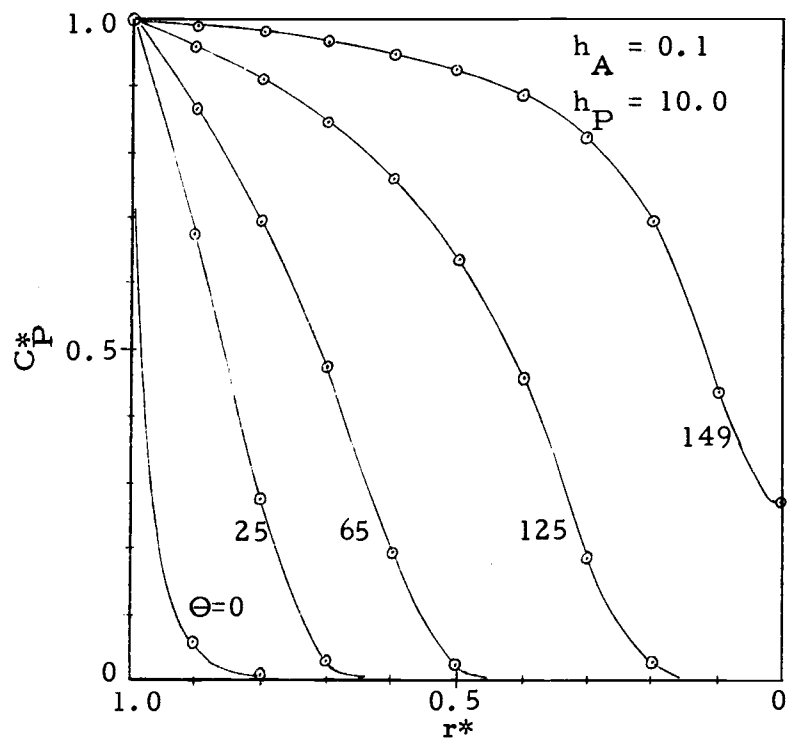


Figure 37. Side-by-side deactivation, C^*_P vs. r^* .

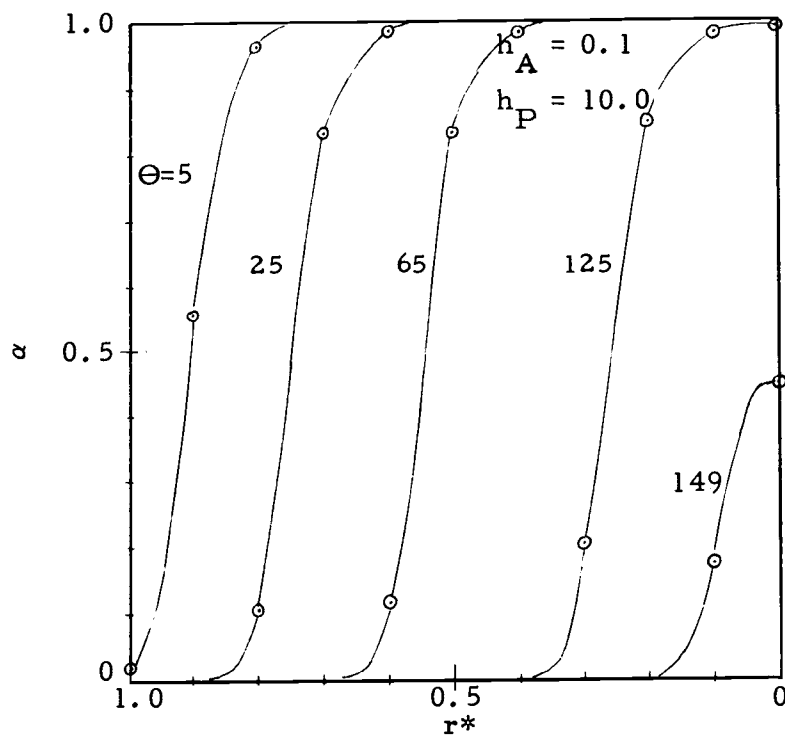


Figure 38. Side-by-side deactivation, α vs. r^* .

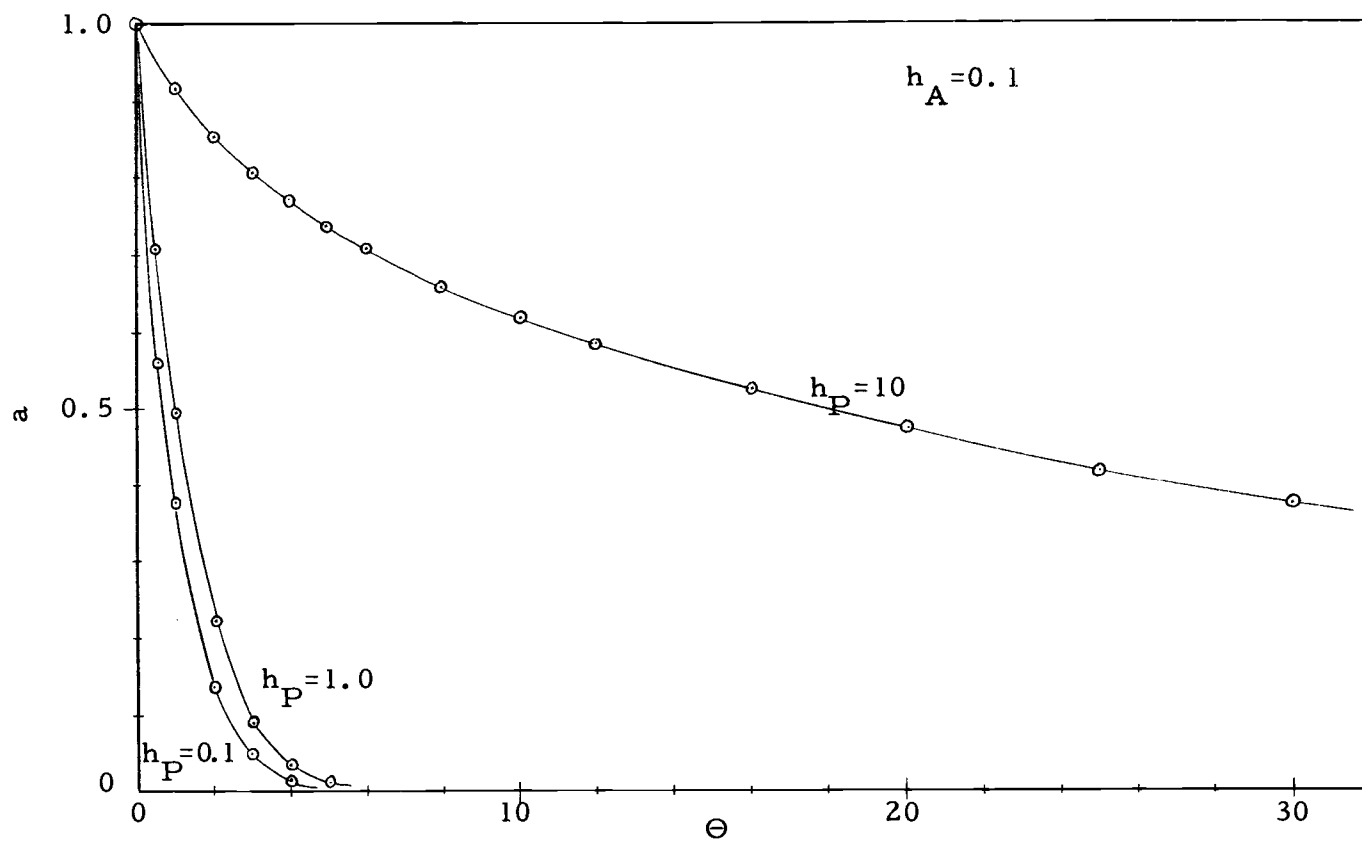


Figure 39. Side-by-side deactivation, a vs. Θ .

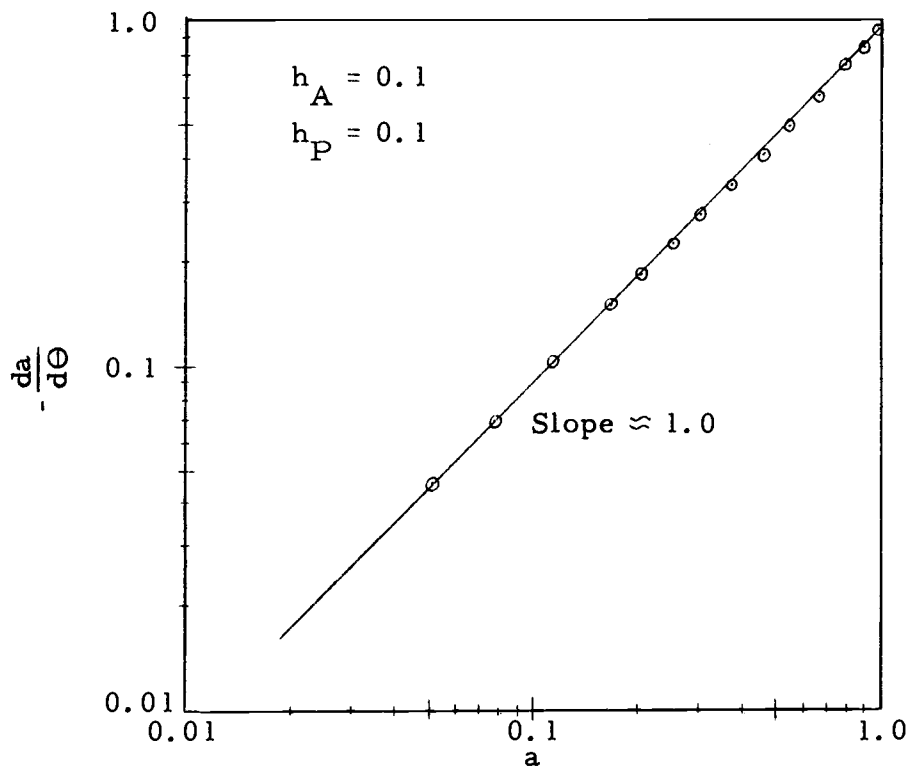


Figure 40. Side-by-side deactivation, $-\frac{da}{d\Theta}$ vs. a .

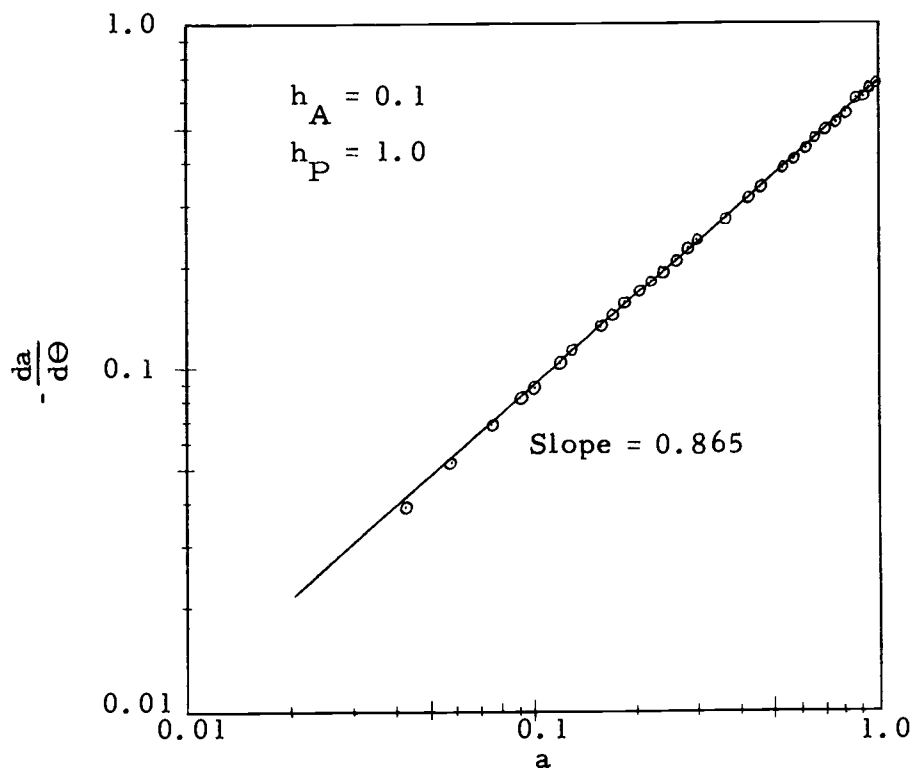


Figure 41. Side-by-side deactivation, $-\frac{da}{d\Theta}$ vs. a .

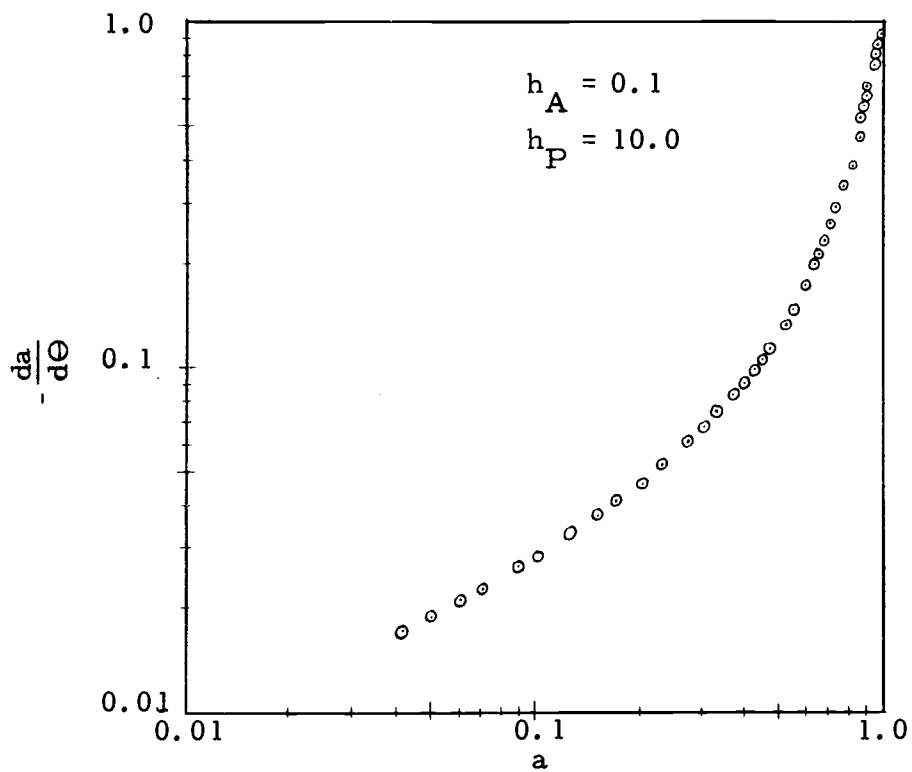


Figure 42. Side-by-side deactivation, $-\frac{da}{d\Theta}$ vs. a .

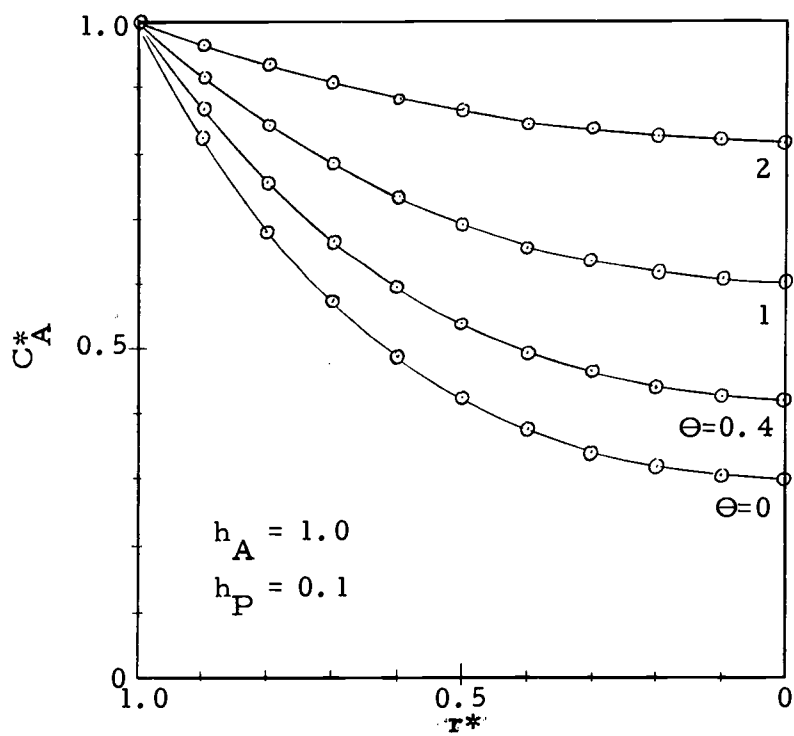


Figure 43. Side-by-side deactivation, C_A^* vs. r^* .

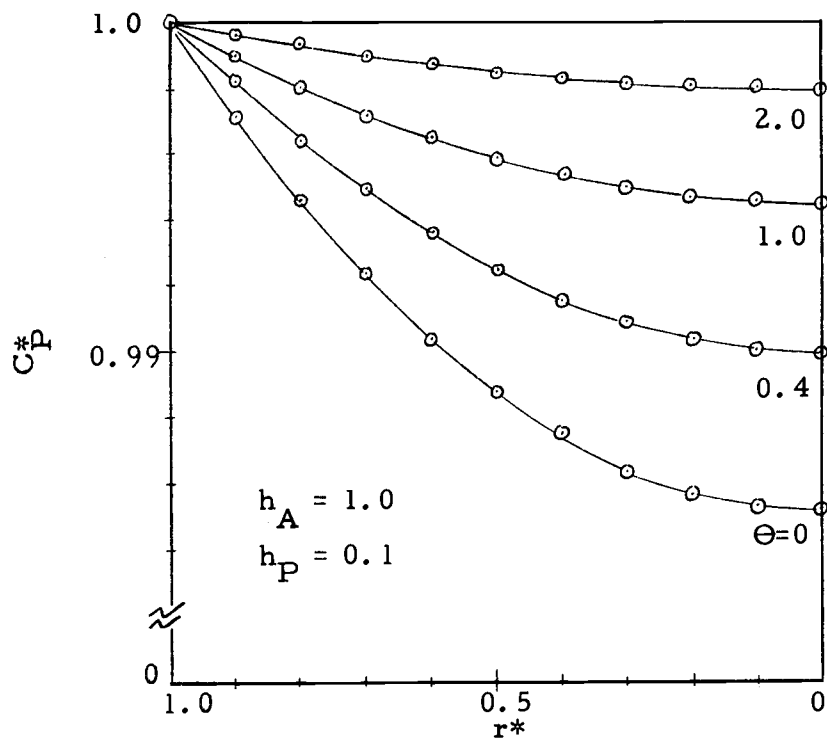


Figure 44. Side-by-side deactivation, C^*_P vs r^* .

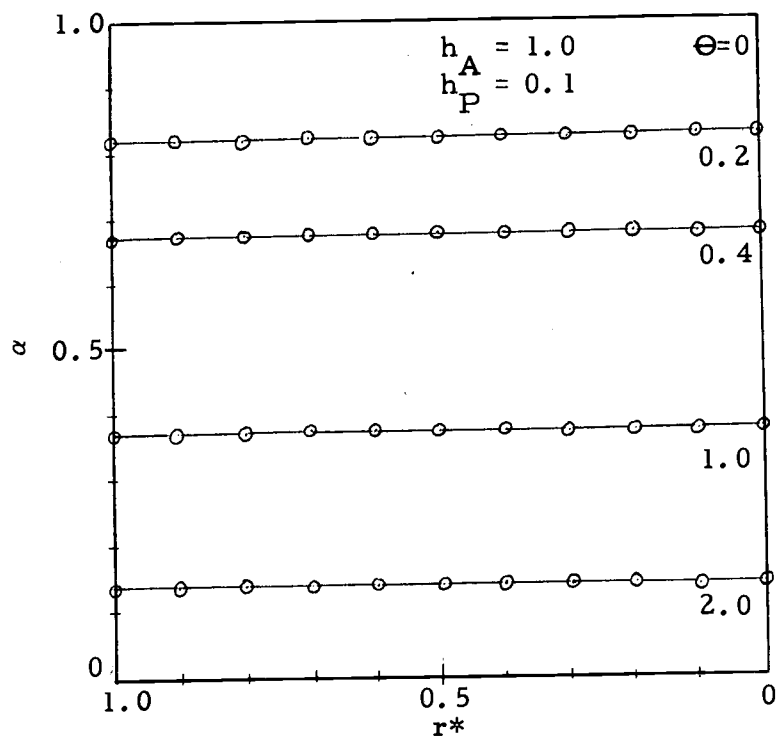


Figure 45. Side-by-side deactivation, α vs r^* .

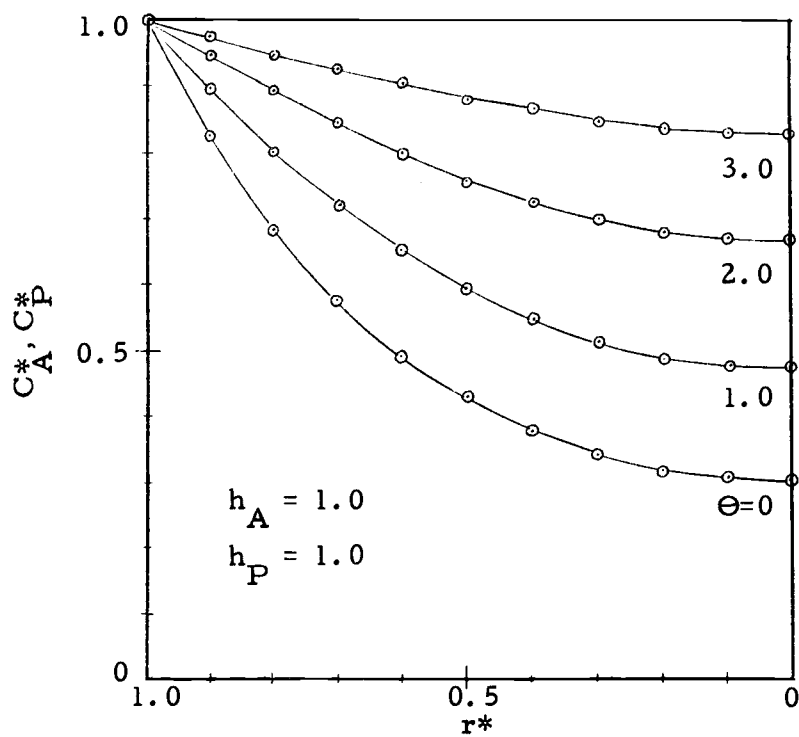


Figure 46. Side-by-side deactivation, C_A^* , C_P^* vs r^* .

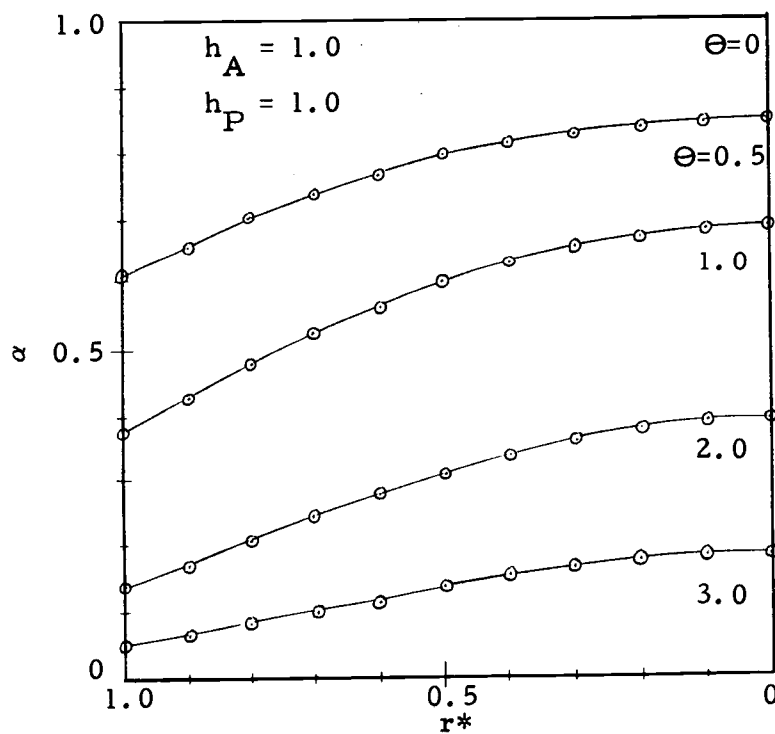


Figure 47. Side-by-side deactivation, α vs r^* .

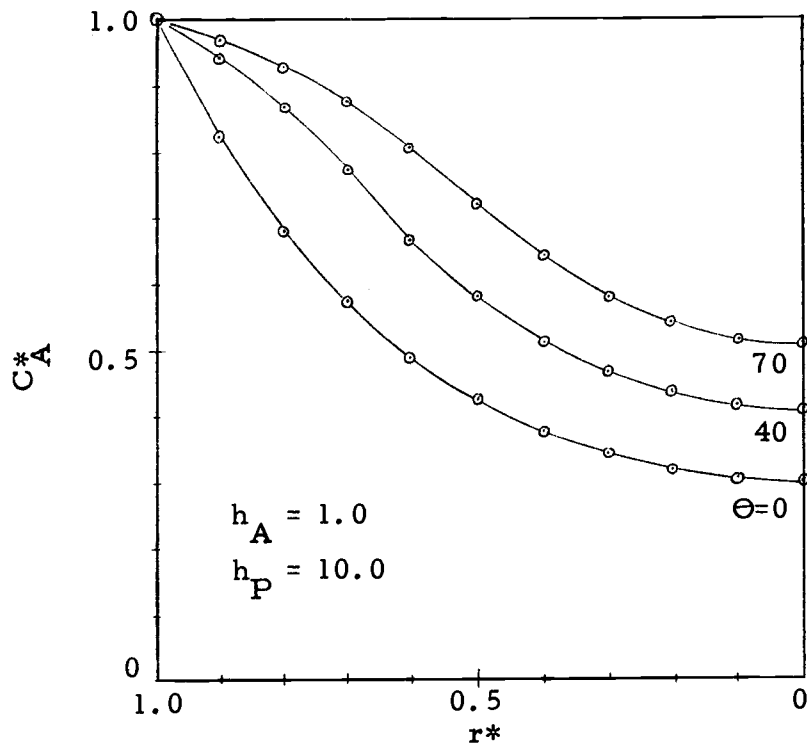


Figure 48. Side-by-side deactivation, C_A^* vs r^* .

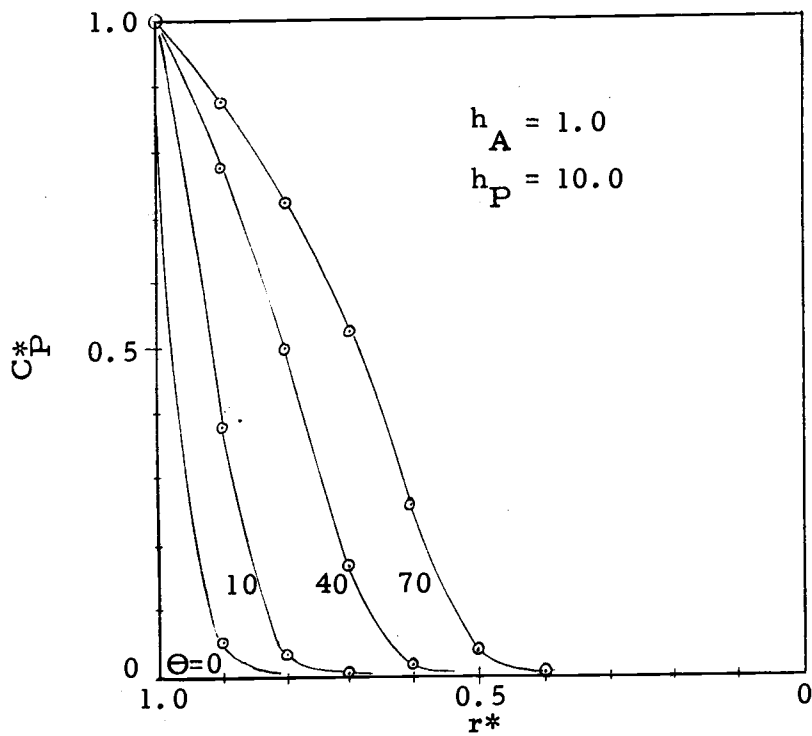


Figure 49. Side-by-side deactivation, C_P^* vs r^* .

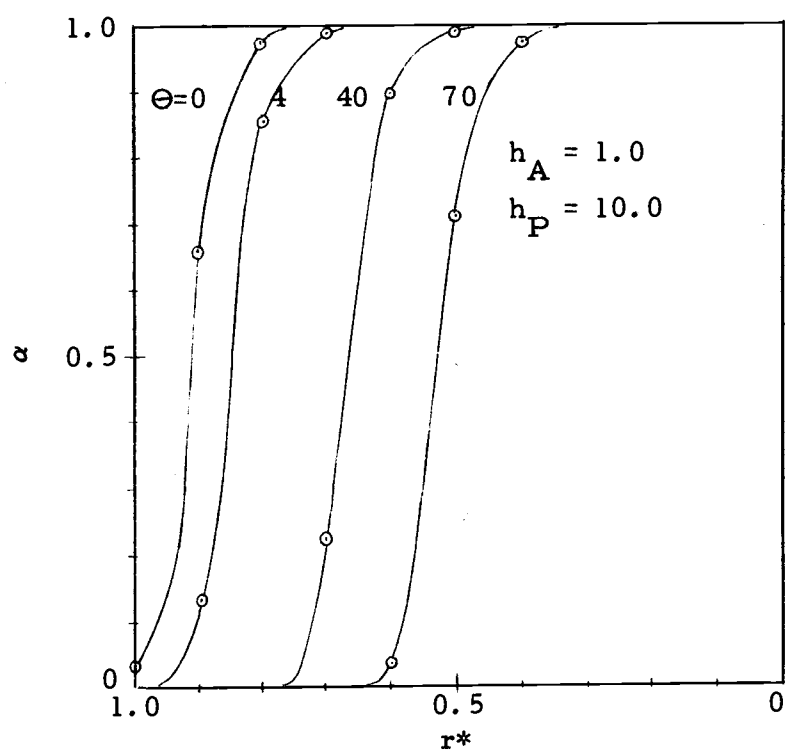


Figure 50. Side-by-side deactivation, α vs r^* .

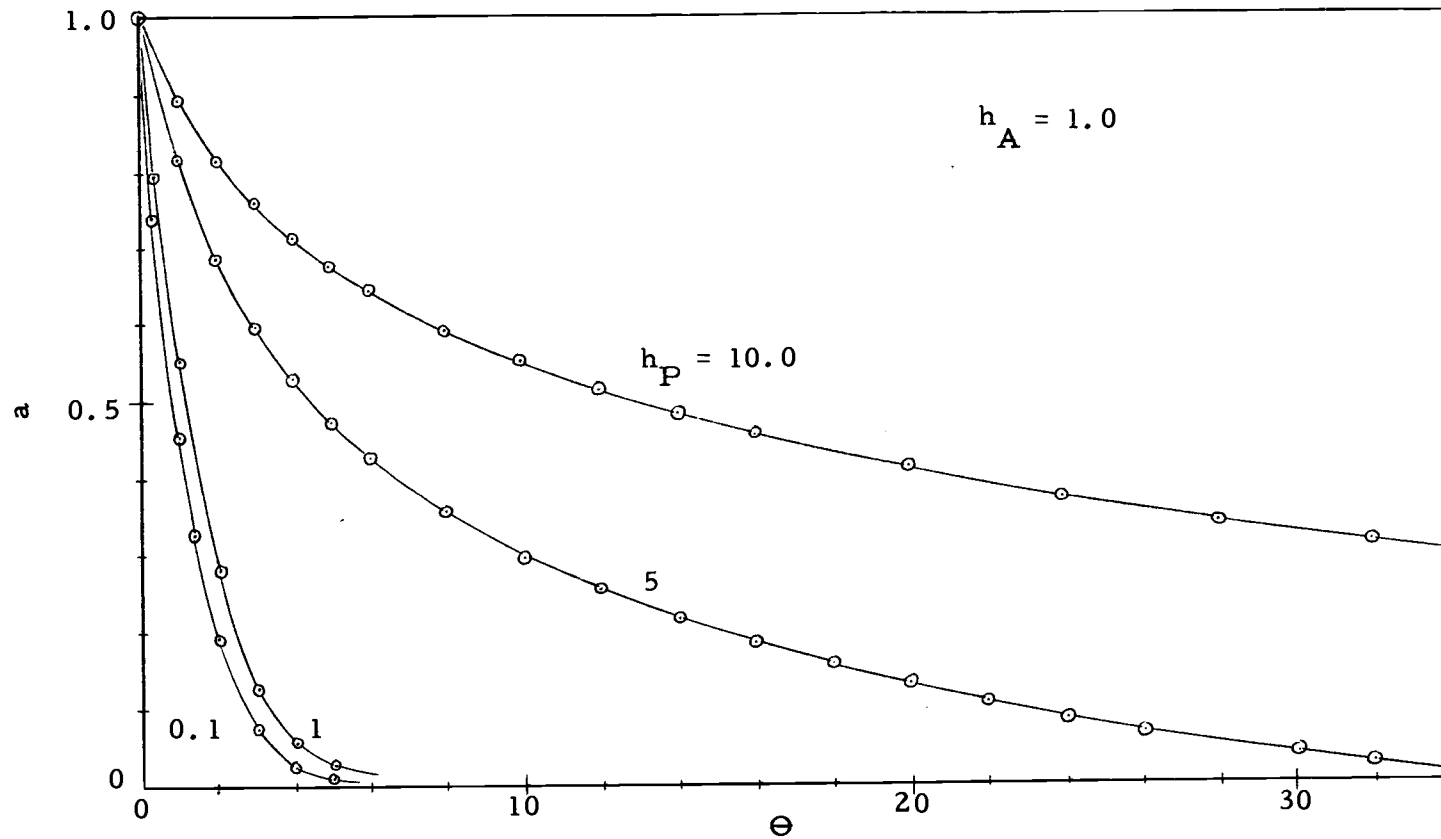


Figure 51. Side-by-side deactivation, a vs Θ .

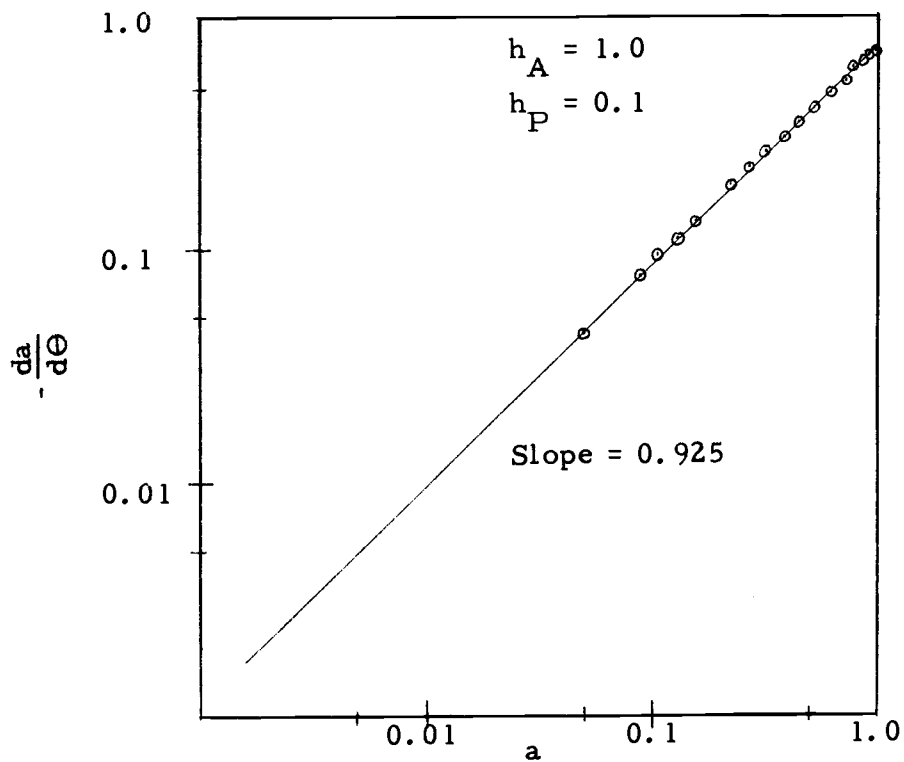


Figure 52. Side-by-side deactivation, $-\frac{da}{d\Theta}$ vs. a .

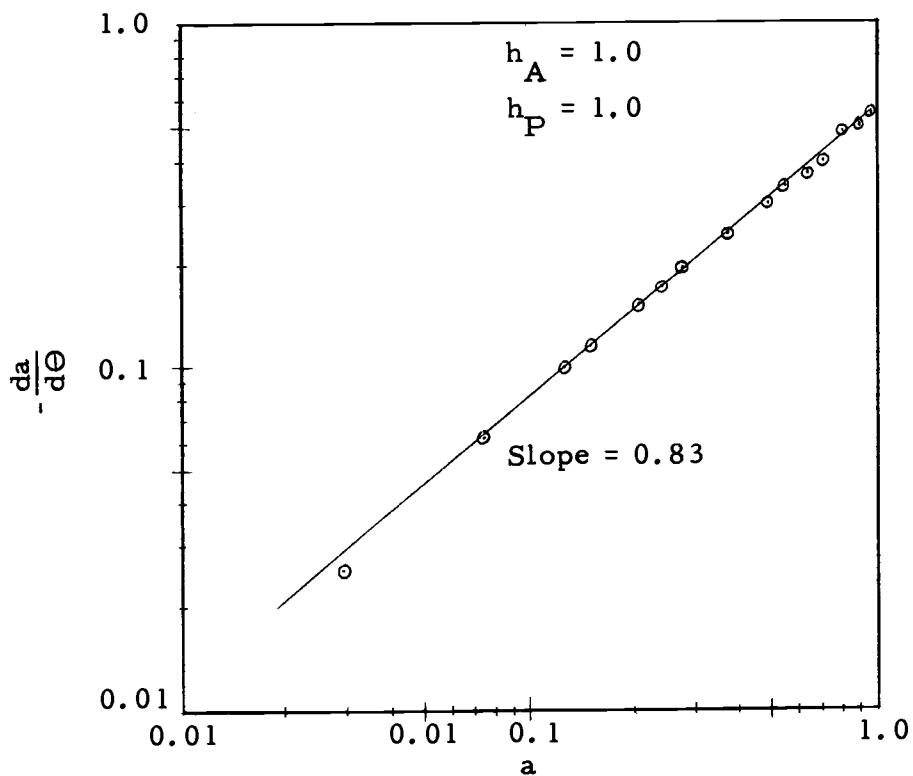


Figure 53. Side-by-side deactivation, $-\frac{da}{d\Theta}$ vs. a .

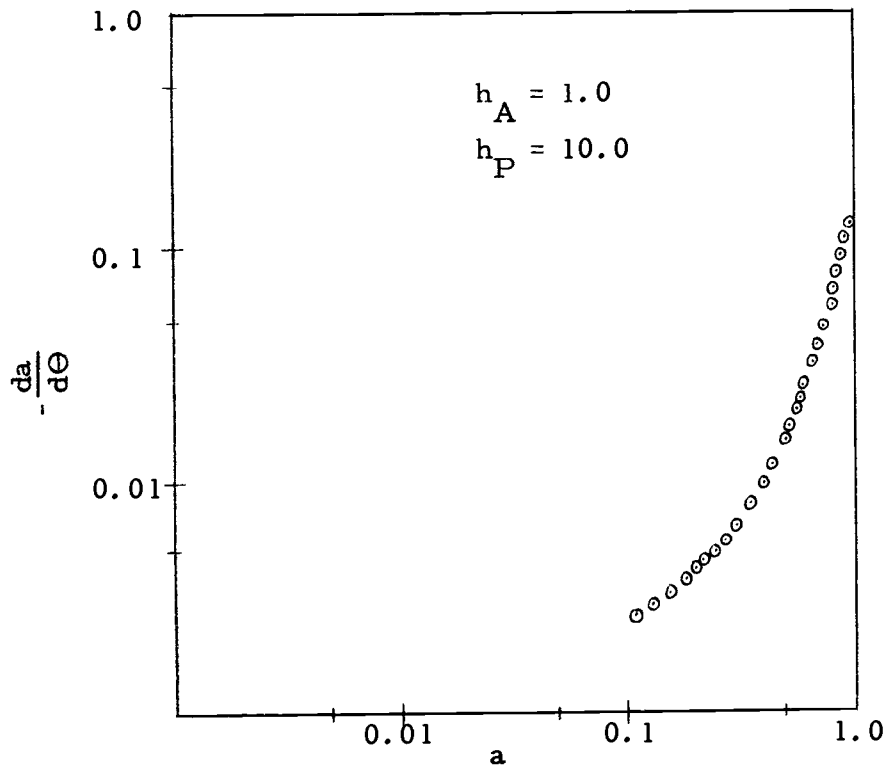


Figure 54. Side-by-side deactivation, $-\frac{da}{d\Theta}$ vs. a .

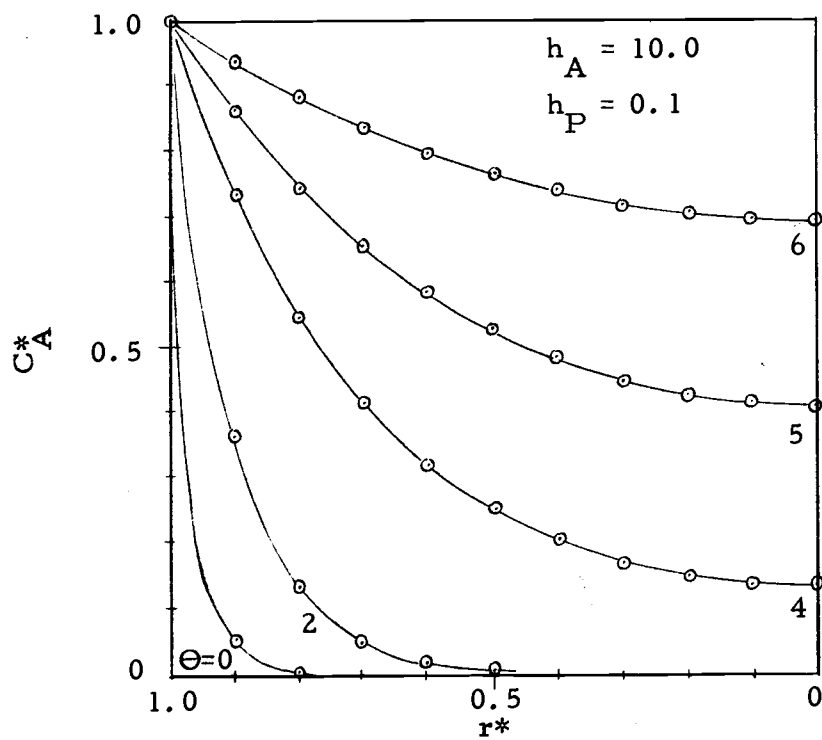


Figure 55. Side-by-side deactivation, C_A^* vs. r^* .

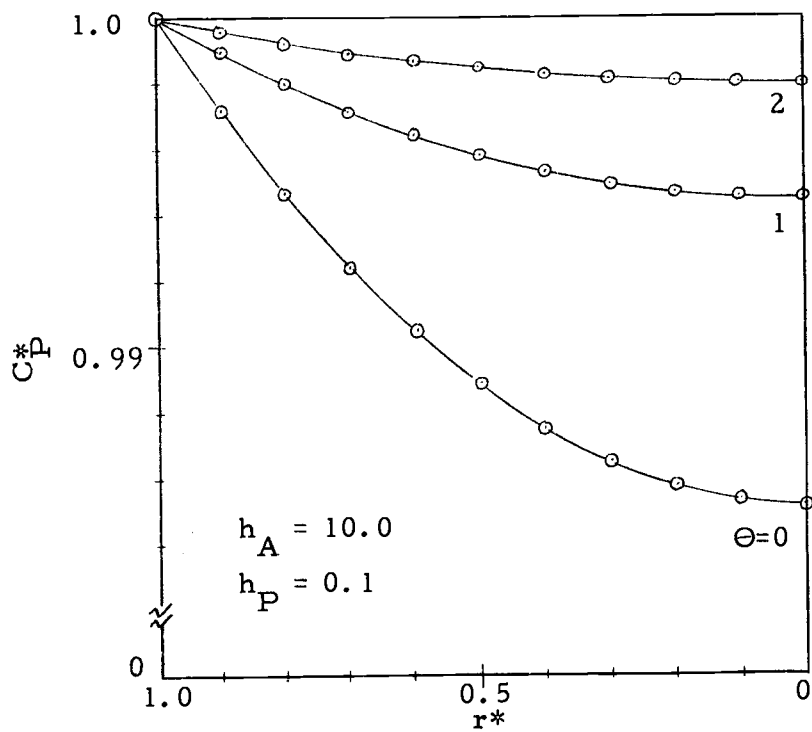


Figure 56. Side-by-side deactivation, C_P^* vs. r^* .

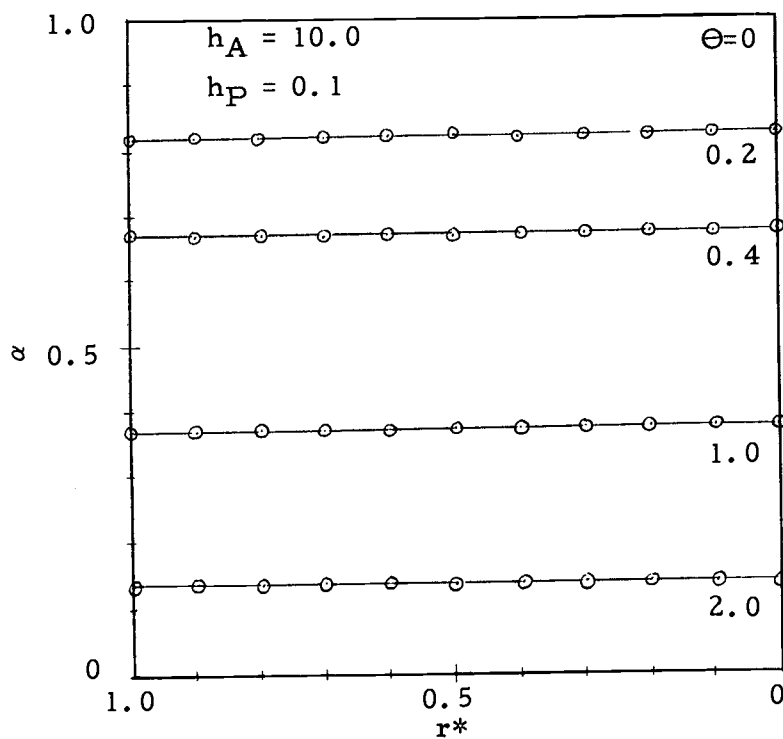


Figure 57. Side-by-side deactivation, α vs. r^* .

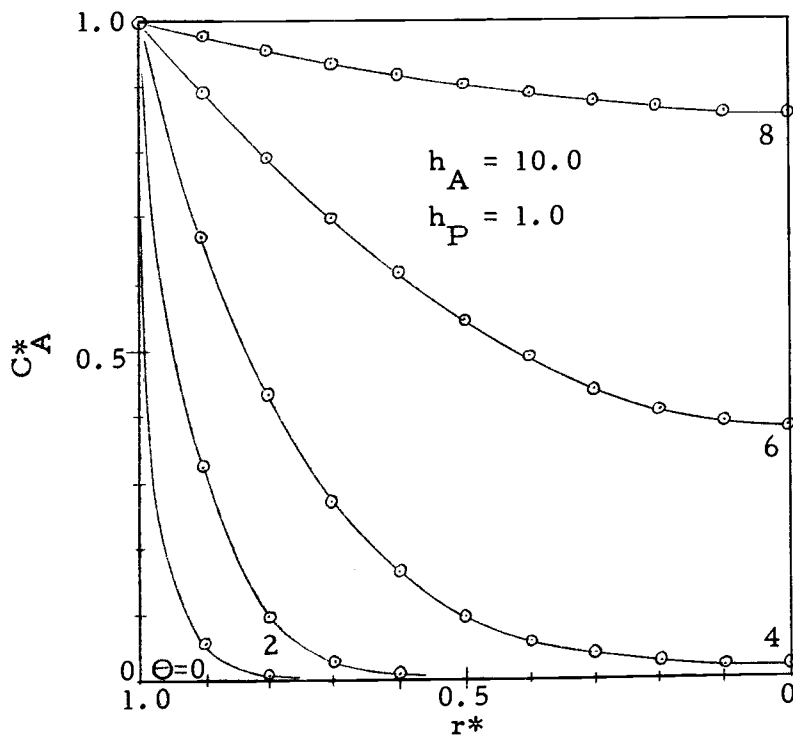


Figure 58. Side-by-side deactivation, C_A^* vs. r^*

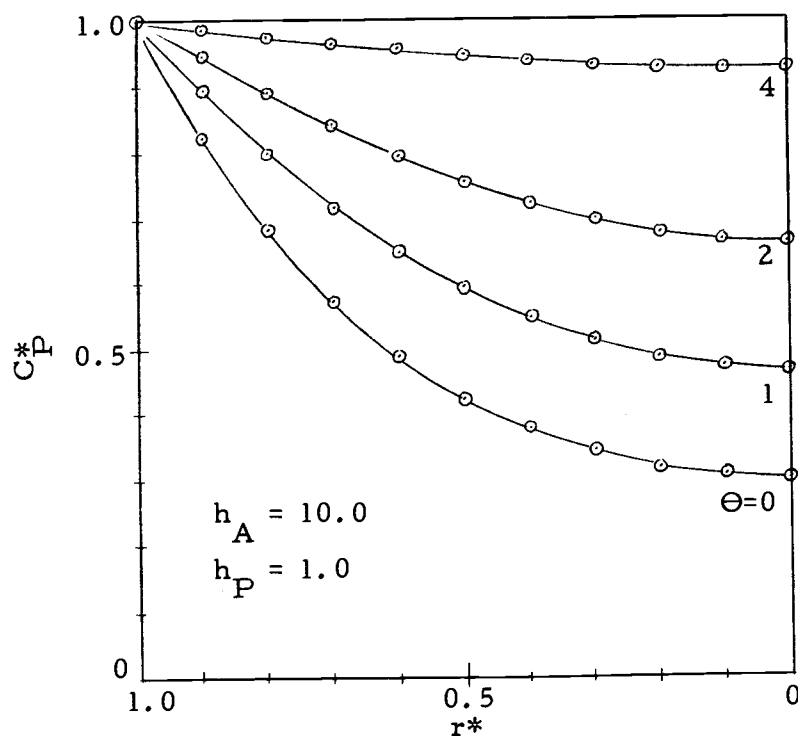


Figure 59. Side-by-side deactivation, C_P^* vs. r^* .

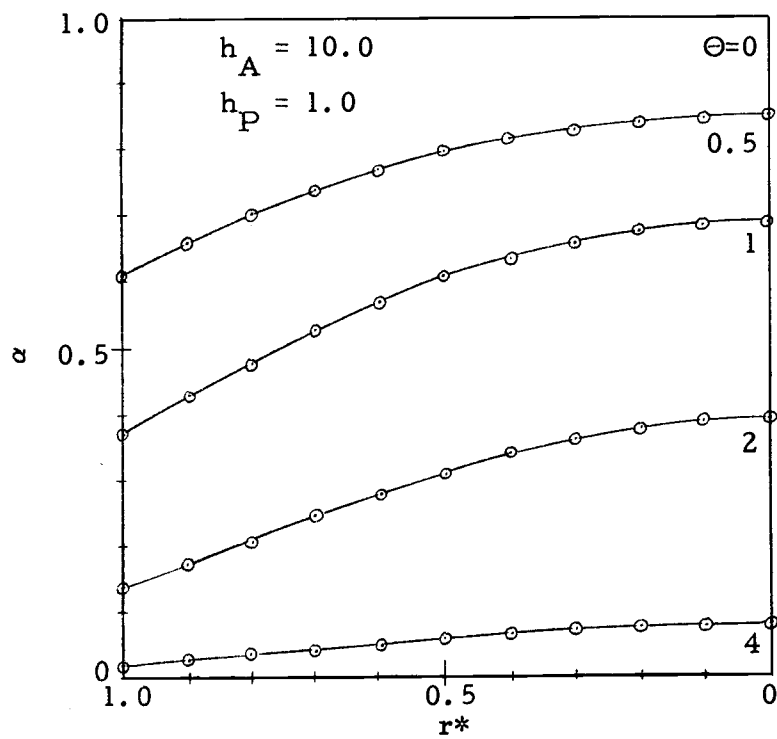


Figure 60. Side-by-side deactivation, α vs r^* .

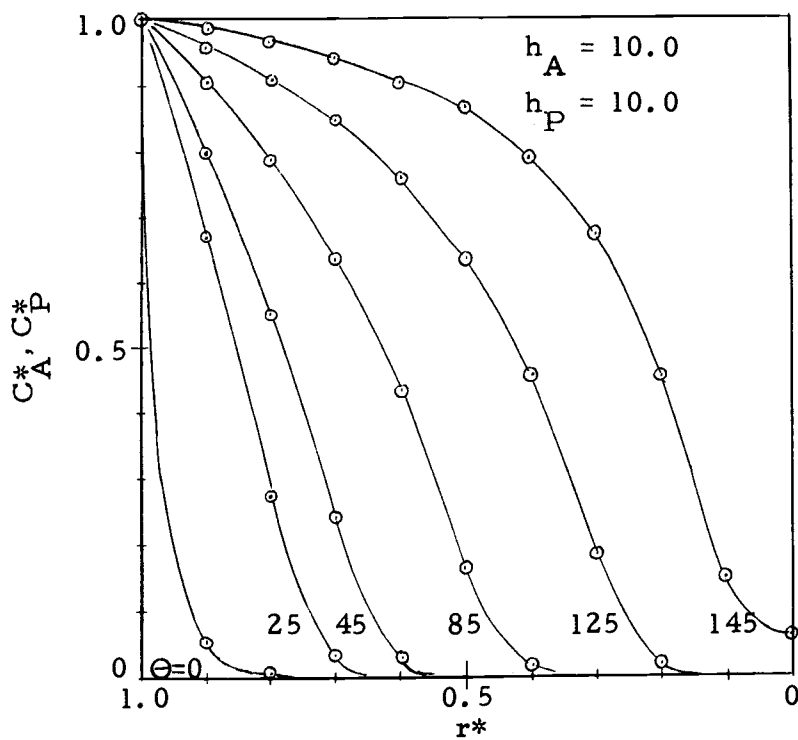


Figure 61. Side-by-side deactivation, C_A^* , C_P^* vs r^* .

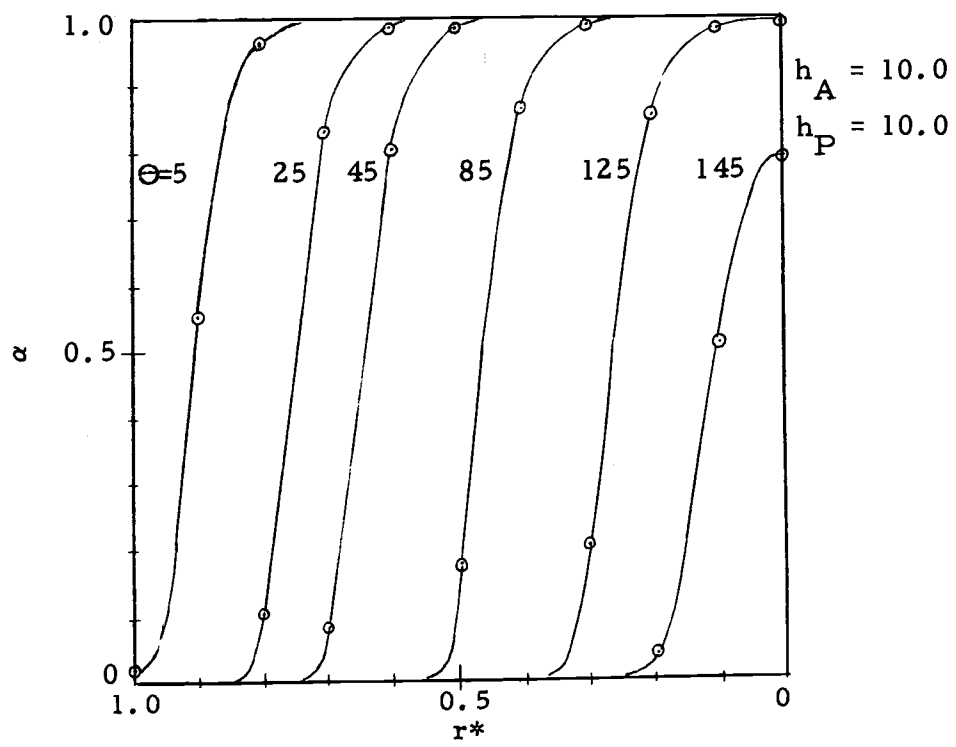


Figure 62. Side-by-side deactivation, α vs. r^* .

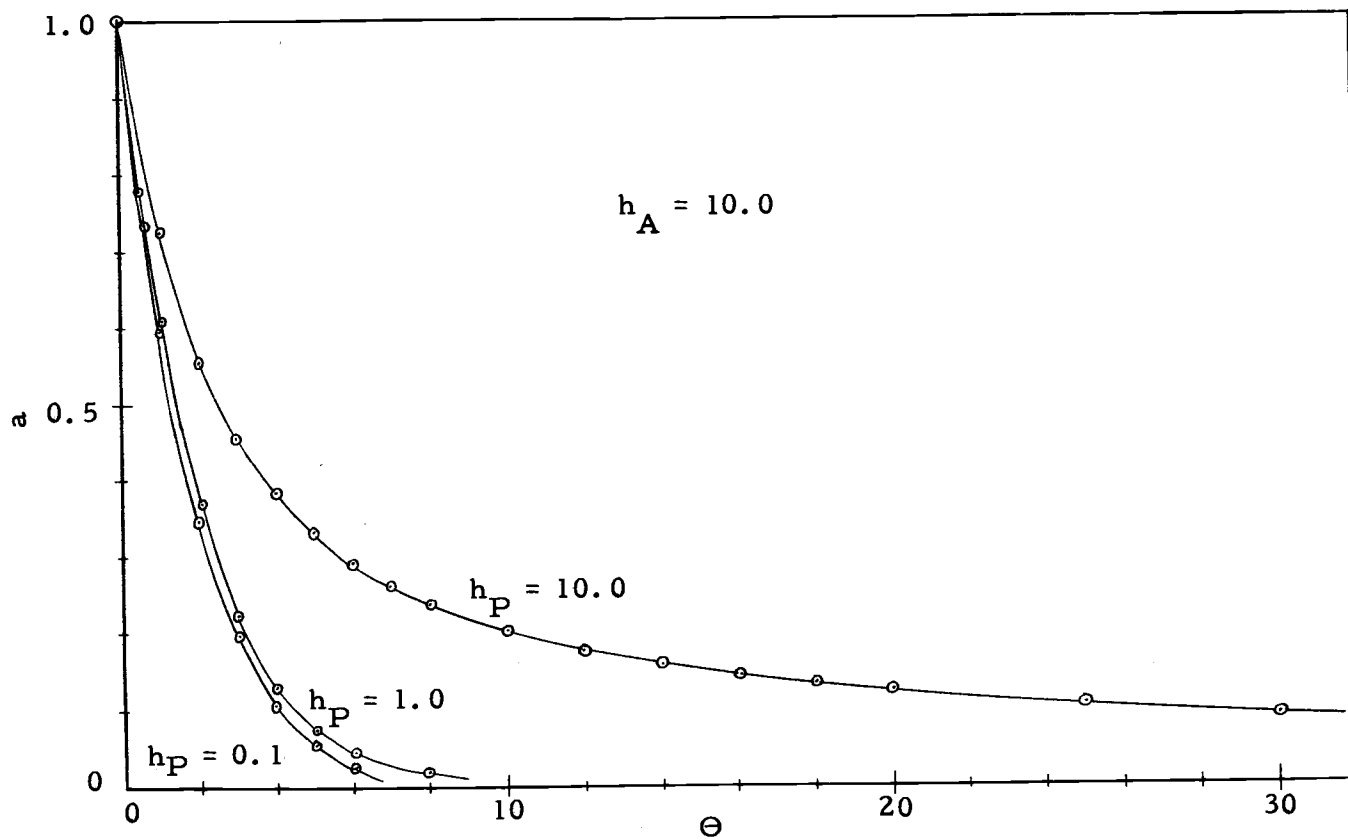


Figure 63. Side-by-side deactivation, a vs. Θ .

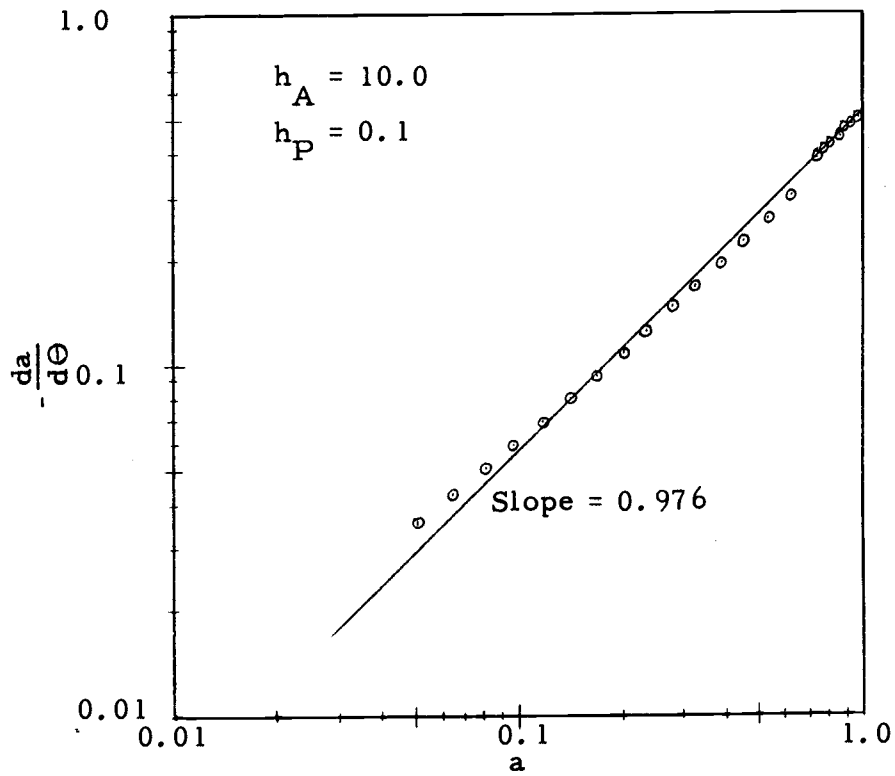


Figure 64. Side-by-side deactivation, $-\frac{da}{d\Theta}$ vs. a .

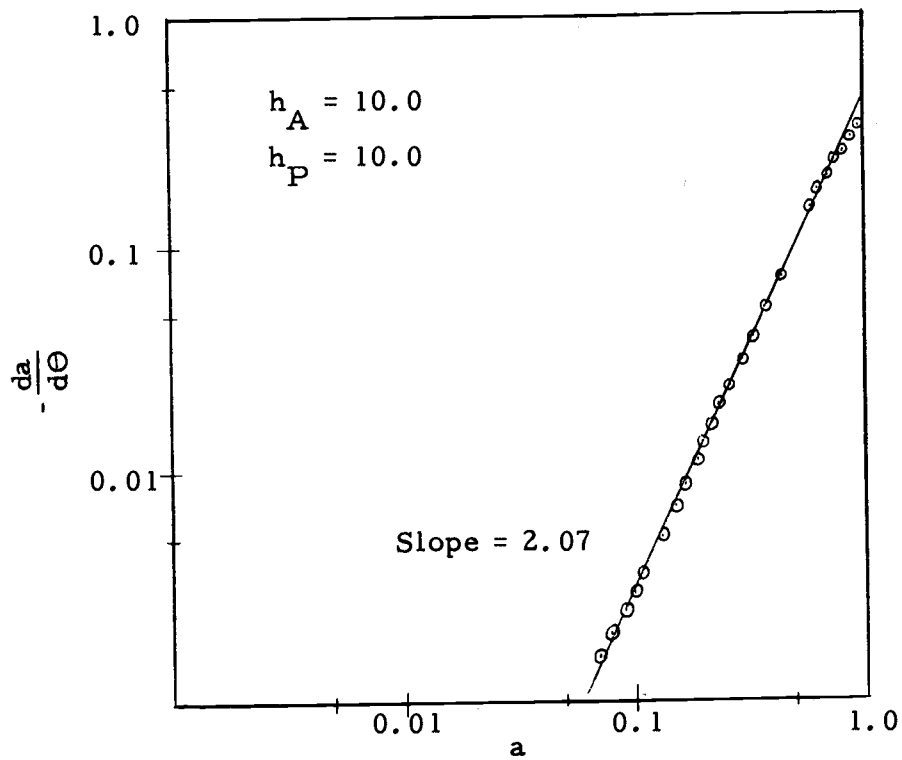


Figure 65. Side-by-side deactivation, $-\frac{da}{d\Theta}$ vs. a .

53 and 64).

If the Thiele modulus for poison is larger than both unity and the Thiele modulus for the main reaction ($h_P > 1$ and $h_P > h_A$), we cannot justify the plot of $-\frac{da}{d\Theta}$ vs. \underline{a} as a straight line (Figures 42 and 54).

Therefore, Equation (5a) with constant d , is valid except when $h_P > h_A$ and $h_P > 1$.

IV. LIMITING CASES

The limiting cases are presented to test the validity of Equation (5a) and the results of the previous chapter.

Parallel Deactivation

We have two limiting cases;

$$\text{i) } h_A \longrightarrow 0$$

$$\text{ii) } h_A \longrightarrow \infty$$

Both these cases were analyzed by Levenspiel (1970) and we will review them in turn.

$$\text{Case i) } \frac{h_A \longrightarrow 0 \quad (\epsilon_A \longrightarrow 1)}{(h_A < 0.5)}$$

In this case, no diffusion resistance is present in the catalyst pellet, the concentration of reactant is uniform, hence, poisoning is uniform throughout the pellet (Figure 66).

The reaction rate of a poisoned catalyst pellet becomes

$$-r_A = k_A \alpha C_{As} \quad (89)$$

$$\frac{d\alpha}{dt} = -k_d \alpha C_{As} \quad (90)$$

$$\alpha = 1, \text{ at } t = 0$$

where α is the point activity which is uniform throughout the pellet.

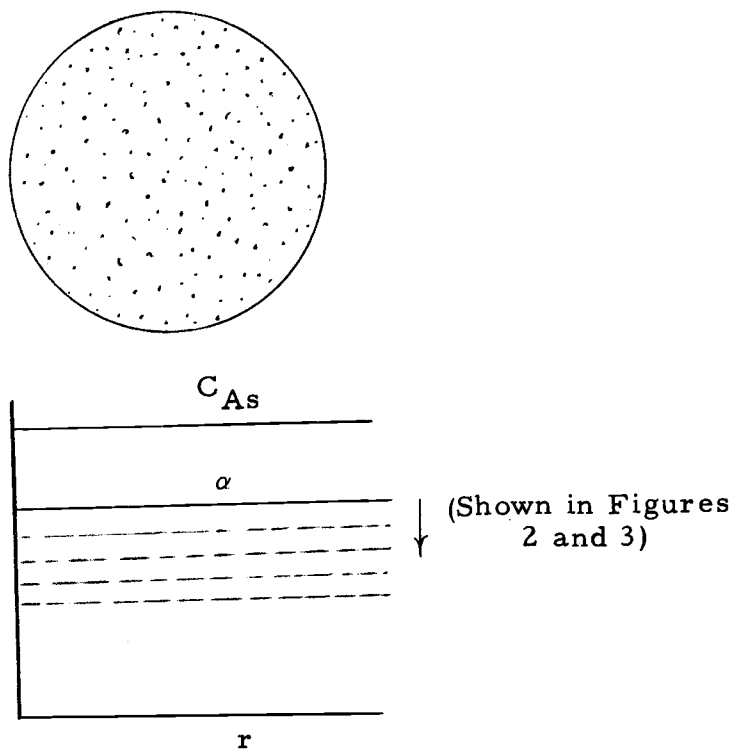


Figure 66. Parallel deactivation, $h_A \rightarrow 0$.

Solving Equation (90), α becomes

$$\alpha = \exp(-k_d C_{As} t) \quad (91)$$

Substituting Equation (91) into Equation (89),

$$-r_A = k_A C_{As} \exp(-k_d C_{As} t) \quad (92)$$

At $t = 0$, we have the reference state of reaction rate

$$-r_{A0} = k_A C_{As}$$

From Equation (3), the activity becomes

$$a \doteq \frac{-r_A}{-r_{A0}} = \frac{k_A C_{As} \exp(-k_d C_{As} t)}{k_A C_{As}} = \exp(-k_d C_{As} t)$$

Differentiating above equation with respect to time, t ,

$$\frac{da}{dt} = -k_d C_{As} \exp(-k_d C_{As} t)$$

or,

$$\frac{da}{dt} = -k_d C_{As} a \quad (93)$$

Thus, the order of deactivation, \underline{d} , approaches unity as h_A goes to zero. This is in good agreement with the results given in Figures 13 and 30.

Case ii) $h_A \longrightarrow \infty$

$$(\underline{C}_A \longrightarrow 0)$$

Even after a large drop in activity has occurred, most of the reaction still takes place within a thin shell close to the outer part of the pellet. Therefore, we can approximate the spherical pellet as a semi-infinite slab, and this is the typical case of pore-mouth poisoning given by Wheeler (Figure 67).

Here we have straight diffusion through the poisoned portion of the pore followed by reaction. Also note that the diffusion rate equals the reaction rate. Thus for a single pellet we write, for the mass transfer step,

$$-r_A = \frac{D_A}{L(L-x)} (C_{As} - C_{Ai}) \quad (94)$$

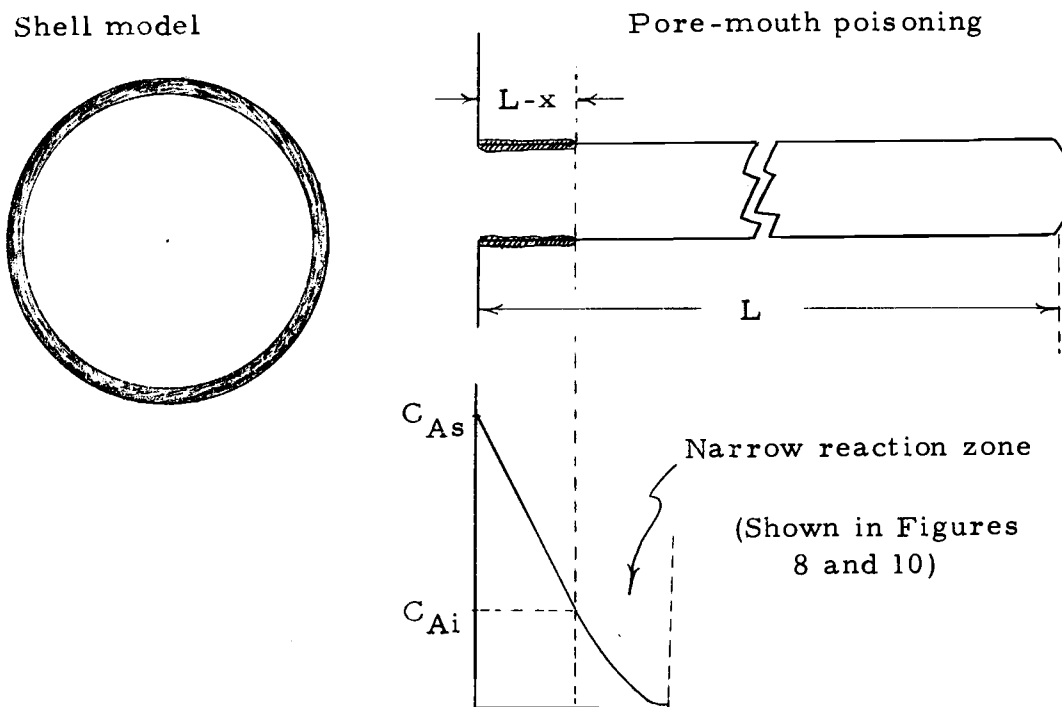


Figure 67. Parallel deactivation, $h_A \rightarrow \infty$.

and for the reaction step

$$-r_A = k_A (x/L) \mathcal{E}_{Ai} C_{Ai} \quad (95)$$

where \mathcal{E}_{Ai} is the pellet effectiveness factor based on the pore length x .

$$\mathcal{E}_{Ai} = \frac{1}{h_{Ai}} = \frac{1}{\sqrt{\frac{k_A}{D_A}} x}$$

Substituting the above equation into Equation (95),

$$-r_A = \frac{k_A C_{Ai}}{\sqrt{\frac{k_A}{D_A}} L} = k_A \mathcal{E}_{Ai} C_{Ai} \quad (96)$$

and eliminating the interface concentration, C_{Ai} , from Equations (95)

and (96),

$$-r_A = \frac{C_{As}}{\frac{L(L-x)}{D_A} + \frac{1}{\mathcal{E}_A k_A}}$$

The initial reaction rate, $-r_{Ao}$, becomes

$$-r_{Ao} = k_A \mathcal{E}_A C_{As}$$

From Equation (3), the activity is written as

$$a = \frac{-r_A}{-r_{Ao}} = \frac{1}{\frac{L-x}{L\mathcal{E}_A} + 1} \quad (97)$$

The progression rate of poisoned area is proportional to the reaction rate, $-r_A$,

$$\frac{d(L-x)}{dt} = k'_d (-r_A) = k'_d \frac{C_{As}}{\frac{L(L-x)}{D_A} + \frac{1}{\mathcal{E}_A k_A}}$$

Differentiating Equation (97) with respect to time, and using the above equation, we have

$$\begin{aligned} \frac{da}{dt} &= - \frac{\frac{1}{L\mathcal{E}_A}}{\left(\frac{L-x}{L\mathcal{E}_A} + 1\right)^2} \frac{d(L-x)}{dt} \\ &= - \frac{k'_d C_{As}}{L} \frac{1}{\left(\frac{L-x}{L\mathcal{E}_A} + 1\right)^3} \end{aligned}$$

or,

$$\frac{da}{dt} = -k_d C_{As} a^3 \quad (98)$$

Therefore, the order of deactivation, \underline{d} , approaches 3 as h_A goes to infinity. The straight line portion in Figures 28 and 29 gives the order of deactivation, \underline{d} , close to 3. And the asymptotic behavior is also given in Figure 30.

Rearranging Equation (98),

$$-\frac{da}{a^3} = k_d C_{As} dt$$

Integrating the above equation,

$$1/2 a^{-2} = k_d C_{As} t$$

$$a = \frac{1}{(2k_d C_{As} t + 1)^{1/2}} \quad (98a)$$

Assuming that the activity of the surface is inversely proportional to the concentration of carbon on the surface, Equation (9) becomes

$$a = A t^{-0.5} \quad (98b)$$

If $2k_d C_{As} t \gg 1$, Equation (98a) becomes Equation (98b).

Therefore, Equation (98) also represents the Voorhies correlation.

Side-by-side Deactivation

We have four limiting cases;

$$i) \begin{cases} h_A \longrightarrow 0 \\ h_P \longrightarrow 0 \end{cases}$$

$$ii) \begin{cases} h_A \longrightarrow \infty \\ h_P \longrightarrow 0 \end{cases}$$

$$iii) \begin{cases} h_A \longrightarrow 0 \\ h_P \longrightarrow \infty \end{cases}$$

$$iv) \begin{cases} h_A \longrightarrow \infty \\ h_P \longrightarrow \infty \end{cases}$$

For each of the above cases, we will develop the expression for deactivation rate and see if the analysis of the previous chapter is reasonable.

$$\text{Case i) } \begin{cases} h_A \longrightarrow 0 & (\mathcal{E}_A \longrightarrow 1) \\ h_P \longrightarrow 0 & (\mathcal{E}_P \longrightarrow 1) \end{cases}$$

Concentrations of reactant A and poison P are uniform, and hence the point activity α is uniform throughout the pellet.

$$-r_A = k_A C_{As} \alpha \quad (99)$$

$$\frac{d\alpha}{dt} = -k_d C_{Ps} \alpha$$

$$\alpha = 1, \text{ at } t = 0$$

Solving the above equation, the point activity becomes

$$\alpha = \exp(-k_d C_{Ps} t)$$

From Equation (3), the activity becomes

$$a = \frac{-r_A}{-r_{A0}} = \frac{k_A C_{As} \exp(-k_d C_{Ps} t)}{k_A C_{As}} = \exp(-k_d C_{Ps} t)$$

Differentiating the above equation with respect to time,

$$\frac{da}{dt} = -k_d C_{Ps} a \quad (100)$$

The order of deactivation, \underline{d} , approaches unity as h_A and h_P goes to zero. This result is also given by Figure 40.

$$\text{Case ii) } \left\{ \begin{array}{ll} h_A \longrightarrow \infty & (\mathcal{E}_A \longrightarrow 0) \\ h_P \longrightarrow 0 & (\mathcal{E}_P \longrightarrow 1) \end{array} \right.$$

Concentration of poison P is uniform, and hence the point activity α is uniform throughout the pellet. The main reaction takes place within a thin shell close to the outer part of the pellet. The reaction rate can be found as

$$-r_A = k_A C_{As} \sqrt{\alpha} \frac{\tanh(h_A \sqrt{\alpha'})}{h_A}$$

where

$$\frac{d\alpha}{dt} = -k'_d C_{Ps} \alpha$$

or,

$$\alpha = \exp(-k'_d C_{Ps} t)$$

From Equation (3), the activity becomes

$$a = \frac{-r_A}{-r_{A0}} = \frac{k_A C_{As} \sqrt{\alpha'} \tanh(h_A \sqrt{\alpha'})}{k_A C_{As} h_A} = \sqrt{\alpha'} \frac{\tanh(h_A \sqrt{\alpha'})}{h_A}$$

For large values of h_A ,

$$a = \sqrt{\alpha'} = \exp(-1/2 k_d' C_{Ps} t)$$

Differentiating the above equation with respect to time, we have

$$\frac{da}{dt} = -k_d' C_{Ps} a \quad (101)$$

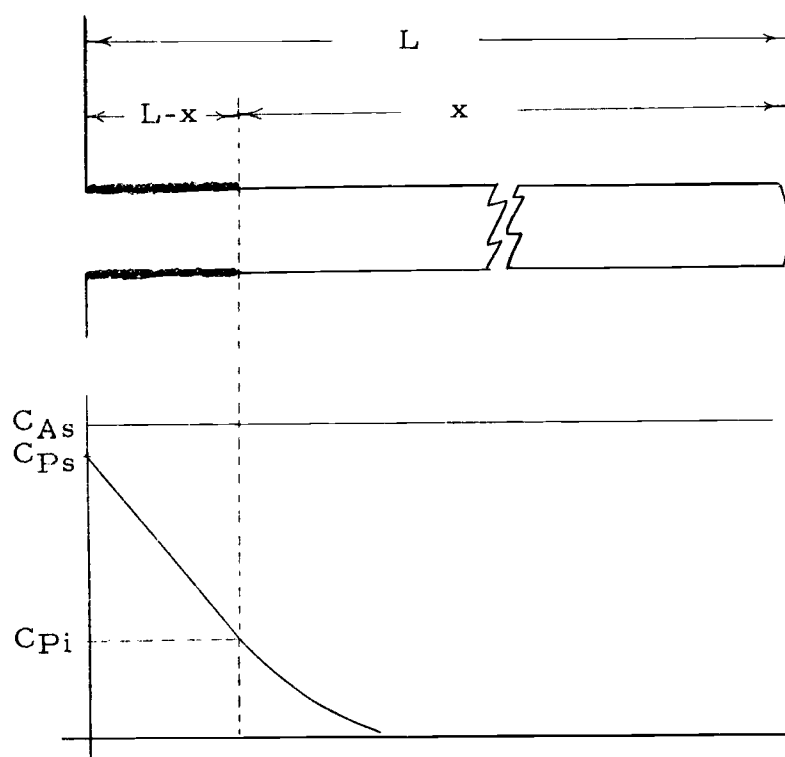
Therefore, the order of deactivation, \underline{d} , approaches unity as h_A goes to infinity and h_P goes to zero. This result is in good agreement with Figure 64.

$$\text{Case iii) } \left\{ \begin{array}{ll} h_A \longrightarrow 0 & (\mathcal{E}_A \longrightarrow 1) \\ h_P \longrightarrow \infty & (\mathcal{E}_P \longrightarrow 0) \end{array} \right.$$

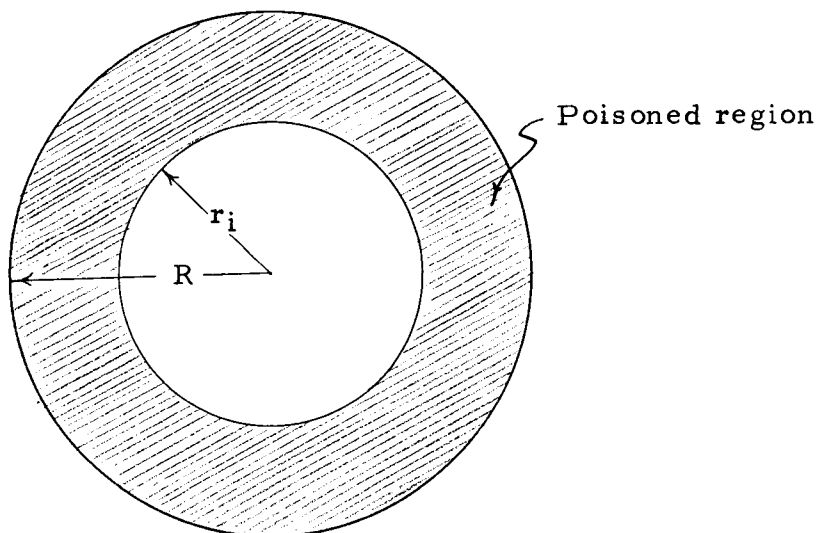
Concentration of reactant A is uniform through the pellet.

Poison is initially confined within a thin shell close to the outer part of the pellet, and moves toward the interior of the pellet after deactivating the active surface (Figure 68).

Even after more than half of the pellet radius is deactivated, the pellet still has a significant amount of activity. In this case, we cannot approximate the spherical pellet as a semi-infinite slab. We will consider both slab and spherical geometries.



a) Slab



b) Sphere

Figure 68. Side-by-side deactivation, $h_A \rightarrow 0$ and $h_P \rightarrow \infty$.

a) A Pellet of Slab Geometry

Consider Figure 68a. The reaction rate for Reactant A is

$$-r_A = k_A C_{As} x/L$$

From Equation (3), activity is written as

$$a = \frac{-r_A}{-r_A} = \frac{k_A C_{As} x/L}{k_A C_{As}} = x/L \quad (102)$$

By the same reason of Case ii in the previous section, the reaction rate for poison P becomes, for the mass transfer step,

$$-r_P = \frac{D_P}{L(L-x)} (C_{Ps} - C_{Pi}) \quad (103)$$

and for the reaction step

$$-r_P = k_P \mathcal{E}_{Pi} C_{Pi} = k_P \mathcal{E}_P C_{Pi} \quad (104)$$

where \mathcal{E}_{Pi} is the pellet effectiveness factor for poison P based on the pore length x

$$\mathcal{E}_{Pi} = 1/h_{Pi} = 1 / \left(\sqrt{\frac{k_P}{D_P}} x \right)$$

Eliminating the interface concentration, C_{Pi} , from Equations (103) and (104),

$$-r_P = \frac{C_{Ps}}{\frac{L(L-x)}{D_P} + \frac{1}{\mathcal{E}_P k_P}}$$

The progression rate of poisoned area is proportional to the reaction rate for poison, $-r_P$,

$$\frac{d(L-x)}{dt} = k'_d(-r_P) = k'_d \frac{C_{Ps}}{\frac{L(L-x)}{D_P} + \frac{1}{\epsilon_P k_P}}$$

or,

$$\frac{d(x/L)}{dt} = - \frac{k'_d k_P}{L} \frac{C_{Ps}}{\frac{1}{\epsilon_P^2} (1 - \frac{x}{L}) + \frac{1}{\epsilon_P}}$$

Substituting Equation (102) into the above equation,

$$\frac{da}{dt} = - \frac{k'_d k_P \epsilon_P}{L} \frac{C_{Ps}}{\frac{1}{\epsilon_P} (1-a) + 1}$$

or,

$$\frac{da}{dt} = - \frac{k'_d k_P}{L h_P} \frac{C_{Ps}}{h_P (1-a) + 1} \quad (105)$$

When $a \ll 1$, Equation (105) reduces to

$$\frac{da}{dt} = - \frac{k'_d k_P}{L h_P^2} C_{Ps} = -k'_d C_{Ps} a^0 \quad (105a)$$

For slab geometry if $h_P \rightarrow \infty$, $h_A \rightarrow 0$ and $a \ll 1$, then Equation (5a) with constant order of deactivation is applicable and the order of deactivation approaches zero.

b) A Spherical Pellet

Consider Figure 68b. The reaction rate for reactant A is

$$\begin{aligned}
 -r_A &= k_A C_{As} \left(\frac{\text{Vol. of inner core}}{\text{Vol. of a whole pellet}} \right) \\
 &= k_A C_{As} (r_i/R)^3
 \end{aligned}$$

From Equation (3), activity becomes

$$a = \frac{-r_A}{-r_{Ao}} = (r_i/R)^3 \quad (106)$$

By the material balance within the poisoned region, we find the following differential equation,

$$\frac{D_P}{r^2} \frac{d}{dr} r^2 \frac{dC_P}{dr} = 0$$

with the boundary conditions

$$C_P = C_{Ps} \quad \text{at } r = R$$

$$C_P = C_{Pi} \quad \text{at } r = r_i$$

Solving the above equations, we have

$$C_P = \frac{(C_{Ps} - C_{Pi})R r_i}{R - r_i} \left(\frac{1}{r} \right) + \frac{RC_{Ps} - r_i C_{Pi}}{R - r_i}$$

The reaction rate for poison P becomes, for the mass transfer step,

$$-r_P = \frac{4\pi R^2}{\frac{4}{3}\pi R^3} D_P \frac{dC_P}{dr} \Bigg|_{r=R} = \frac{D_P (C_{Ps} - C_{Pi})}{R - r_i} \left(\frac{r_i}{R} \right) \left(\frac{3}{R} \right) \quad (107)$$

and for the reaction step

$$-r_P = k_P \xi_{P_i} C_{P_i} \frac{\frac{4}{3} \pi r_i^3}{\frac{4}{3} \pi R^3} = k_P \left(\frac{r_i}{R}\right)^2 \xi_P C_{P_i} \quad (108)$$

where

$$\xi_{P_i} = 1/h_{P_i} = \frac{1}{\sqrt{\frac{k_P}{D_P}} \frac{r_i}{3}}$$

$$\xi_P = 1/h_P = \frac{1}{\sqrt{\frac{k_P}{D_P}} \frac{R}{3}}$$

Eliminating the interface concentration, C_{P_i} , from Equations (107) and (108),

$$-r_P = \frac{C_{P_s}}{\frac{R - r_i}{D_P} \left(\frac{R}{r_i}\right) \left(\frac{R}{3}\right) + \left(\frac{R}{r_i}\right)^2 \frac{1}{\xi_P k_P}}$$

The progression rate of poisoned region is proportional to the reaction rate for poison.

$$\frac{d(\text{poisoned region})}{dt} = k'_d (-r_P) = \frac{k'_d C_{P_s}}{\frac{R - r_i}{D_P} \left(\frac{R}{r_i}\right) \left(\frac{R}{3}\right) + \left(\frac{R}{r_i}\right)^2 \frac{1}{\xi_P k_P}}$$

or,

$$\frac{d(r_i/R)^3}{dt} = - \frac{k'_d k_P C_{P_s} \xi_P}{R} \frac{1}{\frac{3}{\xi_P} \left(\frac{R}{r_i} - 1\right) + \left(\frac{R}{r_i}\right)^2}$$

Substituting Equation (106) into the above equation,

$$\frac{da}{dt} = - \frac{k'_d k_P C_{Ps} \xi_P}{R} \frac{1}{\frac{3}{\xi_P} (a^{-1/3} - 1) + a^{-2/3}}$$

or,

$$\frac{da}{dt} = - \frac{k'_d k_P}{R h_P} \frac{C_{Ps}}{3 h_P (a^{-1/3} - 1) + a^{-2/3}} \quad (109)$$

When $a \ll 1$, Equation (109) reduces to

$$\frac{da}{dt} = - \frac{k'_d k_P C_{Ps}}{3 R h_P^2} a^{1/3} = -k_d a^{1/3} \quad (109a)$$

For a spherical pellet if $h_P \rightarrow \infty$, $h_A \rightarrow 0$ and $a \ll 1$, then Equation (5a) with constant order of deactivation is applicable and the order of deactivation approaches $1/3$.

Comparison With the Numerical Solution

Since C_A is constant throughout the pellet and C_P has the same profile as C_A for parallel deactivation, we may use the same numerical procedures as given in Appendix II except the integration of Equation (33). C_A^* in Equation (33) is replaced by unity.

To test the validity of Equation (109), the plot of $\frac{da}{d\Theta}$ vs.

$\frac{1}{3 h_P (a^{-1/3} - 1) + a^{-2/3}}$ is made on a log-log scale (Figure 69). The plot is acceptable as a straight line and the slope is about unity. The curved portion represents the initial period of deactivation where the

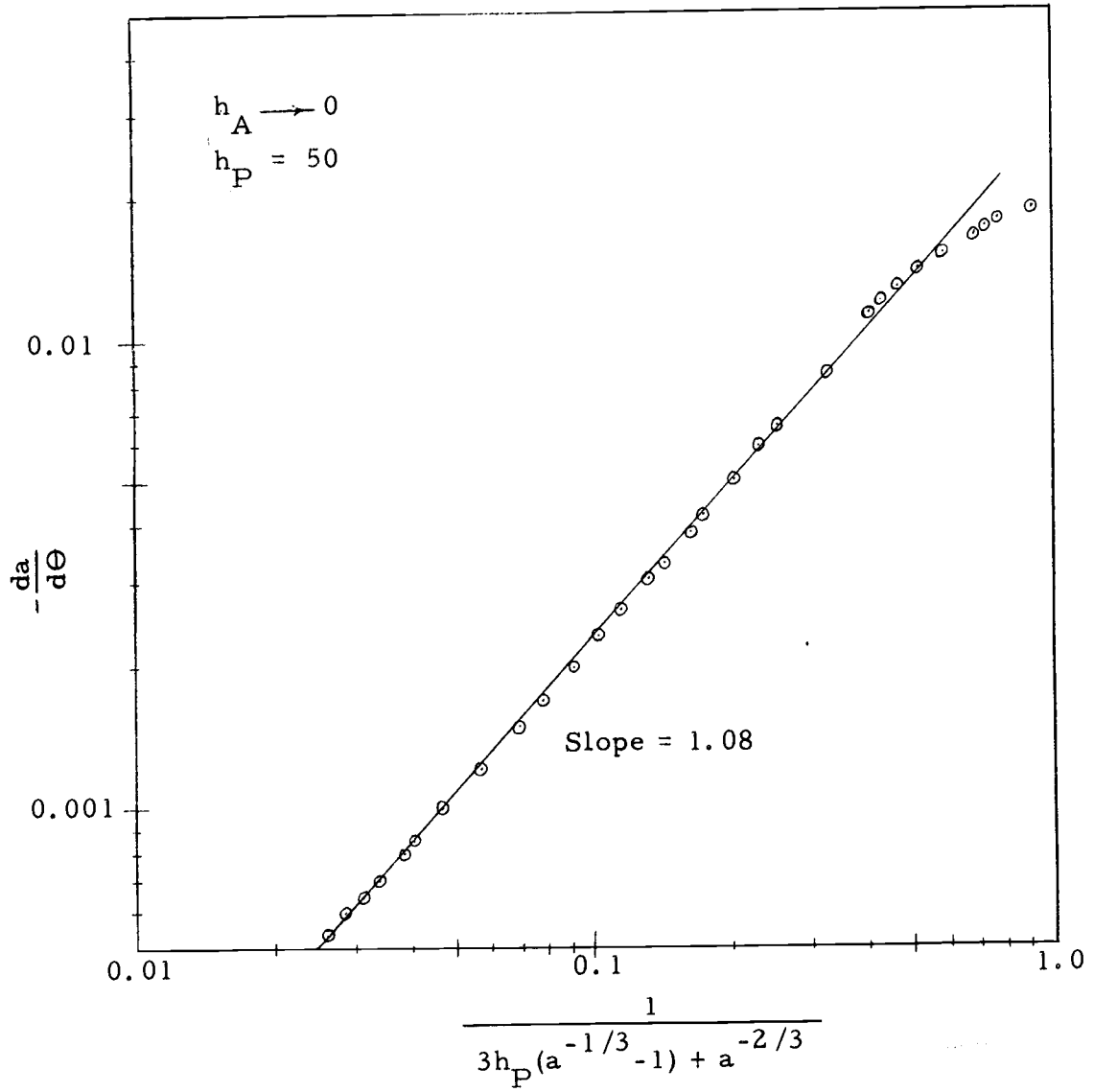


Figure 69. Side-by-side deactivation, limiting case.

α -profile has not yet become S-shaped (see Figures 9 and 11).

Equation (109) is in good agreement with the numerical solution.

$$\text{Case iv) } \left\{ \begin{array}{l} h_A \longrightarrow \infty \quad (\mathcal{E}_A \longrightarrow 0) \\ h_P \longrightarrow \infty \quad (\mathcal{E}_P \longrightarrow 0) \end{array} \right.$$

Even after a large drop in activity has occurred, most of the reaction and deactivation still takes place within a thin shell close to the outer part of the pellet. Therefore, we can approximate the spherical pellet as a semi-infinite slab (Figure 67). By a similar procedure to that of Case ii in the previous section, we find that

$$-r_A = \frac{C_{As}}{\frac{L(L-x)}{D_A} + \frac{1}{\mathcal{E}_A k_A}}$$

$$-r_P = \frac{C_{Ps}}{\frac{L(L-x)}{D_P} + \frac{1}{\mathcal{E}_P k_P}}$$

The progression rate of poisoned region is proportional to the reaction rate for poison.

$$\frac{d(L-x)}{dt} = k'_d (-r_P) = \frac{k'_d C_{Ps}}{\frac{L(L-x)}{D_P} + \frac{1}{\mathcal{E}_P k_P}} \quad (110)$$

The activity becomes

$$a = \frac{-r_A}{-r_{A0}} = \frac{1}{\frac{L-x}{L\mathcal{E}_A} + 1}$$

or,

$$L - x = \sum_A L \left(\frac{1}{a} - 1 \right)$$

Substituting the above equation into Equation (110),

$$\frac{da}{dt} = - \frac{k'_d k_P C_{Ps} \epsilon_P / \epsilon_A}{L} \frac{a^2}{\frac{\epsilon_A}{\epsilon_P} \frac{1}{a} - \frac{\epsilon_A}{\epsilon_P} + 1}$$

or,

$$\frac{da}{dt} = - k'_d C_{Ps} \frac{a^3}{\frac{h_P}{h_A} (1 - a) + a} \quad (111)$$

When $h_P = h_A$, Equation (111) reduces to Equation (5a), and the order of deactivation becomes 3. This result can be drawn from the results in the previous chapters, since when $h_P = h_A$ the differential equations of side-by-side deactivation reduce to those of parallel deactivation and the order deactivation approaches 3 as h_A goes to infinity.

When $h_P \ll h_A$, Equation (111) reduces to Equation (5a), and the order of deactivation becomes 2.

When $h_P \gg h_A$ and $a \ll 1$, Equation (111) reduces to Equation (5a), and the order of deactivation becomes 3.

V. CONCLUSIONS

As a result of the present analysis of a single pellet system, the following conclusions are drawn.

(1) Parallel Deactivation

- a) The proposed model, Equation (5) with a constant for the order of deactivation \underline{d} , is generally acceptable.
- b) The order of deactivation, \underline{d} , is a function of Thiele modulus h_A as given in Figure 30.
- c) If h_A goes to zero, the order of deactivation approaches 1.
- d) If h_A goes to infinity, the order of deactivation approaches 3.

(2) Side-by-side Deactivation

- a) The proposed model, Equation (5) with constant order of deactivation \underline{d} , is applicable except when h_P is larger than both unity and h_A .
- b) If h_P goes to zero, the order of deactivation, \underline{d} , approaches 1, regardless of the value of h_A .
- c) If h_P goes to infinity and h_A goes to zero, Equation (105) is applicable for slab geometry and Equation (109) for spherical geometry.

In addition when $a \ll 1$, both Equations (105) and (109) reduce to Equation (5) with constant order of deactivation. The order of deactivation is zero for slab geometry and

$1/3$ for spherical geometry.

- d) If both h_P and h_A go to infinity, Equation (111) is applicable.

In addition, when $h_P \gg h_A$ and $a \ll 1$, or when $h_P = h_A$ and any a , Equation (111) reduces to Equation (5) with the order of deactivation, $d = 3$.

When $h_P \ll h_A$, Equation (111) reduces to Equation (5) with the order of deactivation, $d = 2$.

- e) These findings are only preliminary and a rough indication since only combination of only three values of h_A and h_P were studied. More values of h_A and h_P should be studied to more definitely fix these conclusions.

The significance of this study is that the formulation of Equations (5) and (5a) to describe deactivating catalysts can be a reasonable representation for parallel deactivation, but probably is not useful for situations where a rapidly adsorbed impurity in the feed is the cause of deactivation.

VI. RECOMMENDATIONS FOR FUTURE WORK

1) Further studies on side-by-side deactivation to fill out the brief findings here.

2) Repeat the present type of analysis for reactions in series deactivation, including limiting cases.

3) Repeat the present type of analysis for the cases of fast deactivation which must include the unsteady-state terms for the mass transfer step (Tables 1, 2, and 3).

4) Use different intrinsic kinetics for deactivation (i. e., Langmuir-Hinshelwood type rate forms,

$$\frac{k_1 C_i^\alpha}{k_2 C_i + 1}) ,$$

and give an analysis similar to the present type.

5) Find a suitable intrinsic rate form for heterogeneous poisoning and give an analysis similar to the present type.

6) Search for a formulation to replace Equation (5) which will fit all kinds of deactivation.

7) Find a proper way to design experiments with deactivating catalysts which will give a correct rate equation.

8) Extend a single pellet system to macroscopic systems of various contacting patterns, and search for a simple formulation for reactor performances.

BIBLIOGRAPHY

- Balder, J. R. and E. E. Peters^en. 1968. Poisoning studies in a single pellet reactor. *Chemical Engineering Science* 23:1287-1291.
- Butt, J. B. 1970. Catalyst deactivation. First International Symposium on Chemical Reaction Engineering. Washington, D.C. June, 1970.
- Carnahan, B., H. A. Luther and J. O. Wilkes. 1969. Applied numerical methods. New York, Wiley. p. 429-519.
- Chu, B. 1963. The sintering of platinum supported on alumina. *Journal of Physical Chemistry* 67:1916-1917.
- Chu, C. 1968. Effect of adsorption of the fouling of catalyst pellets. *I & EC Fundamentals* 7:509-514.
- Dougharty, N. A. 1970. Self-poisoning reactions in the single-pellet catalytic reactor. *Chemical Engineering Science* 25:489-494.
- Gioia, F. 1971. Poisoning of porous particles. *I & EC Fundamentals* 10:204-211.
- Gwyn, J. E. 1970. Effect of operating variables on the permanent deactivation of cracking catalyst. *Chemical Engineering Journal* 1:74-82.
- Herrmann, R. A. et al. 1961. The kinetics of sintering of platinum supported on alumina. *Journal of Physical Chemistry* 65:2189-2194.
- Jeffrey, L. H. and E. E. Peterson. 1970. Poisoning studies in a single-pellet catalytic reactor. *Canadian Journal of Chemical Engineering* 48:147-150.
- Levenspiel, O. 1970. Class lectures on applied reaction engineering (Ch. E. 540). Corvallis, Oregon State University. Winter term.
- _____ 1972. *Chemical Reaction Engineering*. 2nd ed. New York, Wiley. (In press)

- Masamune, S. and J. M. Smith. 1966. Performance of fouled catalyst pellets. *A. I. Ch. E. Journal* 12:384-394.
- Murakami, Y. et al. 1968. Effect of intraparticle diffusion on catalyst fouling. *I & EC Fundamentals* 7:599-604.
- Ozawa, Y. and K. B. Bishoff. 1968. Coke formation kinetics on silica-alumina catalyst. *I & EC Process Design and Development* 7:72-78.
- Szépe, S. and O. Levenspiel. 1968a. Optimal temperature policies for reactors subject to catalyst deactivation. I. Batch reactor. *Chemical Engineering Science* 23:881-894.
- _____ 1968b. Catalyst deactivation. *Proceedings of the Fourth European Symposium on Chemical Reaction Engineering, Brussels, 1971.* London, Pergamon. p. 265-276.
- Voorhies, A., Jr. 1945. Carbon formation in catalytic cracking. *Industrial and Engineering Chemistry* 37:318-322.
- Wheeler, A., Jr. 1951. Reaction rates and selectivity in catalyst pores. In: *Advances in catalysis*, ed. by W. G. Frankenburg et al. Vol. 3. New York, Academic. p. 249-327.
- _____ 1955. Reaction rates and selectivity in catalyst pores. In: *Catalysis*, ed. by P. H. Emmett. Vol. 2. New York, Reinhold. p. 105-165.
- Zaidmann, N. M. et al. 1969. Study of regular features of the crystallization of platinum on carriers. II. Effect of thermal treatment on the degree of dispersion and the activity of platinum oxide. *Kinetics and Catalysis* 10:318-321. (Translated from *Kinetika i Kataliz* 10:386-391. 1969)

APPENDICES

APPENDIX I

NOMENCLATURE

<u>Letter</u>	<u>Meaning</u>	<u>cgs Units</u>
a	activity of a catalyst pellet, see Equation (3)	
A	reactant substance	
C_{Ai}	interface concentration of reactant A, see Equation (94) and Figure 67	mole/cm ³
C_i	concentration of substance i	mole/cm ³
C_i^*	dimensionless concentration of substance i, see Equations (17), (42) and (66)	
C_{is}	concentration of substance i on the exterior surface of a catalyst pellet	mole/cm ³
C_{Pi}	interface concentration of poison P, see Equation (103) and Figure 68	mole/cm ³
d	order of deactivation, see Equations (5), (5a)	
D_i	effective diffusivity of substance i in a porous catalyst pellet	cm ² /sec
h_A	Thiele modulus of reactant A	
h_{AR}	mixed Thiele modulus using the reaction rate constant k_A and diffusivity of product D_R , see Equation (43)	
h_{dA}	mixed Thiele modulus using k_d and D_A , see Equation (21)	
h_{dP}	mixed Thiele modulus using k_d and D_P , see Equation (68)	

<u>Letter</u>	<u>Meaning</u>	<u>cgs Units</u>
h_{dR}	mixed Thiele modulus using k_d and D_R , see Equation (44)	
h_P	Thiele modulus of poison P, see Equation (67)	
k_A	reaction constant for main reaction	1/sec
k_d, k_{do}	deactivation constant	$\frac{1}{\text{sec}} \left(\frac{\text{cm}^3}{\text{mole}} \right)^{n'}$
k'_d	constant for progression rate of poisoned region	cm^2/mole
k_P	reaction constant for poison reaction	1/sec
k''	$= k_d C_i^{n'}$	1/sec
L	pore length	cm
m	grid position of radial increments	
M	total number of grids of radial increments	
n	grid position of time increments	
N	total number of grids of time increments	
P	poison substance	
R	product substance or, radius of a catalyst pellet	cm
r	radius of a catalyst pellet	cm
r^*	dimensionless radius of a catalyst pellet	
r_i	radius of a clean pellet core	cm
$-r_A$	reaction rate based on the concentration of reactant A	$\frac{\text{mole}}{(\text{cm}^3)(\text{sec})}$

<u>Letter</u>	<u>Meaning</u>	<u>cgs Units</u>
$-r_{A_0}$	reference reaction rate based on the concentration of reactant A	$\frac{\text{mole}}{(\text{cm}^3)(\text{sec})}$
$-r_P$	reaction rate based on the concentration of poison P	$\frac{\text{mole}}{(\text{cm}^3)(\text{sec})}$
t	time	sec
x	length of clean pore	cm
Greek letters		
α	point activity, see Equation (12)	
ξ_A	pellet effectiveness factor for reactant A	
ξ_{Ai}	pellet effectiveness factor for reactant A based on the length of a clean pore	
ξ_P	pellet effectiveness factor for poison P	
ξ_{Pi}	pellet effectiveness factor for poison P based on the length of a clean pore	
θ	dimensionless time, see Equations (19) and (66)	

APPENDIX II

SOLUTIONS OF TRIDIAGONAL LINEAR EQUATIONS

Consider the following set of linear equations which has a tridiagonal coefficient matrix,

$$\begin{aligned}
 b_1 v_1 + c_1 v_2 &= d_1 \\
 a_2 v_1 + b_2 v_2 + c_2 v_3 &= d_2 \\
 a_3 v_2 + b_3 v_3 + c_3 v_4 &= d_3 \\
 \dots & \\
 a_i v_{i-1} + b_i v_i + c_i v_{i+1} &= d_i \\
 \dots & \\
 a_{N-1} v_{N-2} + b_{N-1} v_{N-1} + c_{N-1} v_N &= d_{N-1} \\
 a_N v_{N-1} + b_N v_N &= d_N
 \end{aligned}$$

The solution is

$$\begin{aligned}
 v_N &= \gamma_N \\
 v_i &= \gamma_i - \frac{c_i v_{i+1}}{\beta_i} \quad ; \quad i = N-1, N-2, \dots, 2, 1
 \end{aligned}$$

where

$$\beta_1 = b_1$$

$$\gamma_1 = d_1 / \beta_1$$

$$\beta_i = b_i - \frac{a_i c_{i-1}}{\beta_{i-1}}$$

$$\gamma_i = \frac{d_i - a_i \gamma_{i-1}}{\beta_i} \quad ; \quad i = 2, 3, \dots, N$$

If $d_1 = d_2 = \dots = d_{N-1} = 0$ and $d_N = 1$, the solution can be simplified, thus

$$v_N = 1/\beta_N$$

$$v_i = v_{i+1}/\beta_i \quad ; \quad i = N-1, N-2, \dots, 2, 1$$

APPENDIX III

DIFFERENCE EQUATIONS AND PROGRAM LISTINGS
FOR PARALLEL DEACTIVATIONDifference Equations

$$C_{m,1}^A = 0 \quad (a)$$

$$\alpha_{m,1} = 1$$

First approximation;

$$\begin{aligned} \bar{\alpha}_{m,n} &= \alpha_{m,n-1} (-\Delta\Theta C_{m,n-1}^A + 1) \\ -\left(\frac{m-2}{m}\right) \bar{C}_{m-1,n}^A + \left(\frac{m-1}{m}\right) (h\bar{\alpha}_{m,n} + G_2) \bar{C}_{m,n}^A - \bar{C}_{m+1,n}^A \\ &= G \left(\frac{m-1}{m}\right) C_{m,n-1}^A \quad ; \quad m = 3, \dots, M-1 \end{aligned}$$

where

$$G = (3h_{dA} \Delta r)^2 / \Delta\Theta, \quad G_2 = G + 2, \quad h = (3h_A \Delta r)^2, \quad \bar{C}_{m,n}^A = 1 \quad (b)$$

Using the results of Appendix II, solve for $\bar{C}_{m,n}^A$; $m = 2, 3, \dots, M-1$.

Second approximation;

$$\begin{aligned} \alpha_{m,n} &= \alpha_{m,n-1} - \frac{\Delta\Theta}{2} (C_{m,n-1}^A \alpha_{m,n-1} + \bar{C}_{m,n}^A \bar{\alpha}_{m,n}) \\ -\left(\frac{m-2}{m}\right) C_{m-1,n}^A + \left(\frac{m-1}{m}\right) (h\alpha_{m,n} + G_2) C_{m,n}^A - C_{m+1,n}^A \\ &= G \left(\frac{m-1}{m}\right) C_{m,n-1}^A \quad ; \quad m = 3, \dots, M-1 \end{aligned}$$

where

$$C_{M,1}^A = 1$$

Solve for $C_{m,n}^A$; $m = 2, \dots, M-1$.

For slow deactivation, all procedures are the same except

$$(a) \quad C_{m,1}^A = \frac{1}{(m-1)\Delta r} \frac{\sinh[3h_A(m-1)\Delta r]}{\sinh(3h_A)}$$

$$(b) \quad \text{Set } h_{dA} = 0$$

```

PROGRAM PARAL
DIMENSION T(80),DD(401),AA(401),TT(401),A(401)
COMMON MM,MI,II,R,RR,HD,X(11),S(401),UAO(401),UBO(401),
1 SI(11,80),UA(11,80),UB(11,80),X2(401),AC(401),AI(401)
1000 MM=TTYIN(4HM= )
IF(MM.EQ.0)GOTO 2000
50 MC=TTYIN(4HSTAR,4HTING,4H M V,4HALUE,2H= )
MIO=(MM-1)/10
IF((MC-1)/MIO*MIO.NE.(MC-1))GOTO 50
NN=TTYIN(4HN= )
DT=TTYIN(4HDT= )
F=TTYIN(4HTIME,4H FAC,4HTOR=)
KK=TTYIN(4HPRIN,4HT 0U,4HT SE,4HQ= )
HA=TTYIN(4HHA= )
HD=TTYIN(4HHD= )
C CALCULATE CONSTANTS AND INITIAL CONDITIONS
HASP=HA*3.
CALL CALCUL(HA)
CALL INITIAL(HASP,1)
GAO=HD*HD*9.*RR/DT
H=HASP*HASP*RR
CALL FUBAR(EFF)
AA(1)=EFF $ UO=EFF
C CALCULATE CONCENTRATION PROFILE AND ACTIVITY BY CALLING THE
C SUBPROGRAM TRID AND FUBAR
DO 500 N=2,NN
IF(N.LE.21)GOTO 1
C THESE LOOPS ARE FOR THE DIFFERENT TIME INCREMENTS
GA=GAO $ TH=DT $ XX=N-21
TT(N)=XX*TH+TT(21)
GOTO 2
1 GA=F*GAO $ TH=DT/F $ XX=N-1
TT(N)=XX*TH
2 CONTINUE
CALL TRID(H,GA,TH,MC)
NI=N-1
CALL FUBAR(EFF)
AA(N)=EFF
IF(UO.LE.EFF)UO=EFF
C CALCULATE THE DERIVATIVE OF THE EFFECTIVENESS FACTOR
DD(NI)=(AA(N)-AA(NI))/TH
C FOR THE WRITING STEP AT THE LATER PORT,
IF(N.LE.21)GOTO 11
NP=N-20
IF(NP/KK*KK.NE.NP)GOTO 13
NK=NP/KK+21
GOTO 12
11 NK=N
12 T(NK)=TT(N)
DO 61 I=1,MM,II
IK=(I+II-1)/II
UA(IK,NK)=UAO(I)
61 SI(IK,NK)=S(I)
13 CONTINUE
C RESET THE STARTING M VALUE
IF(MC.EQ.1)GOTO 500
IF(UAO(MC).GE.0.00001)MC=MC-MIO
500 CONTINUE
C CHANGE THE DERIV OF EFFECTIVE TO THE DERIV OF ACTIVITY, AND
C THE EFFECTIVE TO THE ACTIVITY

```

```

DO 70 I=1,NN
A(I)=AA(I)/UO
70 DD(I)=DD(I)/UO
DD(I)=0.
NI=(NN-21)/KK+21
C WRITE UP THE RESULTS
WRITE(20,199)HA,HD,MM,NN,DT
WRITE(20,200)(X(I),I=1,11)
WRITE(20,201)(T(I),(UA(J,I),J=1,11),I=1,NI)
WRITE(20,202)
WRITE(20,200)(X(I),I=1,11)
WRITE(20,201)(T(I),(SI(J,I),J=1,11),I=1,NI)
WRITE(20,203)(TT(I),AA(I),A(I),DD(I),I=1,NN)
GOTO 1000
2000 CONTINUE
199 FORMAT(1H1,10X,'***CONCENTRATION PROFILE OF A***'
1 /1H0,'HA='F12.6/' HD='F12.6/' M='17/' N='17/' DT='F12.6)
200 FORMAT(1H0,10X,11(3X,'R='F6.4))
201 FORMAT(1X,'T='F7.4,1X,11F11.7)
202 FORMAT(1H1,10X,'***POINT ACTIVITY***')
203 FORMAT(1H1,10X,'***EFFECTIVENESS FACTOR AND ACTIVITY AS A *
1 'FUNCTION OF TIME***'
2 /1H0,24X'TIME'15X'*EFFECTIVE'14X'*ACTIVITY'13X'*DERIVATIVE*'
3 /(21X,F10.5,2(10X,F15.8),E25.8)
END

```

```

SUBROUTINE CALCUL(HA)
COMMON MM,MI,II,R,RR,HD,X(11),S(401),UAO(401),UBO(401),
1 SI(11,80),UA(11,80),UB(11,80),X2(401),AC(401),A(401)
C CALCULATE CONSTANTS WHICH ARE NEEDED IN THE LATER PART OF THE PR0GM
MI=MM-1 $ II=MI/10 $ R=1./FLOAT(MI)
IF(HA.GE.50.)G0T0 91
II9=0 $ RR=R*R
G0T0 92
91 SCALE=TTYIN(4HSCAL,4HE RA,4HDIUS,4HI0,1,4H00,))
XMI=MI $ II9=(SCALE-1.)*XMI $ R=R/SCALE
RR=R*R $ UA(10,10)=II9
92 CONTINUE
XII9=II9 $ XII=II
X9=XII9*R $ XR=XII*R
D0 21 I=1,MM
XX=II9+I $ AC(I)=(XX-1.)/XX $ A(I)=-((XX-2.)/XX
YY=II9+I-1 $ X2(I)=YY*YY*RR
21 S(I)=1.
D0 22 I=1,11
XX=I-1 $ X(I)=XX*XR+X9
22 SI(I,1)=1.
RETURN
END

```

```

SUBROUTINE INITIAL(HA,K)
DIMENSION U(401)
COMMON MM,MI,II,R,RR,HD,X(11),S(401),UAO(401),UBO(401),
1 SI(11,80),UA(11,80),UB(11,80),X2(401),AC(401),A(401)
C CALCULATE INITIAL CONDITIONS
C FUNCTIONAL KEYS 1;F0R UA, 2;F0R UB,
IF(HD.NE.0.)G0T0 50
IF(HA.GE.150.)G0T0 40
IF(HA.GE.10.)G0T0 21
EH=EXP(HA) $ SINH=EH-1./EH
U(1)=2.*HA/SINH
D0 30 I=2,MM
XX=I-1
ARG=XX*R*HA $ E=EXP(ARG)
30 U(I)=(E-1./E)/(XX*R*SINH)
G0T0 22
40 CONTINUE
II9=UA(10,10) $ I=1
41 CONTINUE
IF(1.GE.MM)G0T0 22
I=I+1
XX=II9+I-1 $ XY=XX*R
HI=-HA*(1.-XY)
IF(ABS(HI).GE.500.)G0T0 90
U(I)=EXP(HI)/XY
G0T0 41
90 U(I)=0.
G0T0 41
21 U(1)=2.*HA*EXP(-HA)
D0 31 I=2,MM
XX=I-1 $ XY=XX*R
HI=-HA*(1.-XY) $ H2=-HA*(1.+XY)
31 U(I)=(EXP(HI)-EXP(H2))/XY
22 CONTINUE
IF(K.EQ.1)G0T0 23
D0 32 I=1,MM
32 UBO(I)=U(I)
D0 33 I=1,MM,11
IK=(I+II-1)/II
33 UB(IK,I)=U(I)
G0T0 24
23 CONTINUE
D0 34 I=1,MM
34 UAO(I)=U(I)
D0 35 I=1,MM,11
IK=(I+II-1)/II
35 UA(IK,I)=U(I)
24 RETURN
50 D0 51 I=1,MM
UAO(I)=0.
51 UBO(I)=0.
D0 52 I=1,10
UA(I,I)=0.
52 UB(I,I)=0.
RETURN
END

```

```

SUBROUTINE TRID(N,G,TH,MC)
DIMENSION B(401),D(401),BETA(401),GAMMA(401),
1 UTEMP(401),STEMP(401)
COMMON MM,MI,II,R,RR,HD,X(11),S(401),UAO(401),UBO(401),
1 SI(11,80),UA(11,80),UB(11,80),X2(401),AC(401),A(401)
C CALCULATE POINT ACTIVITY AND CONCENTRATION PROFILE BY SOLVING
C THE TRIDIAGONAL MATRIX
C FOR THE TIME INCREMENTS, EULER'S SECOND ORDER APPROX IS USED.
MC2=MC+1 $ MC3=MC+2 $ N=MI-MC2
IF(HD.EQ.0.)GOTO 60
G2=G+2
DO 61 M=MC,MM
STEMP(M)=(-TH*UAO(M)+1.)*S(M)
B(M)=AC(M)+(H*STEMP(M)+G2)
61 D(M)=G*AC(M)*UAO(M)
D(MI)=D(MI)+1.
BETA(MC2)=B(MC2) $ GAMMA(MC2)=D(MC2)/BETA(MC2)
DO 62 I=MC3,MI
BETA(I)=B(I)+A(I)/BETA(I-1)
62 GAMMA(I)=(D(I)-A(I)*GAMMA(I-1))/BETA(I)
UTEMP(MI)=GAMMA(MI)
DO 63 I=1,N
K=MI-I
63 UTEMP(K)=GAMMA(K)+UTEMP(K+1)/BETA(K)
UTEMP(MC)=UTEMP(MC2) $ UTEMP(MM)=1.
DO 64 M=MC,MM
S(M)=S(M)-(UAO(M)*S(M)+UTEMP(M)*STEMP(M))*TH/2.
64 B(M)=AC(M)+(H*S(M)+G2)
BETA(MC2)=B(MC2) $ GAMMA(MC2)=D(MC2)/BETA(MC2)
DO 65 I=MC3,MI
BETA(I)=B(I)+A(I)/BETA(I-1)
65 GAMMA(I)=(D(I)-A(I)*GAMMA(I-1))/BETA(I)
UAO(MI)=GAMMA(MI)
DO 66 I=1,N
K=MI-I
66 UAO(K)=GAMMA(K)+UAO(K+1)/BETA(K)
UAO(MC)=UAO(MC2) $ UAO(MM)=1.
RETURN
C FOR THE NO ACC(HD=0) CASE,
60 CONTINUE
DO 67 M=MC,MM
STEMP(M)=(-TH*UAO(M)+1.)*S(M)
BETA(MC2)=(H*STEMP(MC2)+2.)/2.
DO 68 M=MC3,MI
BETA(M)=AC(M)+(H*STEMP(M)+2.)*A(M)/BETA(M-1)
UTEMP(MM)=1. $ UTEMP(MI)=1./BETA(MI)
DO 69 I=1,N
K=MI-I
69 UTEMP(K)=UTEMP(K+1)/BETA(K)
UTEMP(MC)=UTEMP(MC2)
DO 70 M=MC,MM
S(M)=S(M)-(UAO(M)*S(M)+UTEMP(M)*STEMP(M))*TH/2.
BETA(MC2)=(H*S(MC2)+2.)/2.
DO 71 M=MC3,MI
BETA(M)=AC(M)+(H*S(M)+2.)*A(M)/BETA(M-1)
UAO(MM)=1. $ UAO(MI)=1./BETA(MI)
DO 72 I=1,N
K=MI-I
72 UAO(K)=UAO(K+1)/BETA(K)
UAO(MC)=UAO(MC2)
RETURN
END

```

```

SUBROUTINE FUBAR(SS)
COMMON MM,MI,II,R,RR,HD,X(11),S(401),UAO(401),UBO(401),
1 SI(11,80),UA(11,80),UB(11,80),X2(401),AC(401),A(401)
C CALCULATE THE ACTIVITY BY INTEGRATION OF THE POINT ACTIVITY*
C CONCENTRATION PROFILE, USING SIMPSON'S RULE
SS=0.
I=1
MMI=(MM-1)/2
DO 85 K=1,MMI
I1=I+1
I2=I+2
SS=SS+X2(I)*UAO(I)*S(I)+4.*X2(I1)*S(I1)*UAO(I1)
1 +X2(I2)*S(I2)*UAO(I2)
85 I=I+2
SS=SS+R
RETURN
END

```

APPENDIX IV

DIFFERENCE EQUATIONS AND PROGRAM LISTINGS
FOR SIDE-BY-SIDE DEACTIVATIONDifference Equations

$$C_{m,1}^A = C_{m,1}^P = 0 \quad (a)$$

$$\alpha_{m,1} = 1$$

First approximation;

$$\begin{aligned} \bar{\alpha}_{m,n} &= \alpha_{m,n-1} (-\Delta \Theta C_{m,n-1}^P + 1) \\ &- \left(\frac{m-2}{m}\right) \bar{C}_{m-1,n}^P + \left(\frac{m-1}{m}\right) (G_{P2} + h_2 \bar{\alpha}_{m,n}) \bar{C}_{m,n}^P - \bar{C}_{m+1,n}^P \\ &= G_P \left(\frac{m-1}{m}\right) C_{m,n-1}^P \quad ; \quad m = 3, \dots, M-1 \end{aligned}$$

where

$$\begin{aligned} \bar{C}_{M,n}^P &= 1 \\ G_P &= (3h_{dP} \Delta r)^2 / \Delta \Theta \quad (b) \\ G_{P2} &= G_P + 2 \\ h_2 &= (3h_P \Delta r)^2 \end{aligned}$$

Using the results of Appendix II, solve for $C_{m,n}^P$; $m = 2, \dots, M-1$.

Second approximation;

$$\alpha_{m,n} = \alpha_{m,n-1} - \frac{\Delta \Theta}{2} (C_{m,n-1}^P \alpha_{m,n-1} + \bar{C}_{m,n}^P \bar{\alpha}_{m,n})$$

$$\begin{aligned}
& -\left(\frac{m-2}{m}\right)C_{m-1, n}^P + \left(\frac{m-1}{m}\right)(G_{P2} + h_2 \alpha_{m, n})C_{m, n}^P - C_{m+1, n}^P \\
& = G_P \left(\frac{m-1}{m}\right) C_{m, n-1}^P
\end{aligned}$$

$$\begin{aligned}
& -\left(\frac{m-2}{m}\right)C_{m-1, n}^A + \left(\frac{m-1}{m}\right)(G_{A2} + h_1 \alpha_{m, n})C_{m, n}^A - C_{m+1, n}^A \\
& = G_A \left(\frac{m-1}{m}\right) C_{m, n-1}^A
\end{aligned}$$

$$; m = 3, \dots, M-1$$

where

$$C_{M, n}^A = C_{M, n}^P = 1$$

$$G_A = (3h_{dA} \Delta r)^2 / \Delta \Theta \quad (c)$$

$$G_{A2} = G_A + 2$$

$$h_1 = (3h_P \Delta r)^2$$

Solve for $C_{m, n}^A$ and $C_{m, n}^P$; $m = 2, 3, \dots, M-1$.

For slow deactivation, all procedures are the same except

$$(a) \quad C_{m, 1}^A = \frac{1}{(m-1)\Delta r} \frac{\sinh [3h_A (m-1)\Delta r]}{\sinh(3h_A)}$$

$$C_{m, 1}^P = \frac{1}{(m-1)\Delta r} \frac{\sinh [3h_P (m-1)\Delta r]}{\sinh(3h_P)}$$

(b) and (c) Set $h_{dA} = h_{dP} = 0$

```

PROGRAM SIDERY
DIMENSION T(80),DD(401),AA(401),TT(401),A(401)
COMMON MM,MI,II,R,RR,HD,X(11),S(401),UAO(401),UBO(401),
1 SI(11,80),UA(11,80),UB(11,80),X2(401),AC(401),AI(401)
1000 MM=TTYIN(4HM= )
IF(MM.EQ.0)GOTO 2000
50 MC=TTYIN(4HSTAR,4HTING,4HM V,4HALUE,2H= )
MIO=(MM-1)/10
IF((MC-1)/MIO*MIO.NE.(MC-1))GOTO 50
NN=TTYIN(4HM= )
DT=TTYIN(4HDT= )
F=TTYIN(4HTIME,4H FAC,4HTOR=)
KK=TTYIN(4HPRIN,4HT 0U,4HT SE,4HQ= )
HA=TTYIN(4HHA= )
HP=TTYIN(4HHP= )
HD=TTYIN(4HHD= ) $ HDP=TTYIN(4HHDP=)
V=TTYIN(4HOUTE,4HR 10,4HZ?(S,4HDT G,4HE.50,2H) )
C CALCULATE CONSTANTS AND INITIAL CONDITIONS
HASP=HA*3.
HPSP=3.*HP
CALL CALCUL(V)
CALL INITIAL(HASP,1)
CALL INITIAL(HPSP,2)
GAO=HD*HD*9.*RR/DT
HAA=HASP*HASP $ HPP=HPSP*HPSP
HI=HAA*RR $ H2=HPP*RR
GPO=9.*HDP*HDP*RR/DT
CALL FUBAR(EFF)
AA(1)=EFF $ UO=EFF
C CALCULATE CONCENTRATION PROFILE AND ACTIVITY BY CALLING THE
C SUBPROGRAM IRID AND FUBAR
DO 500 N=2,NN
IF(N.LE.21)GOTO 1
C THESE LOOPS ARE FOR THE DIFFERENT TIME INCREMENTS
GA=GAO $ GP=GPO $ TH=DT $ XX=N-1
TT(N)=XX*TH+TT(21)
GOTO 2
1 GA=F*GAO $ GP=GPO*F $ TH=T/F $ XX=N-1
TT(N)=XX*TH
2 CONTINUE
CALL SIDE(HI,H3,GA,GP,TH,MC)
NI=N-1
CALL FUBAR(EFF)
AA(N)=EFF
IF(UO.LE.EFF)UO=EFF
C CALCULATE THE DERIVATIVE OF THE EFFECTIVENESS FACTOR
DD(NI)=(AA(N)-AA(N1))/TH
C FOR THE WRITING STEP AT THE LATER PART,
IF(N.LE.21)GOTO 11
NP=N-20
IF(NP/KK*KK.NE.NP)GOTO 13
NK=NP/KK+21
GOTO 12
11 NK=N
12 T(NK)=TT(N)
DO 61 I=1,MM,11
IK=(I+II-1)/II
UA(IK,NK)=UAO(I)
UB(IK,NK)=UBO(I)
61 SI(IK,NK)=S(I)

```

```

13 CONTINUE
C RESET THE STARTING M VALUE
IF(MC.EQ.1)GOTO 500
IF(UAO(MC).GE.0.00001)MC=MC-MIO
500 CONTINUE
C CHANGE THE DERIV OF EFFECTIVE TO THE DERIV OF ACTIVITY, AND
C THE EFFECTIVE TO THE ACTIVITY
DO 70 I=1,NN
A(I)=AA(I)/UO
70 DD(I)=DD(I)/UO
DD(I)=0.
NI=(NN-21)/KK+21
C WRITE UP THE RESULTS
WRITE(20,199)HA,HP,HD,MM,NN,DT
WRITE(20,200)(X(I),I=1,11)
WRITE(20,201)(T(I),(UA(J,I),J=1,11),I=1,NI)
WRITE(20,204)
WRITE(20,200)(X(I),I=1,11)
WRITE(20,201)(T(I),(UB(J,I),J=1,11),I=1,NI)
WRITE(20,202)
WRITE(20,200)(X(I),I=1,11)
WRITE(20,201)(T(I),(SI(J,I),J=1,11),I=1,NI)
WRITE(20,203)(TT(I),AA(I),A(I),DD(I),I=1,NN)
GOTO 1000
2000 CONTINUE
199 FORMAT(1H1,10X,'***CONCENTRATION PROFILE OF A***'
1 /'OHA='F12.6/' HP='F12.6/' HD='F12.6
2 /' M='F7.4/' N='F7.4/' DT='F12.6)
200 FORMAT(1H0,10X,11(3X,'R='F6.4))
201 FORMAT(1X,'T='F7.4,1X,11F11,7)
202 FORMAT(1H1,10X,'***POINT ACTIVITY***')
203 FORMAT(1H1,10X,'***EFFECTIVENESS FACTOR AND ACTIVITY AS A '
1 'FUNCTION OF TIME***'
2/1H0,24X'TIME*'15X'EFFECTIVE*'14X'ACTIVITY*'13X'DERIVATIVE*'
3 /21X,F10.5,2(10X,F15.8),E25.8)
204 FORMAT(1H1,10X,'*** CONCENTRATION PROFILE OF P ***')
END

```

```

SUBROUTINE SIDE(H1,H2,GA,GP,TH,MC)
DIMENSION B(401),D(401),BETA(401),GAMMA(401),
I UTEMP(401),STEMP(401)
COMMON MM,MI,I1,R,RR,HD,X(11),S(401),UAO(401),UBO(401),
I SI(11,80),UA(11,80),UB(11,80),X2(401),AC(401),A(401)
C CALCULATE POINT ACTIVITY AND CONCENTRATION PROFILE BY SOLVING
C THE TRIDIAGONAL MATRIX
C FOR THE TIME INCREMENTS, EULER'S SECOND ORDER APPROX IS USED.
MC2=MC+1 $ MC3=MC+2 $ N=MI-MC2
IF(HD.EQ.0.)GOTO 60
GA2=GA+2. $ GP2=GP+2.
D0 61 M=MC,MM
STEMP(M)=(-TH*UBO(M)+1.)*S(M)
B(M)=AC(M)*(H2*STEMP(M)+GP2)
61 D(M)=GP*AC(M)*UBO(M)
D(MI)=D(MI)+1.
BETA(MC2)=B(MC2) $ GAMMA(MC2)=D(MC2)/BETA(MC2)
D0 62 I=MC3,MI
BETA(I)=B(I)+A(I)/BETA(I-1)
62 GAMMA(I)=(D(I)-A(I)*GAMMA(I-1))/BETA(I)
UTEMP(MI)=GAMMA(MI)
D0 63 I=1,N
K=MI-1
63 UTEMP(K)=GAMMA(K)+UTEMP(K+1)/BETA(K)
UTEMP(MC)=UTEMP(MC2) $ UTEMP(MM)=1.
D0 64 M=MC,MM
S(M)=S(M)-(UBO(M)*S(M)+UTEMP(M)*STEMP(M))*TH/2.
64 B(M)=AC(M)*(H2*S(M)+GP2)
BETA(MC2)=B(MC2) $ GAMMA(MC2)=D(MC2)/BETA(MC2)
D0 65 I=MC3,MI
BETA(I)=B(I)+A(I)/BETA(I-1)
65 GAMMA(I)=(D(I)-A(I)*GAMMA(I-1))/BETA(I)
UBO(MI)=GAMMA(MI)
D0 66 I=1,N
K=MI-1
66 UBO(K)=GAMMA(K)+UBO(K+1)/BETA(K)
UBO(MC)=UBO(MC2) $ UBO(MM)=1.
D0 91 I=MC,MM
B(I)=AC(I)*(H1*S(I)+GA2)
91 D(I)=AC(I)*GA*UAO(I)
D(MI)=D(MI)+1.
BETA(MC2)=A(MC2) $ GAMMA(MC2)=D(MC2)/BETA(MC2)
D0 92 I=MC3,MI
BETA(I)=B(I)+A(I)/BETA(I-1)
92 GAMMA(I)=(D(I)-A(I)*GAMMA(I-1))/BETA(I)
UAO(MI)=GAMMA(MI)
D0 93 I=1,N
K=MI-1
93 UAO(K)=GAMMA(K)+UAO(K+1)/BETA(K)
UAO(MC)=UAO(MC2) $ UAO(MM)=1.
RETURN
C FOR THE NO ACC(HD=0) CASE,
60 CONTINUE
D0 67 M=MC,MM
STEMP(M)=(-TH*UBO(M)+1.)*S(M)
BETA(MC2)=(H2*STEMP(MC2)+2.)/2.
D0 68 M=MC3,MI
BETA(M)=AC(M)*(H2*STEMP(M)+2.)*A(M)/BETA(M-1)
68 UTEMP(MM)=1. $ UTEMP(MI)=1./BETA(MI)
D0 69 I=1,N
K=MI-1

```

```

69 UTEMP(K)=UTEMP(K+1)/BETA(K)
UTEMP(MC)=UTEMP(MC2)
D0 70 M=MC,MM
S(M)=S(M)-(UBO(M)*S(M)+UTEMP(M)*STEMP(M))*TH/2.
BETA(MC2)=(H2*S(MC2)+2.)/2.
D0 71 M=MC3,MI
71 BETA(M)=AC(M)*(H2*S(M)+2.)*A(M)/BETA(M-1)
UBO(MM)=1. $ UBO(MI)=1./BETA(MI)
D0 72 I=1,N
K=MI-1
72 UBO(K)=UBO(K+1)/BETA(K)
UBO(MC)=UBO(MC2)
BETA(MC2)=AC(MC2)*(H1*S(MC2)+2.)/2.
D0 98 I=MC3,MI
98 BETA(I)=AC(I)*(H1*S(I)+2.)*A(I)/BETA(I-1)
UAO(MM)=1. $ UAO(MI)=1./BETA(MI)
D0 99 I=1,N
K=MI-1
99 UAO(K)=UAO(K+1)/BETA(K)
UAO(MC)=UAO(MC2)
RETURN
END

```